

2002

# Numerical Model of the Transient Effects of a Heat of Fusion Reservoir Interacting with Two-phase Flow

Anne-Marie Bechard Thibodeau

Follow this and additional works at: <http://digitalcommons.library.umaine.edu/etd>



Part of the [Mechanical Engineering Commons](#)

---

## Recommended Citation

Thibodeau, Anne-Marie Bechard, "Numerical Model of the Transient Effects of a Heat of Fusion Reservoir Interacting with Two-phase Flow" (2002). *Electronic Theses and Dissertations*. 307.  
<http://digitalcommons.library.umaine.edu/etd/307>

This Open-Access Dissertation is brought to you for free and open access by DigitalCommons@UMaine. It has been accepted for inclusion in Electronic Theses and Dissertations by an authorized administrator of DigitalCommons@UMaine.

**NUMERICAL MODEL OF THE TRANSIENT EFFECTS OF A HEAT OF  
FUSION RESERVOIR INTERACTING WITH TWO-PHASE FLOW**

By

Anne-Marie Bechard Thibodeau

B.M. Anna Maria College, 1985

B.S. The University of Maine, 1993

M.S. The University of Maine, 1996

A THESIS

Submitted in Partial Fulfillment of the

Requirements for the Degree of

Doctor of Philosophy

(Individualized in Mechanical Engineering)

The Graduate School

The University of Maine

December, 2002

Advisory Committee:

Justin H. Poland, Associate Professor of Mechanical Engineering, Advisor

Richard Sayles, Jr., Associate Professor of Mechanical Engineering

John J. Hwalek, Associate Professor of Chemical Engineering

James Sucec, Professor of Mechanical Engineering

Osama M. Ibrahim, Associate Professor of Mechanical Engineering, U.R.I.

## LIBRARY RIGHTS STATEMENT

In presenting this thesis in partial fulfillment of the requirements for an advanced degree at The University of Maine, I agree that the Library shall make it freely available for inspection. I further agree that permission for "fair use" copying of this thesis for scholarly purposes may be granted by the Librarian. It is understood that any copying or publication of this thesis for financial gain shall not be allowed without my written permission.

Signature: Anne-Marie B. Thibodeau

Date: August 23, 2002

# **NUMERICAL MODEL OF THE TRANSIENT EFFECTS OF A HEAT OF FUSION RESERVOIR INTERACTING WITH TWO-PHASE FLOW**

By Anne-Marie Bechard Thibodeau

Thesis Advisor: Dr. Justin H. Poland

An Abstract of the Thesis Presented  
in Partial Fulfillment of the Requirements for the  
Degree of Doctor of Philosophy  
(Individualized in Mechanical Engineering)  
December, 2002

The object of this thesis is to develop a numerical model that simulates the transient behavior of a coaxial, thermal energy storage system consisting of a phase changing material (PCM) interacting with a two-phase fluid. The purpose of this model would be to have a useful design tool that could be applied when sizing and building ice-on-coil, cooling systems (ice-banks).

The numerical model is an explicit finite volume approximation applied to the enthalpy method. It solves a two-dimensional, axisymmetric, heat conduction problem with conjugate forced convection at its inner boundary. Natural convection is neglected in the PCM.

The conjugate boundary is modeled with existing, empirical correlations for heat transfer coefficient during evaporation/condensation of a two-phase fluid. Pressure drop is also modeled with existing correlations.

The model is validated analytically for small times by comparing it to Paterson's one-dimensional, solidification of a line heat sink in an infinite medium. A test apparatus was built also, to validate the model experimentally. Mean and average deviation between numerical and experimental results fall within 9% and 6%, respectively.

Parametric studies are performed to determine relevant characteristics of a thermal energy storage unit. Results indicate that axial conduction in the PCM cannot be neglected when interacting with high Reynolds number, two-phase flows. It is shown that it is more efficient to increase the volume of PCM by adding length rather than thickness.

The effects of Reynolds number on two-phase, local Nusselt number are investigated. The results of adding sensible heat to the PCM are examined by looking at the effects of Stefan number on wall temperature and on Biot number. The behavior of pressure drop, during evaporation and condensation, is discussed.

The results of applying this numerical approach indicate some important criteria to determining the optimal design of a thermal energy storage system.

## **DEDICATION**

To my beloved father, Joseph Bechard,  
whose time in this world was much too short.

## **ACKNOWLEDGMENTS**

I wish to thank William Wess, a work-study student who assisted in the building of the testing apparatus, and Jim LaBreque whose refrigeration experience solved many technical problems before and after they occurred.

I want to thank also my advisor, Dr. Justin H. Poland, for all of his guidance, and Dr. Richard Sayles, Jr., Professor James Sucec, Dr. John J. Hwalek, and Dr. Osama M. Ibrahim, for having agreed to be on my advisory committee.

## TABLE OF CONTENTS

DEDICATION.....	ii
ACKNOWLEDGMENTS.....	iii
LIST OF TABLES.....	vii
LIST OF FIGURES.....	viii
NOMENCLATURE.....	xii

### Chapter

1. INTRODUCTION.....	1
2. LITERATURE REVIEW.....	5
2.1. Heat Conduction in Heat of Fusion Reservoir (Phase Change Material).....	5
2.2. Two-Phase Flow Heat Transfer Correlations.....	7
2.2.1. Evaporation Heat Transfer.....	7
2.2.2. Condensing Heat Transfer.....	8
3. MODELING APPROACH.....	11
3.1. Problem Description.....	11
3.2. Heat Transfer Models.....	12
3.2.1. Phase Change Material (PCM) in Annular Gap.....	12
3.2.1.1. Solution Methodology.....	12
3.2.1.2. Axial Conduction.....	13
3.2.2. Two-Phase Flow.....	13



3.2.2.1. Pressure Drop Correlations.....	14
3.2.2.2. Two-Phase Heat Transfer Correlation for Evaporation.....	17
3.2.2.3. Two-Phase Heat Transfer Correlation for Condensation.....	22
3.2.3. Single-Phase Flow.....	25
4. MATHEMATICAL MODEL.....	26
4.1. Phase Change Material.....	26
4.2. Two-Phase Fluid-Side Heat Transfer and Pressure Drop.....	31
4.2.1. Evaporating Heat Transfer Coefficient.....	31
4.2.2. Condensing Heat Transfer Coefficient.....	33
4.2.3. Two-Phase Pressure Drop.....	37
4.3. Single-Phase Fluid-Side Heat Transfer and Pressure Drop.....	39
4.4. Numerical Procedure.....	41
5. EXPERIMENTAL APPARATUS AND PROCEDURE.....	48
5.1. Description of Apparatus.....	48
5.1.1. Tap Water Flow Path.....	48
5.1.2. Brine Loop.....	50
5.1.3. Refrigerant Loop.....	51
5.2. Operation of the PCM and Phase-Changing Fluid as an Ice-Bank.....	52
6. MODEL VALIDATION.....	58
6.1. Comparison of Numerical Model to 1-D Exact Solution of Paterson.....	58

6.2. Comparison of Numerical Model to Test Results.....	60
6.3. Uncertainty Analysis.....	68
6.4. Convergence of Model.....	68
7. RESULTS AND DISCUSSION.....	72
7.1. Axial Conduction in PCM.....	72
7.1.1. Freezing Front Position at Different Fourier Number.....	72
7.1.2. Axial Variation of Freezing vs. Reynolds Number.....	74
7.2. Effects of Increasing Volume of PCM on Net Energy/Lost.....	75
7.3. Effects of Stefan Number on Refrigerant Wall Temperature.....	77
7.4. Effects of Reynolds Number and Temperature on Evaporation Heat Transfer.....	78
7.5. Effects of Reynolds Number and Temperature on Condensation Heat Transfer.....	80
7.6. Effect of Reynolds Number on Length of Tube Needed to Evaporate/Condense.....	82
7.7. Effect of Reynolds Number on Pressure Drop.....	84
8. CONCLUSIONS.....	86
REFERENCES.....	88
APPENDIX A: The Algorithm.....	94
APPENDIX B: Sample of Fluid-Side Output.....	121
APPENDIX C: Sample of PCM-Side Output.....	123
BIOGRAPHY OF THE AUTHOR.....	125

## LIST OF TABLES

Table 3.1. Comparison of Total Pressure Drop.....	17
Table 5.1. Refrigerant States in Main Refrigeration Loop.....	51
Table 5.2. Axial and Radial Locations of Temperature Probes.....	53
Table 5.3. Location of Additional Thermocouples and Pressure Transducers.....	54
Table 6.1. Parameters applied during Evaporating Mode.....	60
Table 6.2. Mean and Average Deviation of Numerical vs. Experimental Data for Evaporation Mode.....	64
Table 6.3. Parameters applied during Condensing Mode.....	66
Table 6.4. Mean and Average Deviation of Numerical vs. Experimental Data for Condensing Mode.....	66
Table 6.5. Converging Finite Volume Mesh in j ( $\Delta r$ ) direction.....	69
Table 6.6. Converging Finite Volume Mesh in i ( $\Delta z$ ) direction.....	69
Table 7.1. Parameters used in Thickness vs. Length Study.....	73

## LIST OF FIGURES

Figure 3.1. Thermal Energy Storage (TES) Unit and Cross-Sectional View.....	11
Figure 3.2. Comparison of Frictional Pressure Drop Correlations to Data of Seo & Kim (2000) for R-22 at 5C.....	15
Figure 3.3. Comparison of Frictional Pressure Drop Correlations to Data of Seo & Kim (2000) for R-22 at -5C.....	16
Figure 3.4. Comparison of Frictional Pressure Drop Correlations to Data of Seo & Kim (2000) for R-22 at -15C.....	16
Figure 3.5. Comparison of Heat Transfer Correlations to Data of Seo & Kim (2000) for R-22 in a Tube of O.D.=9.52 mm.....	20
Figure 3.6. Comparison of Heat Transfer Correlations to Data of Seo & Kim (2000) for R-22 in a Tube of O.D.=7.0 mm.....	20
Figure 3.7. Comparison of Gungor-Winterton (1987) to Data of Seo & Kim (2000) for R-22 in a Tube O.D. of 9.52 and 7.0 mm.....	21
Figure 3.8. Comparison of Gungor-Winterton (1987) to Data of Seo & Kim (2000) for Different Saturation Temperatures, at a Heat Flux of 15 kW/m <sup>2</sup> .....	21
Figure 3.9. Comparison of Gungor-Winterton (1987) to Data of Seo & Kim (2000) for Different Saturation Temperatures, at a Heat Flux of 5 kW/m <sup>2</sup> .....	22

Figure 3.10. Comparison of Four Heat Transfer Correlations for Condensing R-22, at a Mass Flux of $75 \text{ kg/m}^2 \text{ s}$ .....	23
Figure 3.11. Comparison of Four Heat Transfer Correlations for Condensing R-22, at a Mass Flux of $300 \text{ kg/m}^2 \text{ s}$ .....	24
Figure 3.12. Comparison of Four Heat Transfer Correlations for Condensing R-22, at a Mass Flux of $650 \text{ kg/m}^2 \text{ s}$ .....	24
Figure 4.1. Finite Volume Element, $(\Delta r, \Delta z)$ .....	28
Figure 4.2. Axisymmetric Cross-Section of Isotherms of Sample Output (Length = 45ft. and Thickness = 1 in.).....	47
Figure 5.1. Schematic of Test Apparatus.....	49
Figure 5.2. View of Water Bath, Compressor and Discharge Accumulator.....	50
Figure 5.3. Ice-Bank with Temperature Probes at Various Axial Locations.....	52
Figure 5.4. View of Radial Locations of Temperature Probes.....	53
Figure 5.5. Flow controls, Data Loggers and Power Supplies.....	56
Figure 6.1. Comparison of Numerical Model to 1-D Exact Solution of Paterson – (Fo Computed with Ice Properties).....	59
Figure 6.2. Comparison of Numerical Model to Experimental Results for Evaporation Mode, $Fo=0.629$ .....	61
Figure 6.3. Comparison of Numerical Model to Experimental Results for Evaporation Mode, $Fo=1.887$ .....	62
Figure 6.4. Comparison of Numerical Model to Experimental Results for Evaporation Mode, $Fo=3.775$ .....	63

Figure 6.5. Comparison of Pressure Drop Along Tube.....	65
Figure 6.6. Comparison of Numerical Model to Experimental Results for Condensing Mode, $Fo_s=7.055$ .....	67
Figure 6.7. Convergence on $\Delta r$ [Top to Bottom: $\Delta r=0.0215625$ ft., 0.01078125 ft., 0.014375 ft.] (Length of PCM is 43 ft., Thickness is 1 in., $\Delta z=0.005$ ft.).....	70
Figure 6.8. Convergence on $\Delta z$ [Top to Bottom: $\Delta z=0.02$ ft., 0.01 ft., 0.005 ft.] (Length of PCM is 43 ft., Thickness is 1 in., $\Delta r=0.01078125$ ft.).....	71
Figure 7.1. Freezing Front Position at Different Times for $D=0.1''$ – ( $Fo$ is Computed with Water Properties and Refrigerant Diameter).....	73
Figure 7.2. Freezing Front Position at Different Times for $D=0.3''$ – ( $Fo$ is Computed with Water Properties and Refrigerant Diameter).....	74
Figure 7.3. Axial Variation of Freezing vs. Saturated Liquid Reynolds Number - $Fo$ Computed with Inner Refrigerant Diameter.....	75
Figure 7.4. Effects of Increasing Volume of Water Annulus by Increasing Length vs. Increasing Outer Radius.....	76
Figure 7.5. Effects of Stefan Number on Wall Temperature.....	77
Figure 7.6. Effects of Stefan Number on Biot Number in the PCM ( $h$ of 2-phase fluid, $k$ of PCM).....	78

Figure 7.7. Effects of Re Number on Evaporation Heat Transfer in a Tube.....	79
Figure 7.8. Effects of Temperature Differential on Evaporation Heat Transfer in a Tube.....	80
Figure 7.9. Effects of Reynolds Number on Condensation Heat Transfer in a Tube.....	81
Figure 7.10. Effects of Temperature on Condensation Heat Transfer in a Tube.....	82
Figure 7.11. Effects of Liquid Reynolds Number on Minimum Length Required to Completely Evaporate Refrigerant.....	83
Figure 7.12. Effects of Vapor Reynolds Number on Minimum Length Required to Completely Condense Refrigerant.....	83
Figure 7.13. Effects of Saturated Liquid Re on Total Pressure Drop when Completely Evaporating Refrigerant.....	85
Figure 7.14. Effects of Saturated Vapor Re on Total Pressure Drop when Completely Condensing Refrigerant.....	85

## NOMENCLATURE

A	area of cell, i,j in PCM [ $\text{ft}^2$ ( $\text{m}^2$ )]
Bi	Biot number, $(hr_w)/k$
Bo	boiling number, $q/G h_{fg}$
$C_p$	specific heat at constant pressure [Btu/lbm-F ( $\text{J/kg-K}$ )]
$c_f$	coefficient of friction
$c_1$	factor applied in Dobson & Chato's stratified flow correlation
$c_2$	factor applied in Dobson & Chato's stratified flow correlation
D	inner diameter of fluid tube [in. (m)]
$E_2$	factor in Gungor & Winterton's correlation
Fo	Fourier number, $kt/\rho C_p D^2$
$Fr_{lo}$	Froude number assuming all mass flowing as liquid, $G^2/\rho_l^2 gD$
f	friction factor
G	mass flux of fluid [ $\text{lbm/ft}^2\text{-hr}$ ( $\text{kg/m}^2\text{-s}$ )]
Ga	Galileo number, $g \rho_l (\rho_l - \rho_v) D^3/\mu_l^2$
g	acceleration of gravity [ $\text{ft/hr}^2$ ( $\text{m/s}^2$ )]
H	enthalpy of the PCM [Btu/lbm ( $\text{J/kg}$ )]
h	heat transfer coefficient [Btu/hr-ft <sup>2</sup> -F ( $\text{W/m}^2\text{-K}$ )]
$h_{tp}$	local, two-phase heat transfer coefficient [Btu/hr-ft <sup>2</sup> -F ( $\text{W/m}^2\text{-K}$ )]
$h_L$	heat transfer coefficient assuming all mass to be flowing as liquid [Btu/hr-ft <sup>2</sup> -F ( $\text{W/m}^2\text{-K}$ )]
$h_{fg}$	latent heat of fluid [Btu/lbm ( $\text{J/kg}$ )]



$Ja_l$	liquid Jakob number, $\frac{C_{p,l}(T_{sat} - T_w)}{h_{fg}}$
$k$	thermal conductivity [Btu/hr-ft-F (W/m-K)]
$L$	length [ft (m)]
$LH$	latent heat of PCM [Btu/lbm (J/kg)]
$Nu_{forced}$	forced, convective Nusselt number, defined by eq. (34)
$P$	pressure [lb/in <sup>2</sup> (kPa)]
$P_c$	critical pressure
$P_r$	reduced pressure, $P/P_c$
$Pr$	Prandtl number, $C_p\mu/k$
$q$	heat flux [Btu/ft <sup>2</sup> -hr (W/m <sup>2</sup> )]
$q_{left}$	heat rate through left face of finite volume [Btu/hr (W)]
$q_{right}$	heat rate through right face of finite volume [Btu/hr (W)]
$q_{top}$	heat rate through top of finite volume [Btu/hr (W)]
$q_{bottom}$	heat rate through bottom of finite volume [Btu/hr (W)]
$r$	radial distance [in (m)]
$r_w$	radius of copper wall through which fluid flows
$Re_l$	liquid Reynolds number, $G(1-x)D/\mu_l$
$Re_L$	Reynolds number assuming all mass flowing as liquid, $GD/\mu_l$
$Re_{vo}$	Reynolds number assuming all mass flowing as vapor, $GD/\mu_v$
$Ste$	Stefan Number, $C_{p,w}(T_m - T_o)/LH$
$v$	velocity [ft/hr (m/s)]
$T$	temperature [F (K)]

$T_o$	initial temperature of PCM [F (K)]
$T_w$	wall temperature [F (K)]
$t$	time
$x$	vapor quality
$z$	axial distance [ft (m)]

### **Subscripts**

exp	experimental
f	fluid
fr	friction
i	cell counter in axial (z) direction
j	cell counter in radial (r) direction
l	liquid
m	melting
mo	momentum
o	outer edge of PCM
p	phase change material
R-22	refrigerant-22
s	solid
sat	saturation
tp	two-phase
v	vapor
w	water

### **Superscripts**

$n$  at old time step

$n+1$  at new time step

### **Greek Symbols**

$\alpha$  void fraction

$\Delta r$  cell thickness [ft (m)]

$\Delta t$  time step [hr (s)]

$\Delta z$  cell width [ft (m)]

$\theta_l$  angle defining liquid level in horizontal tube of condensate

$\mu$  dynamic viscosity [lbm/hr-ft (N-s/m<sup>2</sup>)]

$\rho$  density [lbm/ft<sup>3</sup> (kg/m<sup>3</sup>)]

$\chi_{tt}$  Lockhart-Martinelli parameter for turbulent-turbulent flow

## **Chapter 1**

### **INTRODUCTION**

The application of Thermal Energy Storage (TES) systems can provide benefits to both electric utilities as well as their customers. The use of TES systems makes it possible to shift peak electrical loads to off-peak times, resulting in cost savings for electricity providers and consumers, by temporarily storing hot or cold-temperature energy for later use.

In hot climates, electricity demand is often a problem during peak cooling periods. Often we hear of ‘black-outs’ in these areas during very hot weather days. In fact, some electrical utilities are making it possible for customers to reduce their electricity bills by taking advantage of TES systems. Off-peak rates are offered to customers who shift their use of electricity to low-demand periods of the day. By utilizing TES systems, ice can be generated overnight by operating the TES in a mode such that the Phase Change Material (PCM) is functioning as an evaporator, thus creating a low-temperature energy reservoir. Then, during hot periods of the day, the purpose of the TES would be to function as a supplemental cooling source in an air-conditioning application. At the very least, the low-temperature reservoir could partially cool the air in the existing air-conditioning system. For instance, the city of Pasadena California has installed ice storage systems in its Public Library as well as its Civic Center to take advantage of the Commercial Cool Storage Incentive Program the city started in 1992. The utility company, in Pasadena, offers a rebate of up to \$250,000 on cool storage installations, based on the number of

kilowatts shifted from on-peak to off-peak hours (National Renewable Energy Laboratory, 1995, Cool Storage Using Ice section, paras. 2 & 4). In Hawaii, the Off-Peak/Elite Energy Group has stated that savings have ranged from 42%-58% for all cooling energy shifted from on-peak to off-peak using ice storage and that Hawaii offers a 50% tax credit on the installation of ice storage equipment (2001). These examples show that it is financially advantageous to incorporate TES systems for cooling of buildings. Although the customer is still using electricity to create the ice in the low-temperature TES system (i.e., operating a compressor), the load has been shifted to off-peak demand when lower electricity rates may apply, thus producing monetary savings.

Electrical utilities also benefit financially from TES systems. Having to meet peak demands often requires the electric companies to purchase and install over-sized equipment. During periods of lowered electrical demand, this expensive equipment is operated at conditions which result in lower efficiencies. Convincing customers to shift their electrical demand, through the use of TES systems, makes it possible for the electric companies to size and purchase equipment that can be operated at peak efficiency.

The LaBrecque cycle, discussed by Poland (1990), is a redesign of the conventional refrigeration cycle, aimed at improving the efficiency of household refrigerator/freezer machines by incorporating a TES unit. Upon start up, the liquid PCM in the TES unit would be cooled and changed to its solid phase, operating as a refrigerant evaporator with the machine rejecting heat to the ambient. During normal operation, the TES unit would be operated as a refrigerant condenser, melting some solid, as energy

removed from the cold frozen food storage area is deposited into the PCM. The TES unit would then return to its solid phase by evaporating refrigerant, preparing for more frozen food cooling. This process would continue to cycle between the TES unit performing as condenser then evaporator. The TES unit operating in this fashion needs some development work to determine what configuration of PCM and refrigerant tubing would work best for particular situations.

The object of the current research was to model and test a TES system to determine pertinent parameters that must be applied in the design of such a system. Much research has already been done on the analysis of TES systems with conjugate forced convection but, to the knowledge of this researcher, prior to the present work, none has modeled the two-dimensional, transient effects of a PCM with conjugate forced convection of a two-phase fluid.

The present research has undertaken to model the two-dimensional, time-dependent, freezing and melting of PCM. The PCM is in an annulus that surrounds a metal tube through which flows a phase-changing fluid (i.e., heat-sink/heat-source). The problem is modeled as a conjugate problem of conduction through the PCM with forced convection at one of the boundaries. The numerical model was examined by comparing constant fluid temperature, small-time solutions to that of Paterson's exact solution to a two-phase problem of solidification by a line heat sink in an infinite medium, with cylindrical symmetry (Ozisik, 1993). Parameters that are important to the sizing and selection of a TES system were investigated. The transient evolution of the temperature

distribution in the TES was determined experimentally and compared to the results of the numerical model.

## **Chapter 2**

### **LITERATURE REVIEW**

#### **2.1. Heat Conduction in Heat of Fusion Reservoir (Phase Change Material)**

Many practical heat transfer problems involve a change of phase of a material due to energy absorption or release (i.e., melting or freezing of the phase changing material). Examples would include solar energy storage for night heating, the solidification of castings in industry, and the formation of ice for space cooling.

Several researchers have investigated the behavior of phase change materials analytically and numerically. The analytical solutions are limited by their mathematical complexity. The solution of a phase change problem consists of a transient heat conduction problem, in up to three space dimensions, coupled with a convection problem, or in the case of the present work, coupled with a phase-changing flow problem.

Springer (1969) numerically solved the problem of freezing or melting of cylinders for homogeneous phase change materials (e.g.,  $\rho_w = \rho_s$ ) for a given temperature distribution along the inner wall. Hsu and Sparrow (1981) developed a closed form analytical solution for freezing adjacent to a plane wall cooled by forced convection. Sparrow and Hsu (1981) numerically solved for two-dimensional freezing on the outside of a coolant-carrying tube. The tube consisted of a single-phase gaseous coolant. Hsu, Sparrow and Patankar (1981) set forth a numerical solution of transient, two-dimensional heat conduction problems in which one of the boundaries of the solution domain moves with time. The moving boundary is immobilized through coordinate transformation. Shamsundar (1982) presented a closed-form, analytical solution for freezing outside a



circular tube with axial variation of coolant temperature by ignoring the sensible heat and axial conduction of the phase change material. Cao and Faghri (1990) performed a numerical analysis of freezing in a phase change material with a square cross-section. This analysis included the effects of natural convection but assumed constant, uniform wall temperature. Charach, Keizman, and Sokolov (1991) studied the problem of axisymmetric freezing around a coolant-carrying tube which provided a uniform, constant heat transfer coefficient. Hasan (1994) also used a constant heat transfer coefficient from the coolant when computing the speed of the radial phase transition front around a vertical and horizontal tube. Bellecci and Conti (1993) studied the transient behavior of a cylindrical thermal storage system by using the enthalpy method. The heat transfer fluid was single-phase, incompressible and viscous heating was neglected. Cao and Faghri studied the performance of a thermal energy storage system with conjugate laminar forced convection (1991) and turbulent forced convection (1992) in the tube. Zhang and Faghri (1996) derived a semi-analytical solution for a thermal energy storage system with conjugate laminar forced convection; however, axial heat transfer in the phase change material was neglected. Hamdan and Elwerr (1996) studied a two-dimensional melting process of a phase change material in a rectangular enclosure which had a constant heat flux applied to one side. Lee and Jones (1996) modeled an ice-on-coil thermal energy storage system. Although they applied Shah's evaporation correlation for a two-phase heat transfer coefficient, they simply calculated the heat transfer coefficient at ten different vapor qualities then took a weighted average for the overall heat transfer coefficient. And, most recently, Almogbel modeled heat conduction in ice with conjugate forced convection as a one-dimensional conduction problem (1997). To the knowledge

of this researcher, until the present work, a solution had not been obtained to the transient problem of two-dimensional heat conduction in a phase change material with conjugate forced convection of a two-phase fluid.

## **2.2. Two-Phase Flow Heat Transfer Correlations**

Over the last fifty years, a number of techniques have been devised for predicting the heat transfer coefficients during condensation or evaporation of fluids inside pipes. Most correlations are particular to a certain category of fluids or to specific orientations or flow parameters.

### **2.2.1. Evaporation Heat Transfer**

Flow boiling heat transfer correlations can be classified into three categories: 1) the two-phase flow coefficient is expressed as a function of some dimensionless parameters such as Boiling number and Convection Number; 2) the nucleate boiling term and forced convection term are summed together; 3) the larger of the two terms, microconvective and macroconvective, is applied.

Chen developed an additive model in 1966 but it applies best to water as the phase-changing fluid and exhibits large deviations when applied to refrigerants (Kandlikar, 1991).

Kandlikar proposed a correlation which he claims was tested against 10,000 data points, for fluids including water, refrigerants, and cryogenics (1990). His correlation consists of a fluid-dependent parameter. In order for his correlation to be applied to other fluids, the parameter must first be evaluated. Also, his two-phase heat transfer coefficient

evaluated at nearly zero vapor quality can be at least two times greater than the value obtained by other correlations.

Shah developed a correlation in 1982 which provides a good fit to a large body of data, including water, refrigerants and cryogenics (Gungor & Winterton, 1986). His correlation belongs to category 3 in which the larger of the two heat transfer terms (nucleate boiling vs. convection) is applied. This creates stepwise behavior when his heat transfer coefficient is plotted as a function of quality.

Gungor and Winterton proposed a general correlation for flow boiling in tubes (1986) then went on to simplify their correlation, resulting in a reduction of the number of equations needed to solve, with improved accuracy (1987). Their correlation was developed on the theory of summation of macroconvective and microconvective terms, with an enhancement factor applied to the former and a suppression factor applied to the latter. However, in their most recent version (1987), they replaced the microconvective term, whose range of magnitude is quite narrow, with a simpler expression based on an all-liquid heat transfer coefficient and absorbed it into a general expression for two-phase heat transfer. When compared to over 4300 data points, the mean deviation is only 20.8%. When compared to the Refrigerant-22 data, the mean and average deviation are 15.0% and 6.9%, respectively.

### **2.2.2. Condensing Heat Transfer**

Several flow regimes exist in the process of condensing a two-phase fluid. The two primary types of flow are stratified (wavy) flow and annular flow. Stratified flow condensation is commonly referred to as film condensation. Its dominant heat transfer

mechanism is conduction through the film at the top of the tube (Dobson & Chato, 1998). Annular flow exhibits a film of liquid all around the inner circumference of the tube, with a high-speed vapor core at its center. Annular flow condensation does not experience the resistance to heat transfer which is present in stratified flow, in the form of a pool of liquid, driven by gravity, at the bottom of the tube.

Jaster and Kosky (1976) developed a method for predicting stratified flow condensation in a tube. However, their correlation exhibits a mean deviation of 37% when compared to their own data.

The correlation of Traviss, Rohsenow, and Baron (1973) is applicable in the range of annular flow but the value of their two-phase heat transfer coefficient is not finite at a vapor quality of 100%.

Two of the more commonly used correlations in industry, according to Kandlikar (1999), are those of Cavallini and Zecchin (1974) and of Shah (1979). Cavallini and Zecchin's model is limited to the ranges of Reynolds number from 5,000 to 500,000, Prandtl number from 0.8 to 20, and vapor quality from 0.2 to 0.9. Shah's correlation was based on multiplying an all-liquid heat transfer coefficient by a two-phase multiplier. His correlation is applicable in the range of mass flux from 39,000 to 758,000 kg/m<sup>2</sup>-hr and vapor qualities from 0 to 100%. Although he claimed a modest mean deviation of only 15.4% from his analysis of 474 data points, recently Moser, Webb, and Na have compared his correlation to 1197 data points, for six kinds of refrigerants, and found that the deviation is only 14.37% for all data points (Kandlikar, 1999).

Dobson and Chato have sought to improve on Chato's original correlation by making it applicable to stratified as well as annular flow (1998). However, their

correlation is based on choices of when to apply the stratified or annular correlation. This creates a discontinuous jump in their heat transfer coefficient when the flow straddles between, what they have defined numerically to be, stratified or annular flow.

## Chapter 3

### MODELING APPROACH

#### 3.1. Problem Description

The Thermal Energy Storage (TES) unit being investigated consists of a copper tube surrounded by a coaxial cylinder which forms an annular gap around the tube as shown in Figure 3.1. The gap is filled with Phase Change Material (PCM). The fluid running through the copper tube also undergoes a phase change. When the PCM is in a liquid state, the fluid flowing through the tube enters as a liquid, or mostly liquid, coolant that changes to a vapor as it absorbs energy from the PCM through the copper wall. Likewise, when the PCM is solid, the fluid in the tube enters as a vapor and changes to liquid as it releases energy into the PCM.

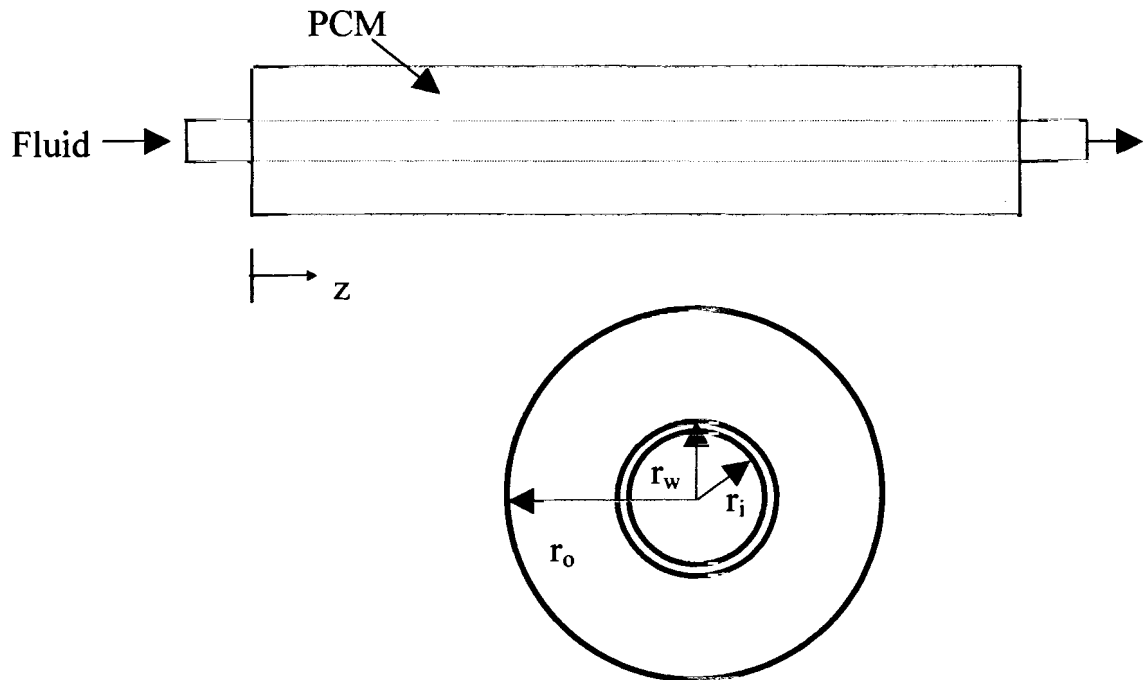


Figure 3.1. Thermal Energy Storage (TES) Unit and Cross Sectional View

The TES unit being analyzed is a two-dimensional, transient, heat conduction problem with conjugate forced convection of a two-phase fluid at its inner boundary. The fluid at the entrance to the annulus is considered to be fully developed, quasi-steady, equilibrium flow. The ends of the outer annulus, consisting of the PCM, are modeled as adiabatic, as is the outer wall of the PCM container.

### **3.2. Heat Transfer Models**

An explicit finite volume approach is used to analyze this two-dimensional, transient heat conduction problem. The conjugate forced convection at the inner boundary of the PCM annulus is modeled by implementing empirical correlations for the heat transfer coefficient. Heat transfer through the copper wall, which separates the fluid from the PCM, is modeled with radial conduction only since the thin wall of the copper tube, typically 0.03 to 0.05 inch thick, makes its ability to transport heat axially much less than either the refrigerant in the tube or the water/ice surrounding it.

#### **3.2.1. Phase Change Material (PCM) in Annular Gap**

The PCM in the outer annulus is considered to have constant thermophysical properties in the liquid and solid regions. The only temperature at which the properties vary is at the single melting/fusion temperature of the PCM.

**3.2.1.1. Solution Methodology.** A finite-volume, enthalpy method is applied to the heat conduction problem (Ozisik, 1993). The PCM in the annular gap is divided into equal lengths ( $\Delta z$ ) and layers of equal thickness ( $\Delta r$ ). In the finite-volume method, the temperature at the center ( $\Delta z/2$ ,  $\Delta r/2$ ) of each lump is considered to be uniform

throughout the lump, at each instant of time (Murray & Landis, 1959). Conservation of energy is applied at each boundary of each finite annular volume. Variation in temperature around the circumference of the horizontal annulus is considered negligible and, therefore, freezing or melting is considered axisymmetric around the tube. Natural convection, in the PCM, is ignored.

**3.2.1.2. Axial Conduction.** Several researchers, including Shamsundar (1982), Charach, Keizman and Sokolov (1991), Zhang and Faghri (1996), Yingqiu, Yinping, Yi and Yanbing (1999), neglected axial conduction in their analysis of TES units due to the complexity it imposes on the problem. However, the effects of axial conduction cannot be neglected in all cases. For instance, in this model, the temperature of the fluid running through the copper tube is a function of the saturation pressure at each finite volume. The pressure drop is computed for each volume. Therefore, as the pressure drops along the length of the tube, so does the temperature. The change in temperature of the fluid causes more energy to be extracted from the PCM or less energy to be absorbed by the PCM. Also, depending upon the mode of operation of the TES unit, when the fluid becomes saturated vapor, during evaporation mode, the fluid commences to increase in temperature for the remainder of the length of the TES unit. This has an effect on the amount of energy extracted along the length of the PCM. It will be shown that Reynolds Number also is a great influence on axial conduction.

### **3.2.2. Two-Phase Flow**

Exact analytical solutions of two-phase flows are not readily achievable. As stated by Hewitt in Kandlikar's text (1999), the interfacial configurations of the two



phases are difficult, and often impossible, to predict. The governing equations can be simplified by averaging over space and/or time. In this study, the flow is considered to be steady and one-dimensional. All dependent variables, whether for liquid or vapor, are constant over a given finite volume and vary only in the axial direction (e.g., bulk temperature of the refrigerant) (Carey, 1992). Therefore, empirical correlations are required for determining the heat transferred from the fluid to the PCM or vice versa. The Separated Flow model is often chosen as the more accurate method to incorporate into a computational model. In the separated flow model, the two phases are considered to be flowing in separated regions and with different velocities; however, the governing equations of the flow are combined (Kandlikar, 1999).

It is assumed that the vapor phase and the liquid phase, in two-phase flow, exist in thermodynamic equilibrium. For a pure substance, this implies that the two phases co-exist at the saturation temperature and that the saturation temperature is a direct function of the saturation pressure. In classical thermodynamics, phase transitions are treated as quasi-equilibrium processes, occurring at the equilibrium saturation conditions of the pure substance (Carey, 1992).

Considering the great importance of the saturation pressure to the study of two-phase flow, it is with great care that the pressure drop is modeled. In doing so, several models were investigated.

**3.2.2.1. Pressure Drop Correlations.** Pressure drop, in two-phase flow, consists of three parts: acceleration (momentum); friction; and, gravity. The horizontal flow in this model makes it possible to neglect the gravitational pressure drop. However, there exist several correlations, established for different flow conditions, to compute each

remaining component of the pressure drop. In one study performed by Seo & Kim, the frictional pressure drop was measured for Refrigerant-22 flowing in a horizontal, copper tube (2000). They recorded data with R-22 at three different temperatures. In an attempt to determine which model to employ in this study, four widely-used correlations for two-phase, friction pressure drop were compared to data obtained by Seo & Kim, as shown in Figures 3.2., 3.3., and 3.4. Those of Chisholm, Chisholm's curve fits of Lockhart and Martinelli's relationships, and Friedel are depicted in Kandlikar's text (1999). Traviss, Rohsenow and Baron's correlation is described in ASHRAE transactions (1973).

Whalley, as mentioned in Kandlikar's text, recommends the following:

For  $\mu_l/\mu_v < 1000$ , the Friedel (1979) correlation should be used.

For  $\mu_l/\mu_v > 1000$  and mass flux  $> 100$ , the Chisholm (1973) correlation should be used.

For  $\mu_l/\mu_v > 1000$  and mass flux  $< 100$ , the Lockhart-Martinelli (1949) correlation should be used.

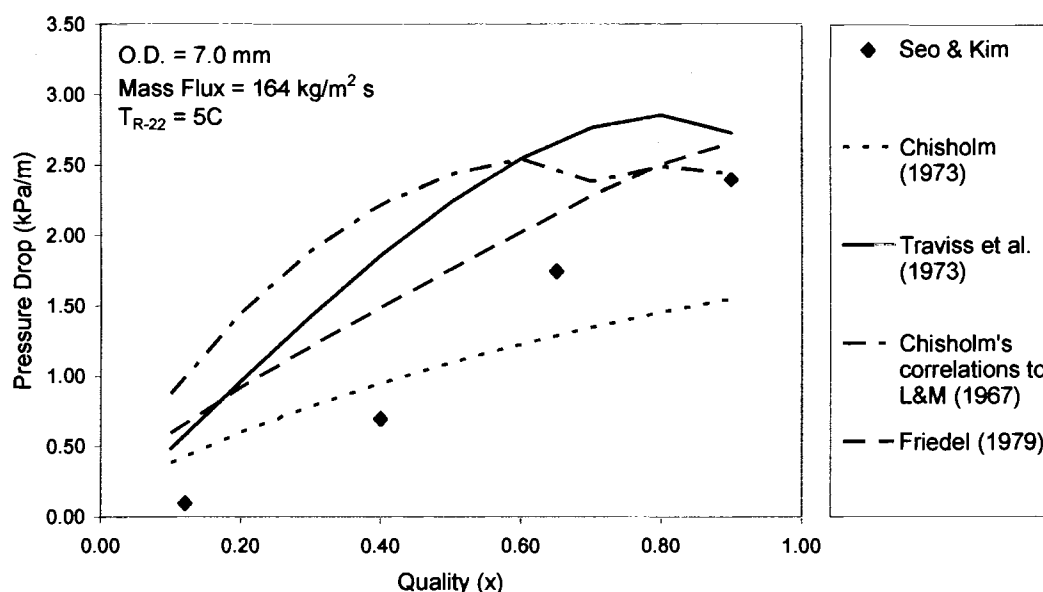


Figure 3.2. Comparison of Frictional Pressure Drop Correlations to Data of Seo & Kim (2000) for R-22 at 5C

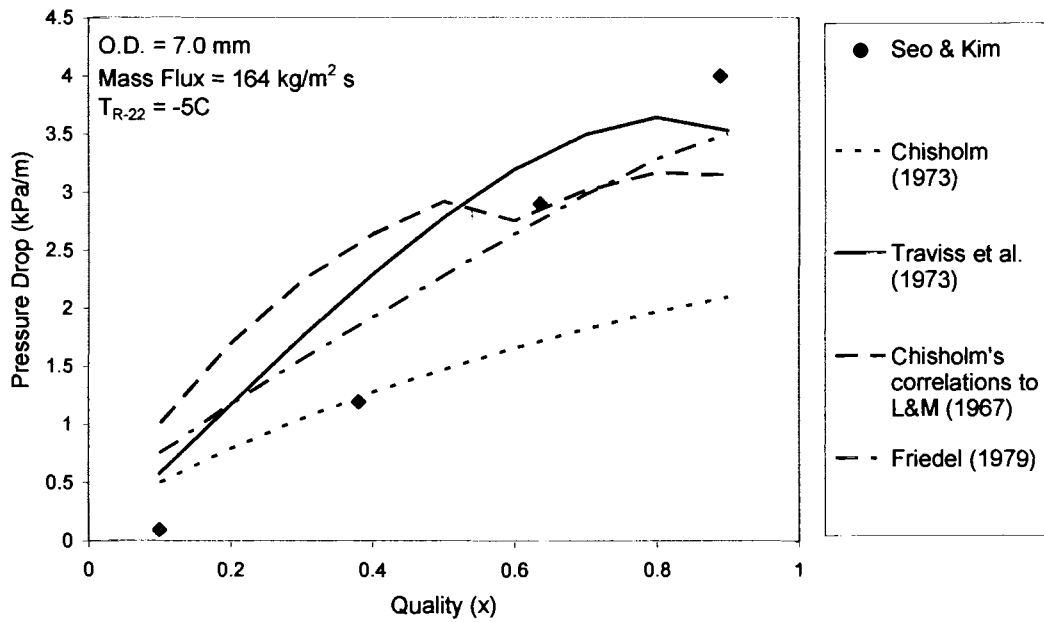


Figure 3.3. Comparison of Frictional Pressure Drop Correlations to Data of Seo & Kim (2000) for R-22 at -5C

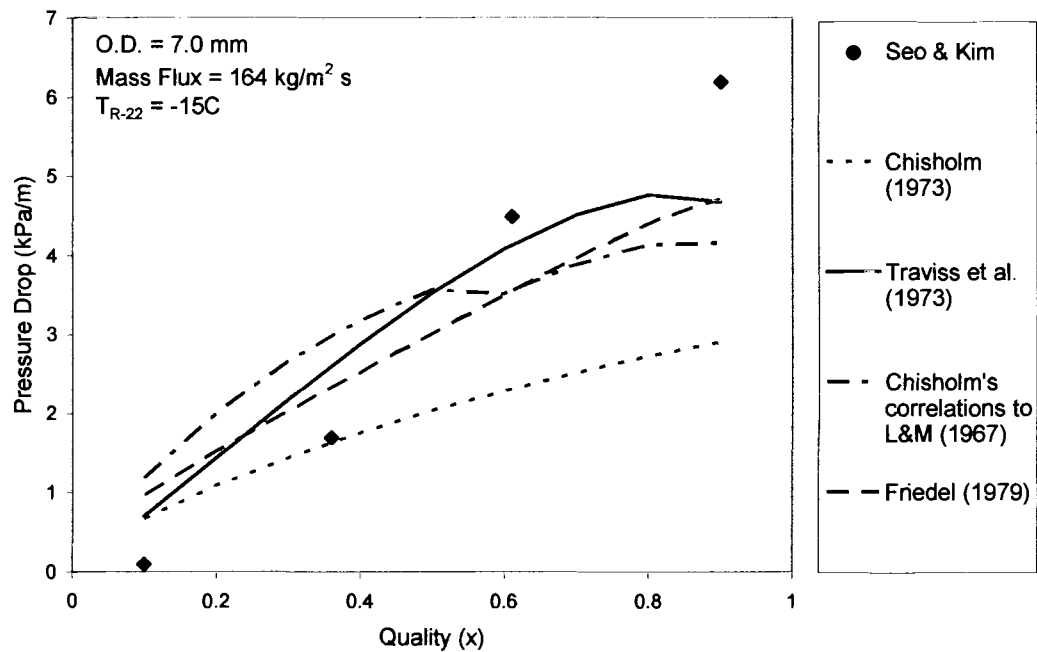


Figure 3.4. Comparison of Frictional Pressure Drop Correlations to Data of Seo & Kim (2000) for R-22 at -15C

It is seen from these figures that:

At  $T = 5^\circ\text{C}$ , the data lay between the Chisholm (1973) and Friedel (1979) correlations.

At  $T = -5^\circ\text{C}$ , the data is closest to Friedel (1979) but with a different slope.

At  $T = -15^\circ\text{C}$ , the data is still closest to Friedel (1979) but, again, with a different slope.

These results were inconclusive; therefore, the momentum pressure drop term was investigated. The Traviss, Rohsenow and Baron model (1973) was compared to the separated-flow model in Kandlikar's text (1999). The total pressure drop for a horizontal tube was then determined from different combinations of the correlations as follows in Table 3.1.

Friction Pressure Drop	Momentum Pressure Drop	Total Pressure Drop (psi/in)
Traviss et al.(1973)	Traviss et al.(1973)	-3.428E-3
Friedel (1979)	Traviss et al.(1973)	-3.611E-3
Friedel (1979)	Separated Flow (1999)	-3.546E-3

Table 3.1. Comparison of Total Pressure Drop

The variables implemented in the above-study were those of Refrigerant-22 at  $-8^\circ\text{C}$  and a mass flux of  $87.2\text{ kg/m}^2\text{s}$ . The combinations resulting in the largest and smallest pressure drops indicate a deviation of only 5%. Therefore, the widely-used Traviss, Rohsenow, and Baron (1973) correlations were implemented in this model.

**3.2.2.2. Two-Phase Heat Transfer Correlation for Evaporation.** The phase change that takes place during evaporation is complex. Evaporation occurs when both the liquid and the vapor are at the saturation condition and the heat provided by the wall

provides the latent heat needed to vaporize the liquid. Two types of boiling occur during this process. At low quality, the nucleate, or pool, boiling has a much greater effect on vaporization than does forced convection. However, the balance of importance of these two methods shifts along the length of the tube. It is important to apply an empirical correlation that characterizes the behavior of these two mechanisms on the particular flow in question. In deciding on a method to implement in this model, several models were investigated.

In 1976, Shah proposed a correlation for flow boiling inside vertical and horizontal tubes. The correlation was specified in graphical form (Carey, 1992). In 1982, he revised his model by implementing computational representation of his chart correlation. Shah's correlation determines the two distinct mechanisms of evaporation, nucleate boiling and forced convection, but the larger of the two contributions is chosen for the heat transfer coefficient. Although his method of predicting heat transfer coefficient compares very well with water, ethylene glycol, and various refrigerants, it is complex and cumbersome to implement.

Gungor and Winterton developed a general correlation for flow boiling inside tubes in 1986. Their correlation was tested against a data bank of over 4300 data points consisting of seven fluids. The mean deviation between their calculated heat transfer coefficient and the experimental data was 21.3% (Gungor & Winterton, 1986). In 1987, these researchers improved upon their correlation, by reducing the number of equations needed to calculate the heat transfer coefficient by more than half, and by increasing the accuracy of their comparison to experimental data to within a mean deviation of only 20.8% (Gungor & Winterton, 1987).

Kandlikar also developed a correlation for saturated flow boiling heat transfer inside horizontal and vertical tubes (1990). His correlation was tested against 10,000 data points consisting of refrigerants, water, and cryogenes. His method is applicable to vapor qualities from 0 to 80%. What is specific about his model is that it requires a fluid-dependent parameter which must be determined for each specific fluid being analyzed.

Since these three correlations are widely used for determining the heat transfer coefficient of a variety of substances, the need to compare them to existing experimental data for R-22, the fluid used in this study, became of prime importance. The three correlations were plotted along with the experimental data obtained by Seo and Kim for R-22 (2000). The results are shown in Figures 3.5. and 3.6. From these figures, it is evident that Gungor and Winterton's correlation is the best fit to Seo and Kim's available data for R-22. To verify that this correlation would be applicable to flow of R-22 at different Reynolds Number, saturation temperature, and heat flux, it was plotted against Seo and Kim's experimental data under these various conditions, as is seen in Figures 3.7., 3.8., and 3.9., respectively. Gungor and Winterton's correlation for local heat transfer coefficient compares very well in all of these cases and is used in this study's numerical model.

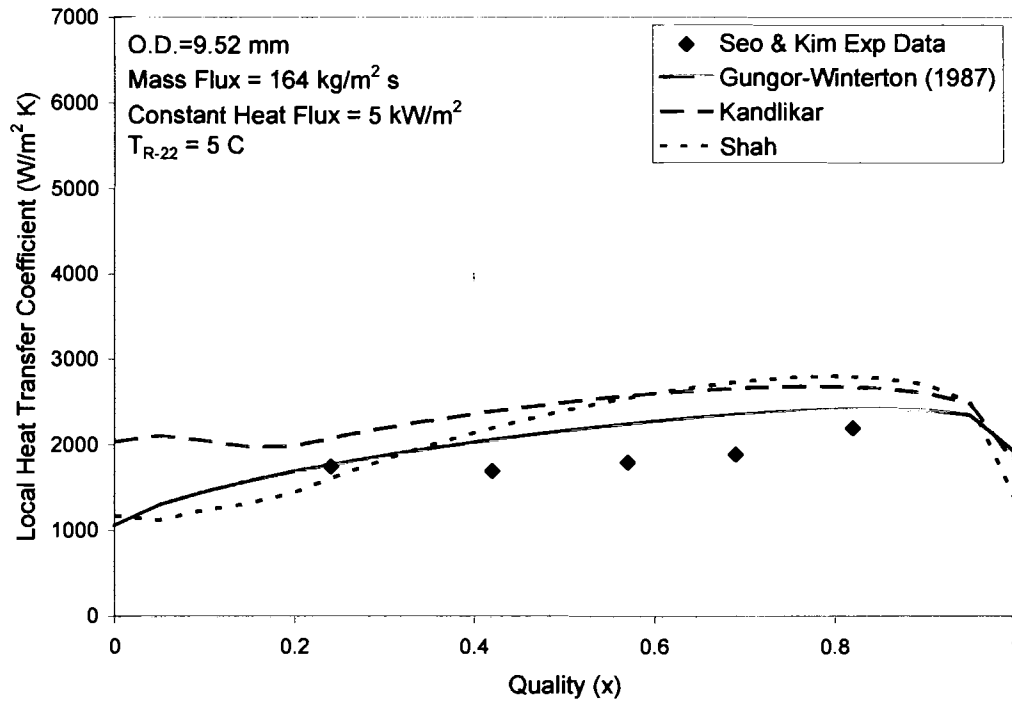


Figure 3.5. Comparison of Heat Transfer Correlations to Data of Seo & Kim (2000) for R-22 in a Tube of O.D.=9.52 mm

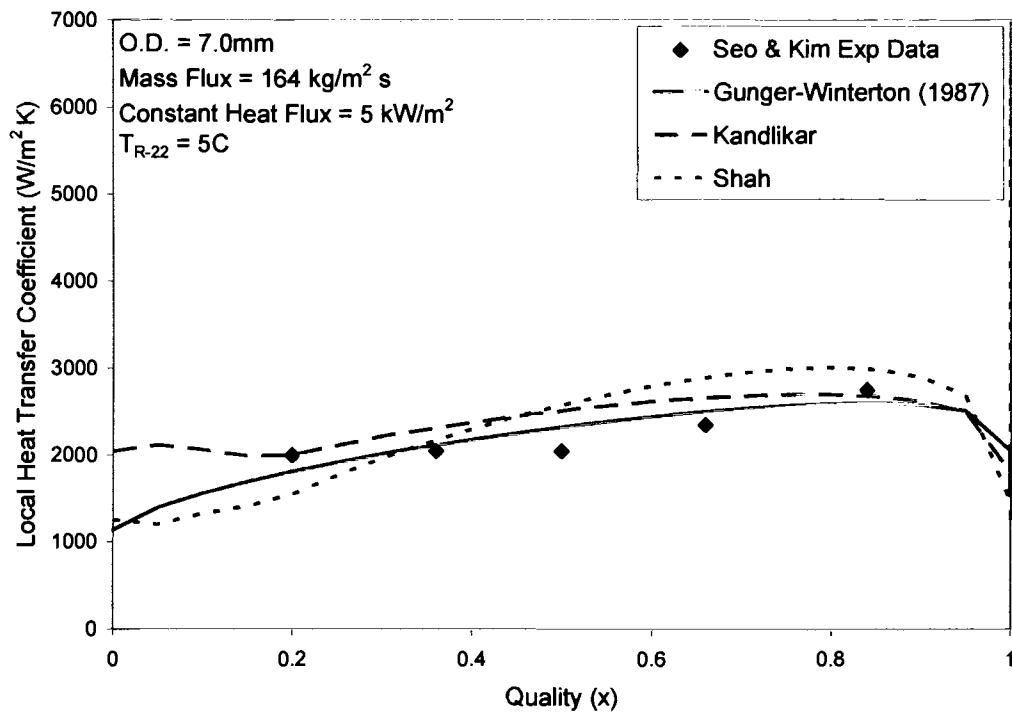


Figure 3.6. Comparison of Heat Transfer Correlations to Data of Seo & Kim (2000) for R-22 in a Tube of O.D.=7.0 mm

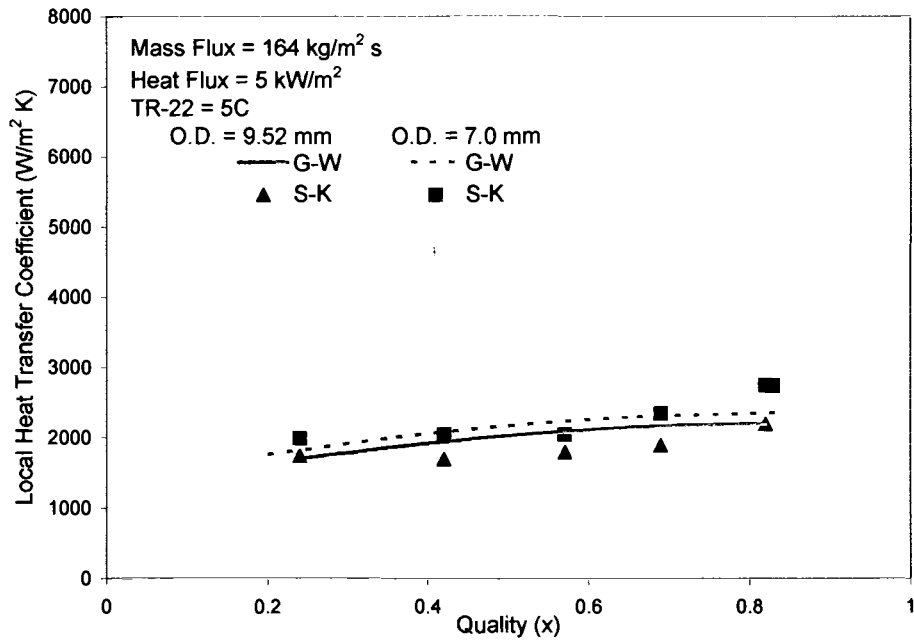


Figure 3.7. Comparison of Gungor-Winterton (1987) to Data of Seo & Kim (2000) for R-22 in a Tube of O.D. of 9.52 and 7.0 mm

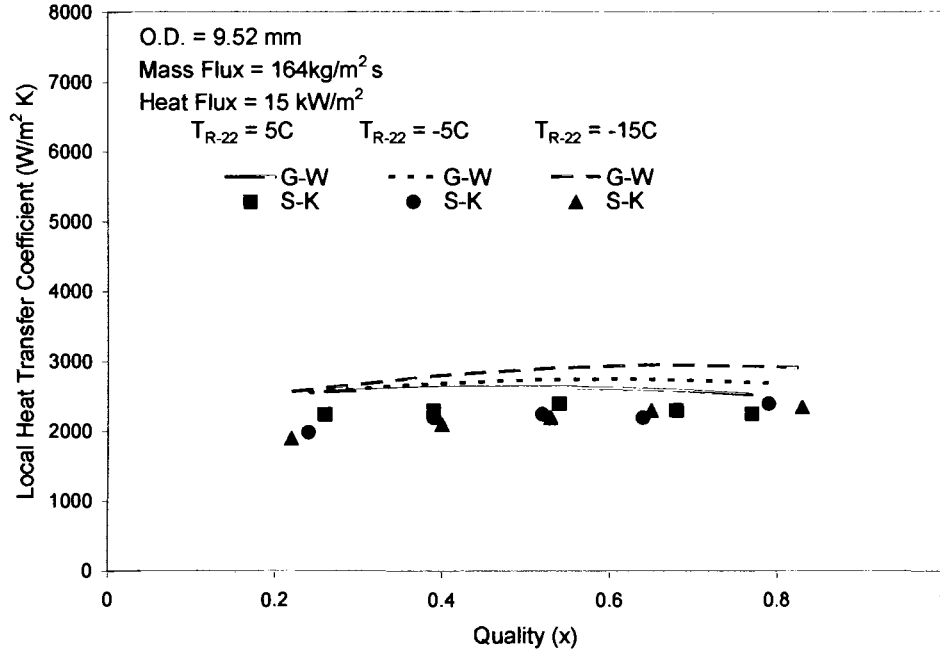


Figure 3.8. Comparison of Gungor-Winterton (1987) to Data of Seo & Kim (2000) for Different Saturation Temperatures, at a Heat Flux of  $15 \text{ kW/m}^2$



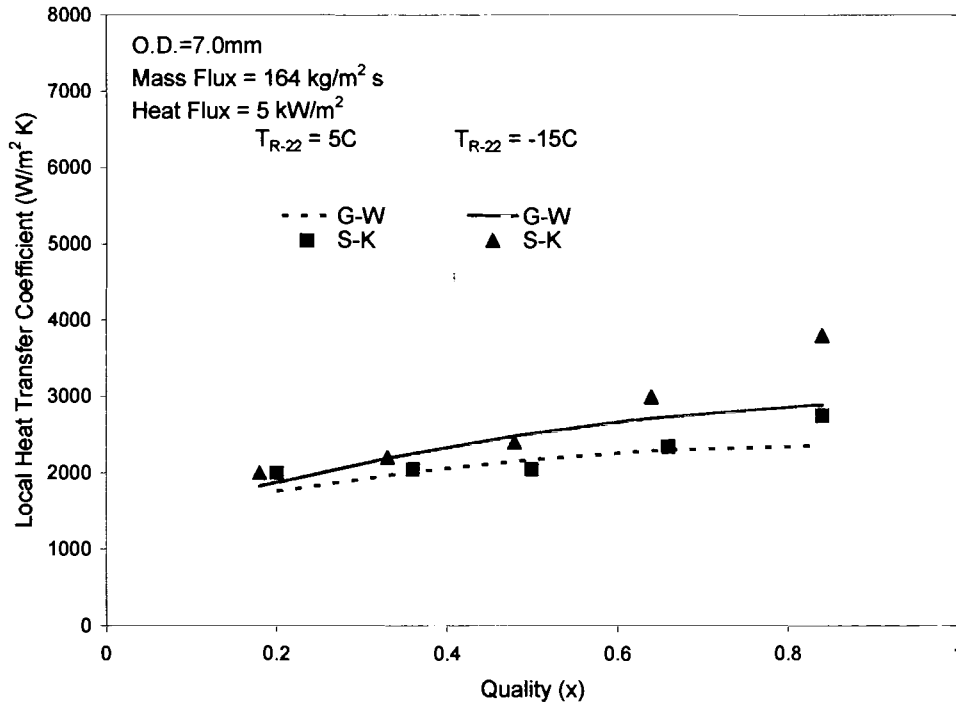


Figure 3.9. Comparison of Gungor-Winterton (1987) to Data of Seo & Kim (2000) for Different Saturation Temperatures, at a Heat Flux of 5 kW/m<sup>2</sup>.

**3.2.2.3. Two-Phase Heat Transfer Correlation for Condensation.** At low vapor velocities, gravitational forces dominate the condensation process and the liquid condensate formed at the top of the horizontal tube flows into a pool at the bottom of the tube. This type of flow is categorized as stratified, or wavy, flow. In this flow regime, the local heat transfer coefficient is largely temperature dependent. The greater the wall-to-refrigerant temperature difference, the bigger the pool of liquid at the bottom of the tube to inhibit heat transfer (Dobson & Chato, 1998). However, at a mass flux of approximately 100 kg/m<sup>2</sup> s, the flow transitions to annular flow which, from experimental evidence, is negligibly affected by temperature difference. Annular flow exhibits a nearly uniform liquid layer all around the inside of the tube, with a vapor core flowing through the center. Three of the more widely used correlations in industry are those of

Shah (1979), Cavallini and Zecchin (1974), and Travis, Rohsenow, and Baron (1973). However, these correlations apply primarily to the annular regime. Dobson and Chato (1998) attempted to develop a correlation that would apply to both the stratified and the annular regimes. In order to select which correlations to incorporate into this model for condensing heat transfer coefficient, the four correlations were plotted against experimental data obtained by Dobson and Chato (1998) for stratified, annular, and transitional flows, as depicted in Figures 3.10., 3.11., and 3.12. It is clear from the plot of flow at  $300 \text{ kg/m}^2 \text{ s}$  and  $650 \text{ kg/m}^2 \text{ s}$  that Shah's correlation is the best fit to the data in the annular flow regime. However, at  $75 \text{ kg/m}^2 \text{ s}$ , all of the correlations underpredicted the heat transfer coefficient for the given parameters. Since, Dobson and Chato have the closest correlation and since stratified flow is not that common in industrial applications,

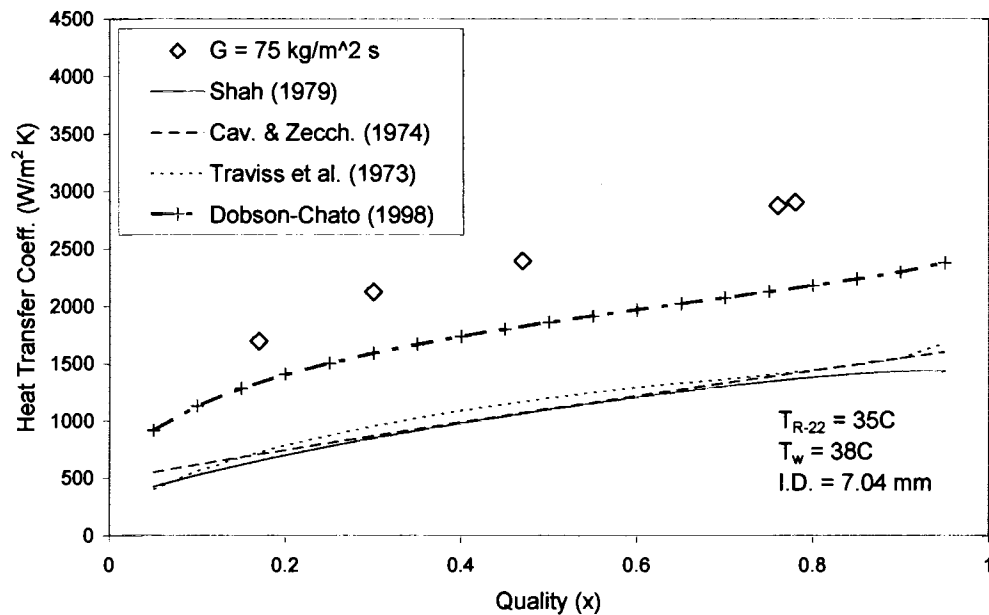


Figure 3.10. Comparison of Four Heat Transfer Correlations for Condensing R-22, at a Mass Flux of  $75 \text{ kg/m}^2 \text{ s}$

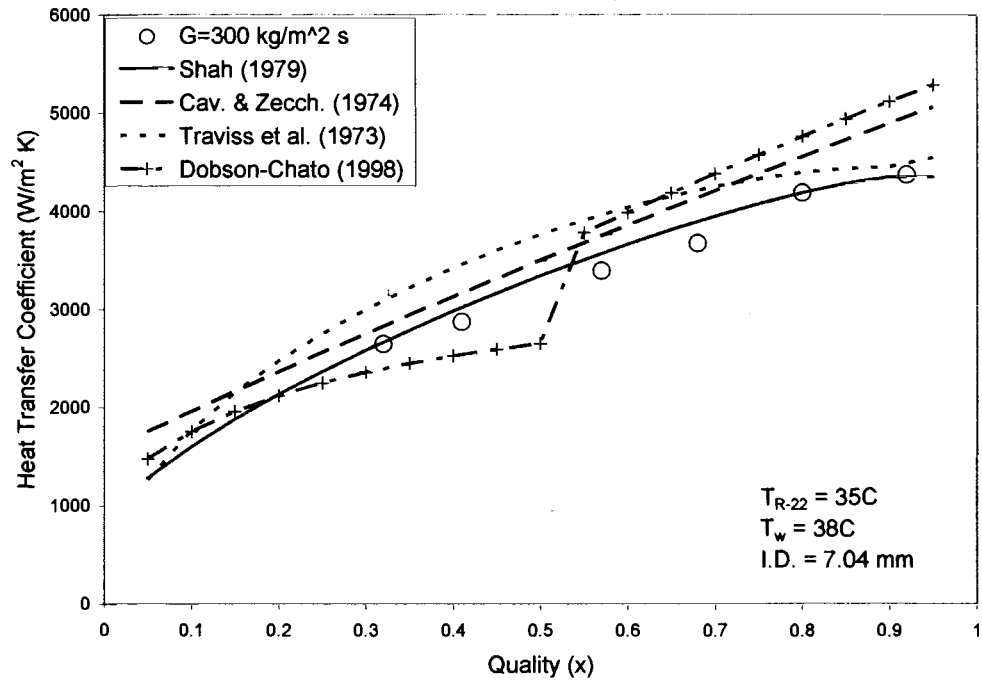


Figure 3.11. Comparison of Four Heat Transfer Correlations for Condensing R-22, at a Mass Flux of  $300 \text{ kg/m}^2 \text{ s}$

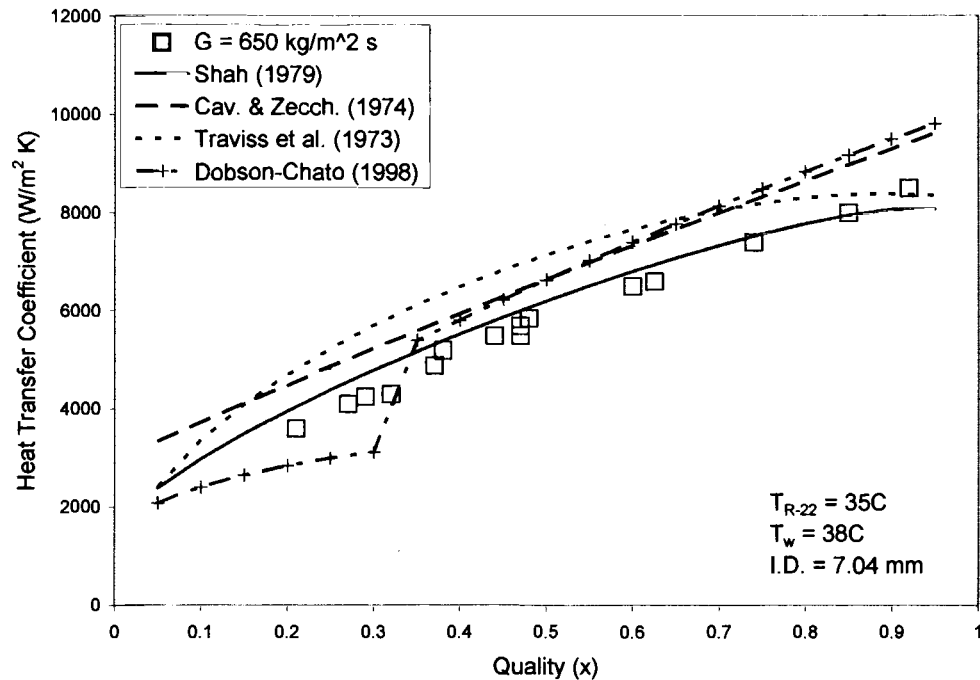


Figure 3.12. Comparison of Four Heat Transfer Correlations for Condensing R-22, at a Mass Flux of  $650 \text{ kg/m}^2 \text{ s}$

because of the low heat transfer associated with it, the stratified portion of Dobson and Chato's correlation is applied to flows less than  $100 \text{ kg/m}^2 \text{ s}$  for the purpose of this numerical model.

### **3.2.3. Single-Phase Flow**

At some point along the length of the TES unit, the fluid becomes 100% vapor, when the TES is used as an evaporator, or 100% liquid, when used as a condenser. For the remaining length of tube, the heat transfer must be computed for single-phase flow. For a circular tube with fully-developed, flow, it is found that Gnielinski's equation for heat transfer coefficient is valid over the range of Prandtl number from 0.5 to 2000, and Reynolds number from 2300 to  $5 \times 10^6$  (Kays & Crawford, 1993). A coefficient of friction is required for this equation. For Reynolds number below  $10^4$ , an expression incorporating D'Arcy's friction factor is applied; equal to or above this value of Reynolds number, Petukhov's friction coefficient is used. The fluid thermophysical properties needed in the afore-mentioned equations are computed as a function of the arithmetic average of the bulk fluid temperature and the wall temperature.

Having selected which theories to apply, the following numerical model was then derived for determining two-dimensional, heat conduction, with conjugate forced convection of two-phase flow, in a horizontal, co-axial TES unit.

## Chapter 4

### MATHEMATICAL MODEL

The energy propagation inside the TES unit is governed by the energy equations, written for the PCM, the copper wall, and the fluid, as described in the following sections.

#### 4.1. Phase Change Material

The PCM is assumed adiabatic at the outer radius,  $r_o$ , and at each end. This is a two-dimensional, cylindrical problem, with axisymmetric solidification/melting of a PCM having a single fusion/melting temperature,  $T_m$ . The thermophysical properties of the PCM are independent of temperature but can be different in the solid and liquid phases. They also have a range of variation over the fusion/melting temperature. The effect of natural convection in the liquid PCM is ignored.

The governing equation and boundary conditions for energy conservation in the PCM are:

$$\rho_p \frac{\partial H}{\partial t} = k_p \left[ \frac{\partial^2 T_p}{\partial r^2} + \frac{1}{r} \frac{\partial T_p}{\partial r} + \frac{\partial^2 T_p}{\partial z^2} \right] \quad (1)$$

At a given time,  $t=0$ , the entire PCM is at a uniform temperature,  $T_o$ .

$$\begin{aligned} T_p(r, z) &= T_o & r_w \leq r \leq r_o & \quad t=0 \\ & & 0 \leq z \leq L & \end{aligned} \quad (2)$$

The adiabatic boundary conditions at the outer wall,  $r_o$ , and at the ends of the TES are represented as:

$$\frac{\partial T_p}{\partial r} = 0 \quad r = r_o \quad t > 0 \quad (3)$$

$$0 \leq z \leq L$$

$$\frac{\partial T_p}{\partial z} = 0 \quad z = 0 \quad \text{and} \quad z = L \quad (4)$$

$$r_w \leq r \leq r_o$$

The inner boundary of the PCM is a convective type boundary condition where all of the energy into/out of the fluid is released from/into the PCM.

$$h(T_f - T_w) = -k_p \frac{\partial T_p}{\partial r} \quad r = r_w \quad (5)$$

$$0 \leq z \leq L$$

The material properties are as follows:

$$\begin{aligned} \text{If the PCM is solid, } T_p(r, z) < T_m, \quad & k_p = k_s \\ & \rho_p = \rho_s \\ & H(r, z) = C p_s [T_p(r, z) - T_m] - LH \end{aligned} \quad (6)$$

$$\begin{aligned}
& k_p = k_w \\
& \text{If the PCM is liquid, } T_p(r, z) > T_m, \quad \rho_p = \rho_w \\
& H(r, z) = C p_w [T_p(r, z) - T_m]
\end{aligned} \tag{7}$$

And, if the PCM is mixed (solid and liquid mixture),  $T_p(r, z) = T_m$ ,

$$k_p = k_w - \frac{H}{LH} (k_s - k_w) \tag{8}$$

$$\rho_p = \rho_w - \frac{H}{LH} (\rho_s - \rho_w)$$

A finite volume approximation is applied to a control volume of the PCM, as shown in

Figure 4.1.

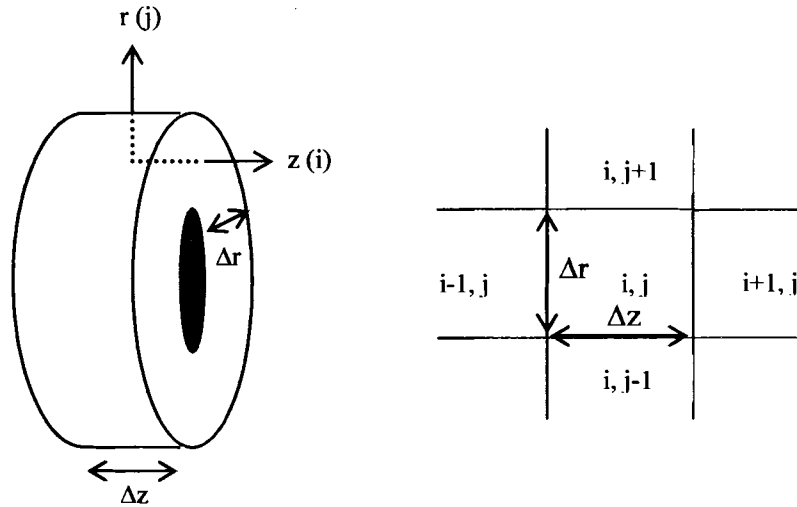


Figure 4.1. Finite volume,  $(\Delta r, \Delta z)$ .

The Enthalpy Method is applied to the governing equation (1).

$$\rho_p V_{i,j} \frac{\partial H_{i,j}}{\partial t} = k_p A_j \frac{\partial T}{\partial r} \Big|_j - k_p A_{j-1} \frac{\partial T}{\partial r} \Big|_{j-1} - k_p A_{i-1} \frac{\partial T}{\partial z} \Big|_{i-1} + k_p A_i \frac{\partial T}{\partial z} \Big|_i \tag{9}$$

where,

$$A_j = 2\pi r_j \Delta z \quad (10a)$$

$$A_{j-1} = 2\pi r_{j-1} \Delta z \quad (10b)$$

$$A_i = A_{i-1} = \pi(r_j^2 - r_{j-1}^2) \Delta z \quad (10c)$$

$$V_{i,j} = \pi(r_j^2 - r_{j-1}^2) \Delta z \quad (10d)$$

Since the finite annular volumes are of even thickness, they are not constant volumes from  $r_w < r < r_o$ . Therefore, we want to weight the material properties, based on volume, in the radial direction. The separate contributions of energy applied to the finite volume approximation are:

Energy through the left boundary:

$$q_{\text{left}} = -\frac{(k_{i-1,j} + k_{i,j})}{2} A_{i-1} \frac{(T_{i-1,j} - T_{i,j})}{\Delta z} \quad (11)$$

Energy through the right boundary:

$$q_{\text{right}} = -\frac{(k_{i,j} + k_{i+1,j})}{2} A_i \frac{(T_{i,j} - T_{i+1,j})}{\Delta z} \quad (12)$$

Energy through the bottom:

$$q_{\text{bottom}} = -\frac{(k_{i,j-1} V_{i,j-1} + k_{i,j} V_{i,j})}{(V_{i,j-1} + V_{i,j})} A_{j-1} \frac{(T_{i,j-1} - T_{i,j})}{\Delta r} \quad (13)$$



Energy through the top:

$$q_{\text{top}} = \frac{(k_{i,j} V_{i,j} + k_{i,j+1} V_{i,j+1})}{(V_{i,j} + V_{i,j+1})} A_j \frac{(T_{i,j} - T_{i,j+1})}{\Delta r} \quad (14)$$

Substituting equations (11)-(14) into the governing energy equation and performing the required differencing to the energy stored term results in:

$$H_{i,j}^{n+1} = H_{i,j}^n + \frac{\Delta t}{\rho_{i,j} V_{i,j}} (q_{\text{left}} + q_{\text{bottom}} - q_{\text{right}} - q_{\text{top}})^n \quad (15)$$

where superscript n+1 is the value at the new time step and superscript n refers to the value at the old time. The first row of finite volumes, immediately adjacent to the refrigerant tube, is treated differently. The copper wall is treated as the j-1 node and ‘q<sub>bottom</sub>’ is the conjugate boundary condition between the refrigerant and the PCM. (See Appendix A.) For stability, when applying an explicit solution technique to a conduction problem in cylindrical coordinates, (Smith, 1985),

$$\frac{k\Delta t}{\rho C_p (\Delta r)^2} + \frac{k\Delta t}{\rho C_p (\Delta z)^2} \leq \frac{1}{2} \quad (16)$$

For a worst case, let k=k<sub>s</sub>, ρ=ρ<sub>s</sub>, and Cp=Cp<sub>s</sub>. Simplifying equation (16), we have the following for the time step in our numerical model.

$$\Delta t = \frac{\rho_s C_{p_s}}{2k_s} \left( \frac{\Delta r^2 \Delta z^2}{\Delta r^2 + 2\Delta z^2} \right) \quad (17)$$

## **4.2. Two-Phase Fluid-Side Heat Transfer and Pressure Drop**

The phase-changing fluid in the copper tube enters the TES unit in either a saturated vapor state, when the TES unit is used as a condenser, or as a liquid whose quality is 3-17% vapor. The temperature of the phase-changing fluid is purely a function of the saturated pressure. Curve fits were established for saturation temperature, as well as for thermophysical properties of R-22, as a function of saturated pressure. The specific equations used may be seen in Appendix A., under 'Subroutine Refrigprops'. These expressions apply only to the range of  $2 \text{ psia} < P_{\text{sat}} < 210 \text{ psia}$  and are accurate to within two percent. The fluid-side tube is a one-dimensional, forced convection problem. The fluid is treated as being fully-developed. The tube is divided into equal lengths,  $\Delta z$ , and the heat transfer coefficient is determined for each constant volume of fluid.

### **4.2.1. Evaporating Heat Transfer Coefficient**

In a phase-changing fluid, it is assumed that the fluid is at saturated conditions and that all of the energy removed from, or released to, the PCM does not affect the fluid temperature. It merely changes the quality of the fluid. The local heat transfer coefficient applied to each control volume of length,  $\Delta z$ , is based on Gungor and Winterton's correlation for saturated flow boiling (1987). This correlation is based on summing the macroconvective (forced convection) contribution and the microconvective (nucleate boiling) contribution. However, the nucleate (pool) boiling term is not clearly visible from the overall expression for the heat transfer coefficient. Gungor and Winterton simplified their 1986 expression by replacing the microconvective term with a

relationship which is a function of the single-phase, liquid heat transfer coefficient and summing it to the expression for forced convection. The result is:

$$h_{tp} = h_l \left[ 1 + 3000Bo^{0.86} + 1.12 \left( \frac{x}{1-x} \right)^{0.75} \left( \frac{\rho_l}{\rho_v} \right)^{0.41} \right] \quad (18)$$

The single-phase, liquid heat transfer coefficient,  $h$  is computed from the well-known Dittus-Boelter equation

$$h_l = 0.023Re_l^{0.8}Pr_l^{0.4} \frac{k_l}{D} \quad (19)$$

where  $Re_l$  is the liquid Reynolds number

$$Re_l = \frac{G(1-x)D}{\mu_l} \quad (20)$$

$Pr_l$ ,  $k_l$ , and  $\mu_l$  are the Prandtl number, thermal conductivity, and viscosity of the liquid.  $D$  is the inner diameter of the copper tube and  $G$  is the mass flux through the tube. The only other values needed in expression (18) are the density ratio of the liquid and vapor, at bulk temperature, the quality of the fluid, and the Boiling number,  $Bo$ . The boiling number is a dimensionless measure of the importance of the generation of vapor in the boiling process (Gungor & Winterton, 1986).

$$Bo = \frac{q}{h_{fg} G} \quad (21)$$

where  $q$  is the heat flux and  $h_{fg}$  is the heat of vaporization of the fluid. For horizontal tubes with Froude number less than 0.05, the right-hand side of equation (18) must be multiplied by a factor to take account of partial wetting of the tube wall. The Froude number is the ratio of inertial force to gravitational force and can be considered a measurement of the wall wetness (Gungor & Winterton, 1987). Therefore, when  $Fr < 0.05$ , equation (18) must be multiplied by the following factor,  $E_2$ .

$$E_2 = Fr_{lo}^{(0.1-2Fr_{lo})} \quad (22)$$

$Fr_{lo}$  is the Froude number of all liquid.

$$Fr_{lo} = \frac{G^2}{\rho_l g_c D} \quad (23)$$

#### 4.2.2. Condensing Heat Transfer Coefficient

The local heat transfer coefficient applied to each control volume of length,  $\Delta z$ , is contingent upon the mass flux of fluid running through the tube. If the mass flux,  $G$ , is greater than or equal to 73730 lb/ft<sup>2</sup>hr, the fluid is considered to be transitioning to annular flow and the Shah (1979) correlation is applied. If the mass flux is less, the stratified flow part of the Dobson and Chato (1998) correlation is used.

Shah has tested his correlation on various fluids, in horizontal, vertical, and inclined pipes of diameters ranging from 7 to 40 mm. He has concluded that his correlation is accurate over the range of reduced pressures from 0.002 to 0.44, vapor velocities from 3 to 300 m/s, vapor qualities from 0 to 100%, liquid Reynolds number from 100 to 63000, and liquid Prandtl number from 1 to 13, and mass flux from 39000 to 758000 kg/m<sup>2</sup>hr. His method was compared to 474 data points and found to have a mean deviation of 15.4% (Shah, 1979). From this researcher's analysis, the lower limit of mass flux in Shah's correlation has been increased for better accuracy. Shah's two-phase heat transfer coefficient for condensing has the following form.

$$h_{tp} = h_L \left[ (1-x)^{0.8} + \frac{3.8x^{0.76}(1-x)^{0.04}}{P_r^{0.38}} \right] \quad (24)$$

The parameter  $P_r$  is the reduced pressure and  $h_L$  is the Dittus-Boelter equation, assuming all the mass flowing as liquid.

$$h_L = 0.023 Re_L^{0.8} Pr_L^{0.4} \frac{k_l}{D} \quad (25)$$

Equation (25) differs from equation (19) in the Reynolds number term.

$$Re_L = \frac{GD}{\mu_l} \quad (26)$$

If, however, the mass flux is less than 73730 lb/ft<sup>2</sup>hr (100 kg/m<sup>2</sup>s), then the stratified flow portion of the Dobson and Chato (1998) correlation is applied.

$$h_{tp} = \frac{k_l}{D} \left\{ \frac{0.23 \text{Re}_{vo}^{0.12}}{1 + 1.11 \chi_{tt}^{0.58}} \left[ \frac{\text{GaPr}_l}{\text{Ja}_l} \right]^{0.25} + \left( 1 - \frac{\theta_l}{\pi} \right) \text{Nu}_{\text{forced}} \right\} \quad (27)$$

where

$$\text{Re}_{vo} = \frac{GD}{\mu_v} \quad (28)$$

Equation (27) represents the two types of heat transfer that take place during stratified flow conditions: film condensation in the upper part of the horizontal tube and forced convective heat transfer in the bottom pool of liquid (Dobson & Chato, 1998). The parameter  $\chi_{tt}$  is the often-used, turbulent-turbulent, Lockhart-Martinelli parameter.

$$\chi_{tt} = \left( \frac{\rho_v}{\rho_l} \right)^{0.5} \left( \frac{\mu_l}{\mu_v} \right)^{0.1} \left( \frac{(1-x)}{x} \right)^{0.9} \quad (29)$$

Ga and  $\text{Ja}_l$  are the Galileo number and the liquid Jakob number, respectively.

$$\text{Ga} = \frac{g_c \rho_l (\rho_l - \rho_v) D^3}{\mu_l^2} \quad (30)$$

$$Ja_1 = \frac{C_{p,l}(T_{sat} - T_w)}{h_{fg}} \quad (31)$$

The angle which is formed by extending an imaginary line from the top of the tube to the liquid level in the bottom of the horizontal tube is represented as  $\theta_1$  in equation (27) and is geometrically related to the void fraction,  $\alpha$ , of Zivi (1964). The void fraction,  $\alpha$ , represents the ratio of the vapor-flow cross-sectional area of the tube to the total cross-sectional area.

$$\alpha = \frac{\theta_1}{\pi} - \frac{\sin(2\theta_1)}{2\pi} \quad (32)$$

However, since this would require solving a transcendental equation which would be challenging to model numerically, Jaster and Kosky (1976) approximated this relationship as

$$\frac{\theta_1}{\pi} = 1 - \frac{\arccos(2\alpha - 1)}{\pi}. \quad (33)$$

The forced-convective Nusselt number, in equation (27), is represented as follows:

$$Nu_{forced} = 0.0195 Re_l^{0.8} Pr_l^{0.4} \phi_1(\chi_{tt}) \quad (34)$$

$$\phi_1(\chi_{tt}) = \sqrt{1.376 + \frac{c_1}{\chi_{tt}^{c_2}}}. \quad (35)$$

If  $0 < Fr_{lo} \leq 0.7$ ,

$$c_1 = 4.172 + 5.48Fr_{lo} - 1.564Fr_{lo}^2 \quad (36a)$$

$$c_2 = 1.773 - 0.169Fr_{lo} \quad (36b)$$

If  $Fr_{lo} > 0.7$ ,

$$c_1 = 7.242 \quad (37a)$$

$$c_2 = 1.655 \quad (37b)$$

#### 4.2.3. Two-Phase Pressure Drop

Accurate computation of the pressure drop is especially important in two-phase flow heat transfer calculations because the saturation temperature of the fluid, and all of its thermophysical properties, are computed as a function of the saturation pressure. The method accepted and used by industry is the Traviss, Rohsenow, and Baron (1973) technique. The pressure drop due to friction is represented as:

$$\left( \frac{\Delta P}{\Delta z} \right)_f = -0.09 \left( 1 + 2.85\chi_{tt}^{0.523} \right)^2 \frac{\mu_v^{0.2} (Gx)^{1.8}}{g_c \rho_v D^{1.2}} \quad (38)$$



The momentum pressure drop has the following relationship:

$$\left(\frac{\Delta P}{\Delta z}\right)_{mo} = -\frac{G^2}{g_c \rho_v} \frac{\Delta x}{\Delta z} \left[ 2x + (1-2x) \left(\frac{\rho_v}{\rho_l}\right)^{\frac{1}{3}} + (1-2x) \left(\frac{\rho_v}{\rho_l}\right)^{\frac{2}{3}} - (2-2x) \left(\frac{\rho_v}{\rho_l}\right) \right] \quad (39)$$

The term  $\Delta x/\Delta z$  in equation (39) is representative of the change in quality of the fluid per cell increment. This is determined from an energy balance over a cell of length,  $dz$ .

When condensing, this is

$$\frac{\Delta x}{\Delta z} = \frac{4h_{tp}(T_{sat} - T_w)}{G h_{fg} D} \quad (40a)$$

When evaporating,

$$\frac{\Delta x}{\Delta z} = \frac{4h_{tp}(T_w - T_{sat})}{G h_{fg} D} \quad (40b)$$

The representation of the gravitational term, although not applicable to this study because of horizontal flow, may be viewed in the same source (Traviss, Rohsenow, & Baron, 1973).

### 4.3. Single-Phase Fluid-Side Heat Transfer and Pressure Drop

The temperature of the single-phase fluid is modeled as steady-state, fully-developed flow. The heat transfer coefficient is modeled through an empirical correlation, as is the pressure drop through the tube. The refrigerant properties are determined as a function of an arithmetic average of the refrigerant and wall temperatures. Upon solving for the heat transfer coefficient, the heat flux through the copper wall is computed. The wall temperature is then determined. If the wall temperature is not what was estimated when solving for the refrigerant properties, to within a designated tolerance, the heat transfer coefficient is solved for again. This iteration takes place until the desired tolerance is met. The differential equation for the local bulk mean temperature of the fluid is then derived by an energy balance on the fluid flowing through the tube:

$$T_{f,i+1} = T_{f,i} + \frac{4 \Delta z h_i}{\rho v D C_p} (T_{w,i} - T_{f,i}). \quad (41)$$

The single-phase heat transfer coefficient,  $h_i$ , is computed according to Gnielinski (1976) from a text by Kays and Crawford (1993). This correlation is valid over the range of  $0.5 < Pr < 2000$  and  $2300 < Re < 5e+06$ , which adequately covers the range of applicability for industrial use.

$$h_i = \frac{k}{D} \left[ \frac{(Re - 1000) Pr^{1/4} c_f / 2}{1 + 12.7 \sqrt{c_f / 2} \left( Pr^{2/3} - 1 \right)} \right] \quad (42)$$

If  $Re < 10000$ , the coefficient of friction is determined using the method of D'Arcy for laminar flow (Kays & Crawford, 1993).

$$c_f = \frac{16}{Re} \quad (43)$$

If the flow is turbulent, Petukhov's friction coefficient is applied (Kays & Crawford, 1993).

$$c_f = 2(2.236 \ln(Re) - 4.639)^{-2} \quad (44)$$

Applying the summation of forces over a control volume of fluid in the pipe, we obtain the pressure drop equations for single-phase flow. The equations apply to fully developed, laminar or turbulent flow, as long as it is understood that in turbulent flow the shear stress is an apparent shear stress that is the combination of the viscous stress and the apparent turbulent shear stress (Kays & Crawford, 1993).

$$\left( \frac{\Delta P}{\Delta z} \right) = \frac{-f G^2}{2g_c D \rho} \quad (45)$$

In equation (45),  $f$  is the friction factor and is dependent upon Reynolds number.

If  $Re \leq 10000$ ,

$$f = \frac{64}{Re}. \quad (46a)$$

Otherwise,

$$f = 0.3164 Re^{-0.25} \quad (46b)$$

Equations (42-46b) are quality dependent and are determined for either vapor or liquid, depending on the subroutine.

#### **4.4. Numerical Procedure**

The program “Ice Bank Model” which is attached hereto as Appendix A., is a computer model for the two-dimensional, heat conduction, problem in a TES unit, with conjugate forced convection of a two-phase fluid at its inner boundary. It is written specifically to model the freezing/melting of ice as a PCM and Refrigerant-22 as the two-phase fluid. However, the only modifications that would be required to make this applicable to other substances would be to change the subroutine REFRIGPROPS to contain curve fit equations for the thermophysical properties of another two-phase fluid that was tested and compared to Gungor and Winterton’s (1987) evaporating correlation, and to Shah (1979) and Dobson and Chato’s (1998) condensing correlations. The other

modification would be to change the properties in subroutine ICEBANKPROPS to contain material properties for the PCM being modeled.

The program was written in Fortran and compiled with Microsoft Fortran PowerStation. It begins by letting the user select in which units he/she would like to obtain results, U.S. units, or S.I. units.<sup>1</sup> The user is then asked to select in which mode he/she would like to operate the program. Mode 1 runs the program in condensing mode, mode 2 in evaporating mode, and mode 3 in start-up mode which always begins with evaporating but is used when alternating between evaporating and condensing. The ice needs to be created before it can be melted. The next choice is to select whether you want to run the program in only one mode for a given period of time or alternate between modes, whose times will be specified in subroutine VARIABLEPROPS. It then calls the subroutine VARIABLEPROPS where the user is allowed to set the saturation pressure for condensing and/or evaporating, set the flow rate for condensing and/or evaporating (i.e., The program can be run in alternating mode, at different flow rates for each mode.), inner diameter of fluid tube, outer diameter of fluid tube, outer diameter of PCM, initial wall temperature, length, time limit on condensing mode, time limit on evaporating mode, time limit on start-up mode, and total time. Total time must be a summation of all the time limits, over however many cycles are desired.

The program sets initial conditions for the fluid tube as well as the PCM, based on the variable properties already set by the user in VARIABLEPROPS. It then begins by calling the CONDENSING or EVAPORATING subroutine where the entering quality must be set by the user (e.g., 0.15 for evaporation; 0.999 for condensing -- The condensing subroutine will not permit beginning with 1.0 for quality.).

In subroutine EVAPORATING, the two-phase heat-transfer correlation will only be applied while the vapor quality is less than 100%, the parameter  $z$  is less than the given length of the tube, and the time counter is less than the end time designated in subroutine VARIABLEPROPS. The Gungor and Winterton heat transfer correlation is iterative, based on making an initial guess of the heat flux (which the user does in VARIABLEPROPS). Upon obtaining the value of the local heat transfer coefficient, the wall temperature is computed. The heat flux is then calculated based upon the new value of wall temperature. If this new value of heat flux has not converged to within a designated tolerance with the old value, the new value becomes the old value and the iteration continues. If, however, the value of heat flux has converged, the change in quality of the fluid is computed. The program continues on to determine the pressure drop for that particular cell. It then updates the saturation pressure to reflect the pressure drop, moves onto the next cell, and updates all of the fluid properties as a function of saturation pressure, in subroutine REFRIGPROPS.

If the quality reaches 100% vapor before the tube length or the time limit have been reached, the program moves onto to the All-Vapor zone where it continues to compute heat transfer with the Gnielinski correlation. In the All-Vapor zone, the fluid properties are dependent upon the arithmetic average of the bulk fluid temperature and the wall temperature. The heat transfer coefficient is determined and an energy balance is performed to determine the wall temperature. If the updated wall temperature has not converged to within a given tolerance, the new wall temperature becomes the old wall temperature and the iteration continues. If the wall temperature has converged, the program moves onto the pressure-drop equations for all-vapor flow. The fluid

temperature of the next cell is then computed through an energy balance between cells. This continues until  $z$  has reached the designated length of tube or the time counter has reached the designated time limit for evaporating.

Normally, the program returns to the main program and proceeds to the transient, two-dimensional, conduction problem in the PCM. However, at this point, the CONDENSING subroutine will next be described.

In subroutine CONDENSING, the two-phase heat-transfer correlation will only be applied while the vapor quality is greater than 0%, the parameter  $z$  is less than the given length of the tube, and the time counter is less than the end time designated in subroutine VARIABLEPROPS. If the mass flux is greater than or equal to  $73730 \text{ lb/ft}^2\text{hr}$  ( $100 \text{ kg/m}^2\text{s}$ ), the program jumps ahead to the Shah correlation for determining the two-phase heat transfer coefficient. The Shah correlation applies to annular flow where there is very little dependence on wall temperature. Therefore, upon computing the heat transfer coefficient, the new wall temperature is determined. Next the quality change is found by applying an energy balance on a finite volume of fluid. The pressure drop is then computed, similarly to that in subroutine EVAPORATING. The program proceeds on to the next cell and updates the fluid properties as a function of the newly computed saturation pressure by calling subroutine REFRIGPROPS. If the vapor quality has reached 0% before the end of the tube is seen or the designated time has expired, the subroutine continues on to the All-Liquid zone.

If the mass flux is less than  $73730 \text{ lb/ft}^2\text{hr}$  ( $100 \text{ kg/m}^2\text{s}$ ) at the start of CONDENSING, the Dobson and Chato correlation for two-phase heat transfer coefficient is applied. The heat transfer coefficient in stratified flow is temperature dependent.

Therefore, upon computing the heat transfer coefficient, the wall temperature is determined. If the wall temperature has not converged to within a given tolerance, the program returns to the beginning of Dobson and Chato's calculations and continues to iterate until convergence is achieved. When this happens, the fluid's quality change is computed and the pressure drop for that given cell is found by the Traviss, Rohsenow, and Baron (1973) equations. The program then proceeds to the next cell and updates the refrigerant properties as a function of saturation pressure. If the quality reaches 0% vapor before the tube length or the time limit have been reached, the program moves on to the All-Liquid zone where it continues to compute heat transfer with the Gnielinski correlation, as described in the section on evaporating.

This continues until  $z$  has reached the designated length of tube or the time counter has reached the designated time limit for condensing. At which time, the program proceeds to the transient heat conduction problem in the PCM.

In the main part of the program, the transient heat transfer in the PCM, the time step is first computed, based on the criterion that will keep this explicit solution stable. The boundary conditions are updated to insure insulated boundaries at the outer radius of the PCM and at each end of the TES unit. The material properties are updated for each finite volume, based on the quality of the cell (i.e., solid, liquid, or mixed). The enthalpy method is then applied to the first row of finite volumes, the row which computes its temperature as a function of an energy balance with the temperature of the fluid in the tube and the wall temperature of the copper. The program then proceeds to compute the enthalpy of each remaining finite volume. The quality and temperature of each volume is determined as a function of its newly computed enthalpy. The new values are then placed



in old arrays for the next iteration at the next time step. If the limiting value of the time counter has not been reached, the program calls either subroutine EVAPORATING or CONDENSING based on choices made by the user at the start of the program.

Samples of the output may be seen in Appendix B., for fluid-side output, and Appendix C. for PCM-side output. The output for the PCM may be imported into a graphics software package where the data may be displayed as profiles of temperature contours within the PCM. An example of such may be seen in Figure 4.2. The plots are the result of having run the program only once, in which the water (PCM) is initially at 70°F. The refrigerant, initially at 57.6psia, flows at 30 lbm/hr for 48 minutes. The program, still in the same run, switches over to condensing mode, flowing refrigerant at 160psia at rate of 26 lbm/hr for 15 minutes. It then returns to evaporating mode, flowing refrigerant at 57.6psia, at a rate of 28 lbm/hr for 21 minutes. The program continues cycling between condensing mode and evaporating mode for the duration of the given time limit.

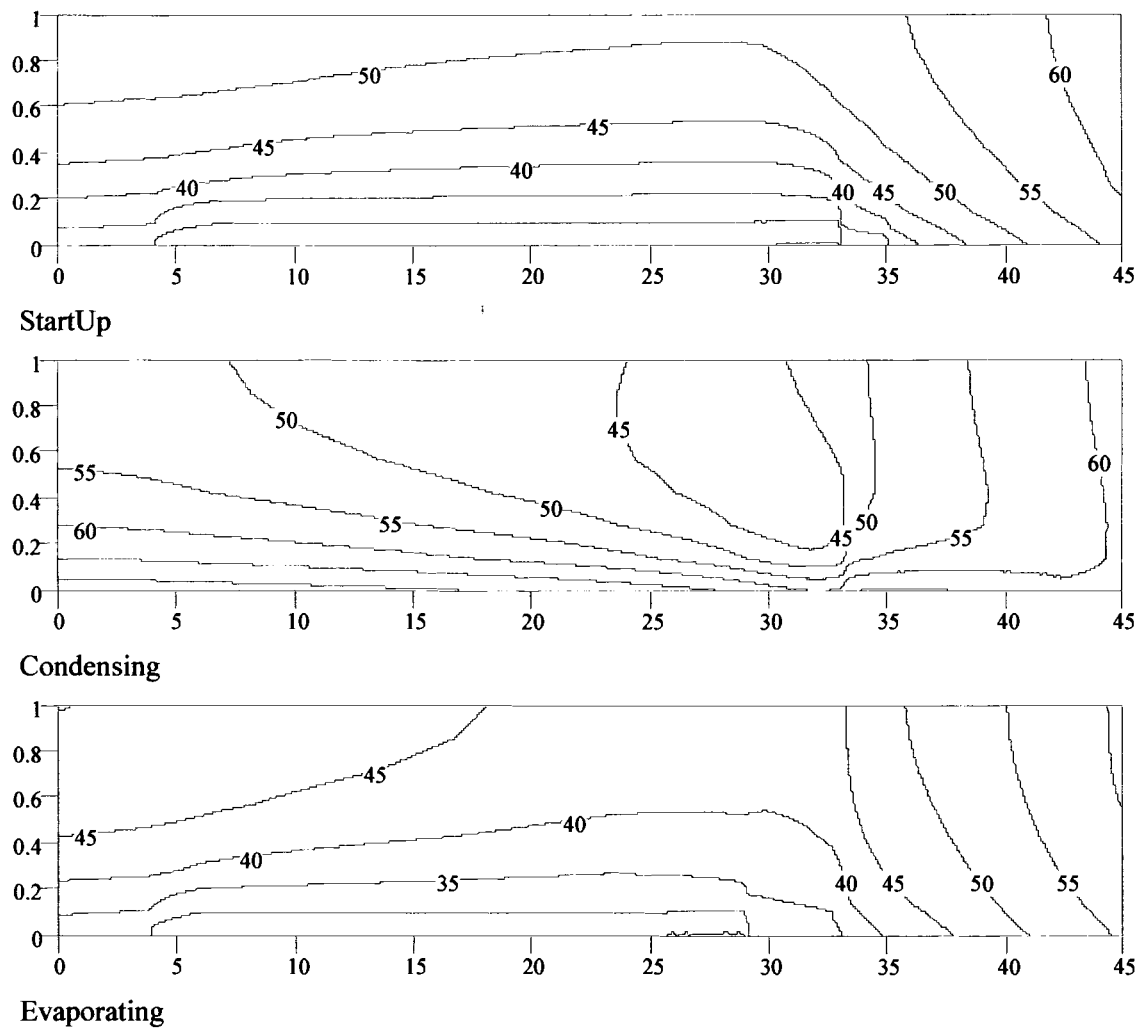


Figure 4.2. Axisymmetric Cross-Section of Isotherms of Sample Output (Length = 45ft. and thickness = 1in.)

## **Chapter 5**

### **EXPERIMENTAL APPARATUS AND PROCEDURE**

#### **5.1. Description of Apparatus**

The testing reported here was performed on a thermal energy storage (TES) unit designed and assembled at the University of Maine, Crosby Laboratory. The TES system uses refrigerant-22 as the two-phase fluid and water as the phase change material (PCM). The apparatus consists of three major loops, Figure 5.1.,: 1) a tap water flow path to remove excess heat from the refrigerant loop; 2) a closed brine loop to cycle energy between the auxiliary condenser and the auxiliary evaporator; and, 3) a closed refrigerant loop which contains a main loop but also releases some refrigerant to the ice-bank loop when performing as condenser or evaporator. The purpose of the test is to validate the numerical model of heat transfer between PCM and phase changing fluid.

##### **5.1.1. Tap Water Flow Path**

Tap water flows through a water flow regulating valve into a five-gallon plastic pail. The water flow is regulated by refrigerant condensing pressure by means of a sensor which is mounted in the condensed liquid refrigerant line and connected to the valve's regulating mechanism. The valve automatically opens slightly on refrigerant pressure increase and closes slightly on pressure decrease to maintain an essentially constant refrigerant condensing pressure and temperature. The water exits the pail by gravity driven forces, through a hose attached to the side of the pail. A mixer was added to the

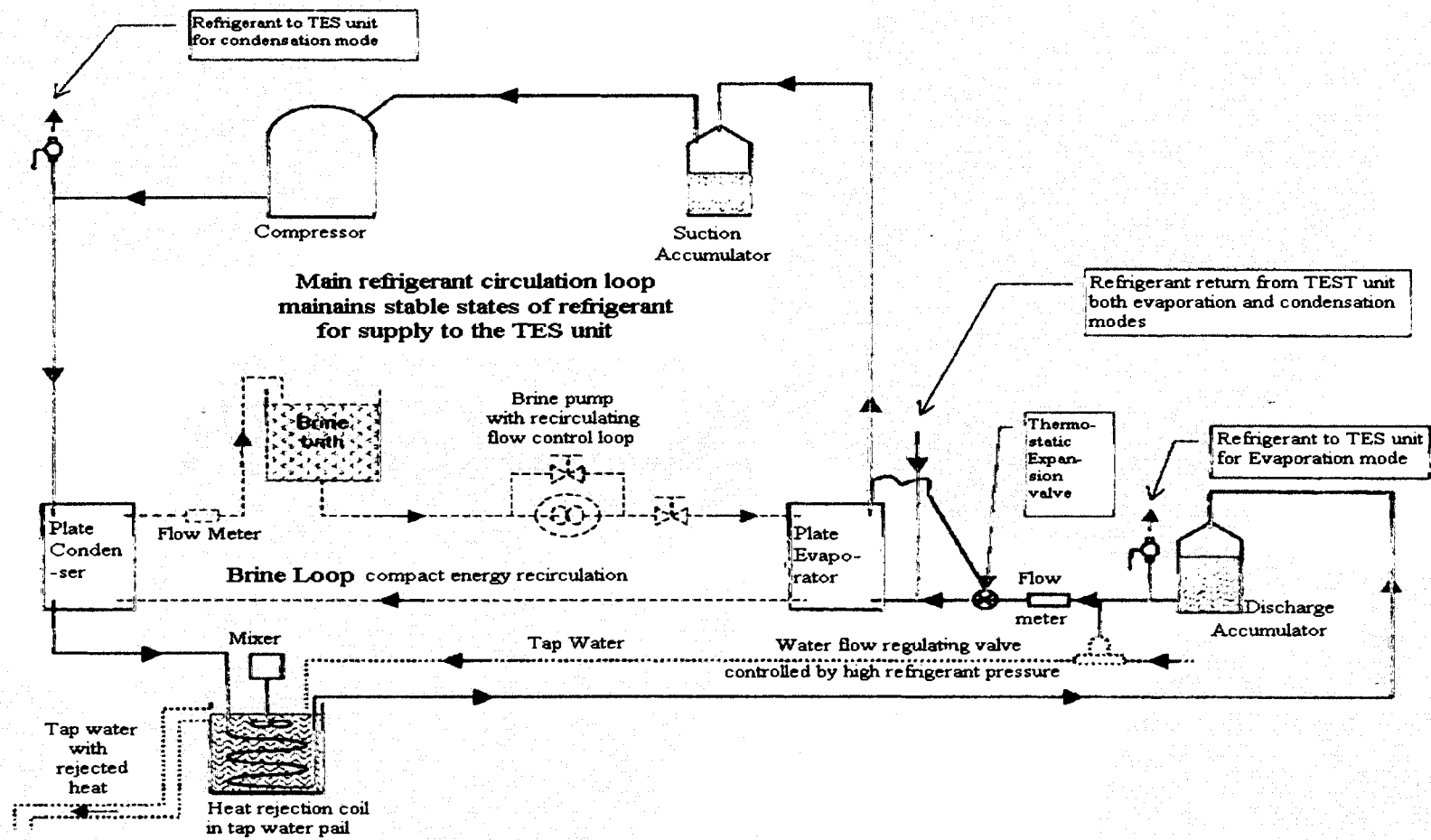


Figure 5.1. Schematic of Test Apparatus

pail to increase forced convection. The water bath, with mixer, is shown in Figure 5.2., along with the compressor and discharge accumulator. The purpose of the water flow path is to reject the energy added to the refrigerant by the compressor so that the main refrigerant loop can operate continuously as a cycle.

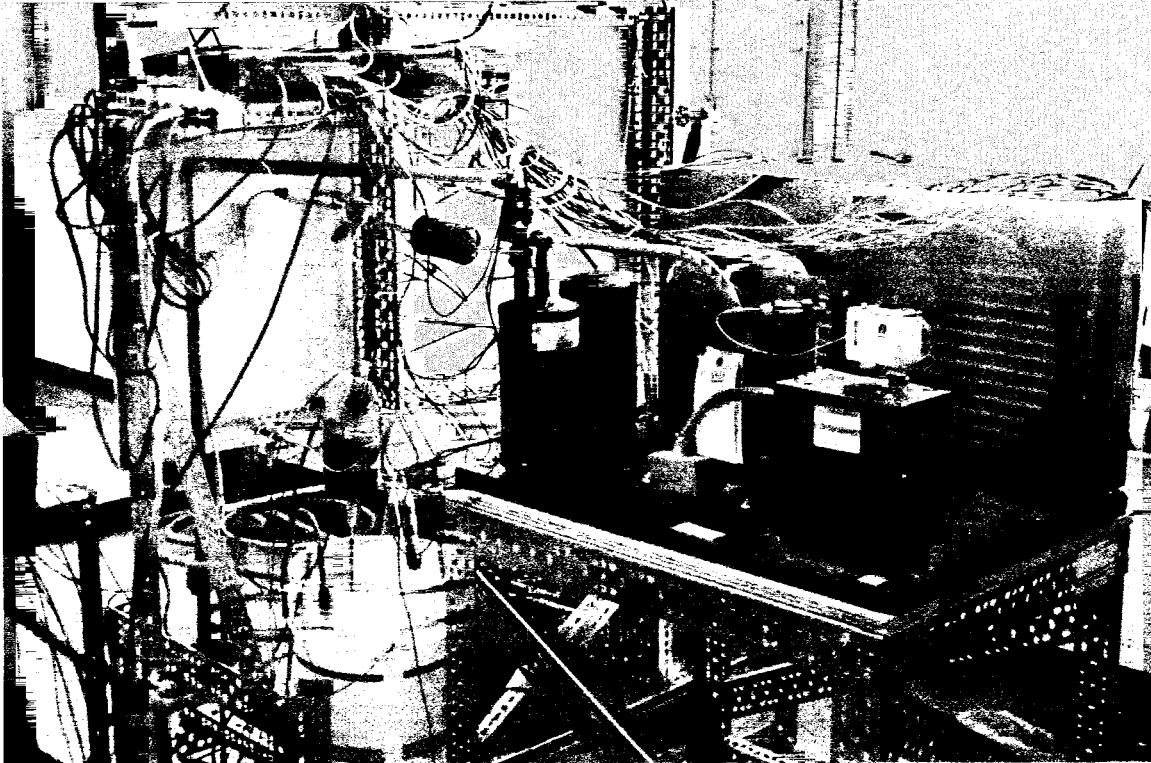


Figure 5.2. View of Water Bath, Compressor and Discharge Accumulator

### 5.1.2. Brine Loop

The brine solution is equal weights of water and antifreeze. It is pumped from an open reservoir in a five-gallon plastic pail, by a positive displacement pump with a recirculating flow loop, through the main refrigerant loop's plate evaporator, to the main refrigerant loop's plate condenser, through a flowmeter, and back to the plastic pail. The brine solution recycles the energy removed from the refrigerant in the plate condenser back into the refrigerant in the plate evaporator.

When the ice-bank is functioning as a condenser, the refrigerant entering the ice-bank must be pre-cooled from a super-heated gas which has just exited the compressor to a state closer to saturated vapor, at approximately 60-80 F. Upon leaving the ice-bank, the refrigerant should be sub-cooled to ensure that the vapor has been totally condensed prior to flowing through the flow meter. However, in the early stages of condensing, the refrigerant could exit the ice-bank at a temperature below freezing. Therefore, the R-22 would require being heated in order to prevent the flow meter from icing. The exchange of energy takes place in the brine bath which is part of the brine loop.

### 5.1.3. Refrigerant Loop

The main refrigerant loop consists of a compressor and the auxiliary condenser and evaporator mentioned in the previous two sections. In order to provide saturated vapor refrigerant to the ice-bank for condensing, or nearly saturated liquid to the ice-bank for evaporating, the main refrigerant loop must be able to operate at stable conditions. The desired conditions are listed in Table 5.1.

State Location	T (F)	P (psia)	h (Btu/lbm)	x (quality)	$\rho$ (lbm/ft <sup>3</sup> )
Compressor exit	162	211	125.0	1.00	3.33
Brine loop condenser exit	100	211	54.0	0.20	16.129
Tap water condenser exit	85	211	33.0	0.00	71.429
Evaporator exit	22	40	108.0	1.00	0.7142

Table 5.1. Refrigerant States in Main Refrigeration Loop

## 5.2. Operation of the PCM and Phase-Changing Fluid as an Ice-Bank

The PCM is able to function as an evaporator or condenser. The refrigerant flows through copper tubing, Type L,  $\frac{1}{4}$ " nominal diameter. The copper tubing runs through the center of 2  $\frac{1}{2}$ " nominal diameter, Schedule 40, PVC pipe, approximately 43 feet in length. The gap in the annulus, formed by the PVC, is filled with water, initially at room temperature. The PVC pipe is wrapped in 1 inch of Imcolock engineered polymer foam insulation. Calculations of heat transfer through the PVC pipe and insulation, based on testing conditions, result in a maximum of 7% energy loss/gain at peak conditions of heat transfer, which enable the outer boundary of the PCM to be modeled as adiabatic.

A series of twenty, Omega, copper-constantan temperature probes were placed at different axial and radial locations along the ice-bank, as shown in Figure 5.3. and 5.4.

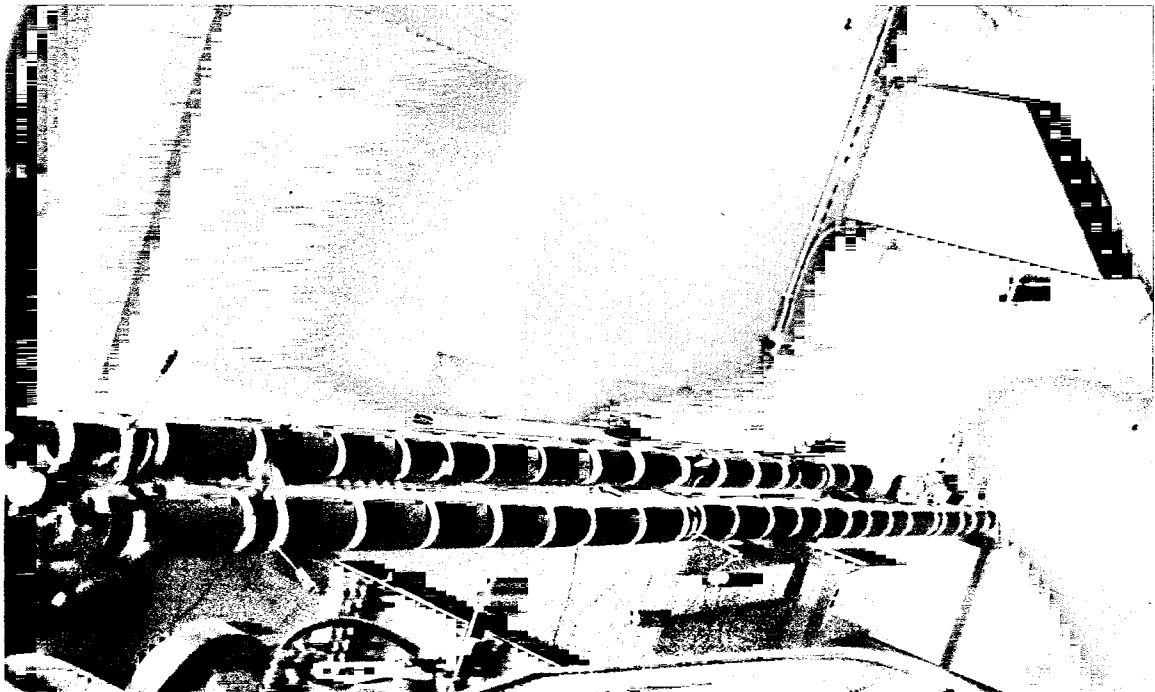


Figure 5.3. Ice-Bank with Temperature Probes at Various Axial Locations

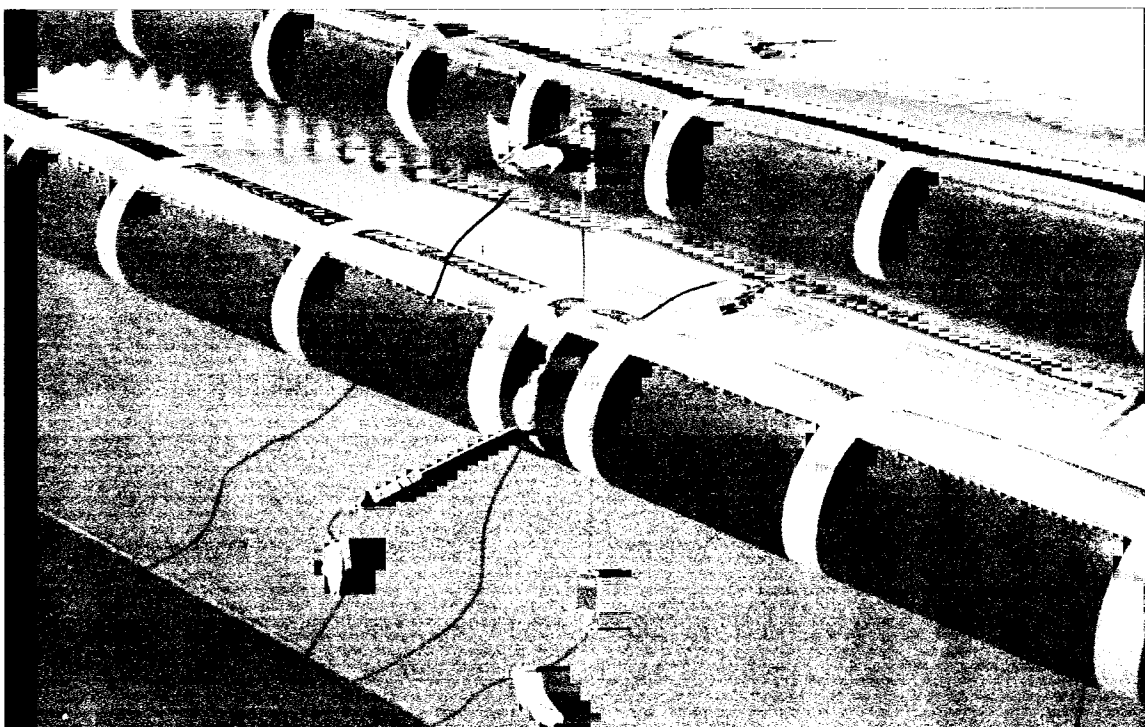


Figure 5.4. View of Radial Locations of Temperature Probes

The axial locations of the temperature probes are listed in Table 5.2.

<b>Temperature Probe</b>	<b>Axial Distance from Entry to Ice Bank (ft)</b>	<b>Radial Distance Away from Refrigerant Tube (in.)</b>
1	1	1/4
2-3-4-5	8	0-1/2-3/4
6-7-8-9	13	0-1/4-1/2
10-11-12-13	24	0-1/2
14-15-16-17	25	0-1/4-1/2
18-19	35	1/4-1/2
20	42	0

Table 5.2. Axial and Radial Locations of Temperature Probes



Omega pressure transducers, Model #PX603, were placed at the inlet, the mid-point, and the exit to the ice bank in order to measure the saturation pressure of the refrigerant. It is expected to measure a larger pressure drop in the ice-bank than the model predicts due to the ‘U’ that was required when building the ice-bank. In order to collect data for a period of time, a TES unit of at least 40 feet was required. Lack of available space required a bend in the horizontal unit, which also facilitated connecting both ends of the ice bank to the main refrigeration loop. The numerical model assumes horizontal flow with no pressure drop due to sharp bends in the piping. Additional points that are monitored for temperature and pressure are listed in Table 5.3.

<b>Location</b>	<b>Temperature</b>	<b>Pressure</b>
At Site Glass	x	x
Liquid R-22 returning from ice bank	x	
Liquid R-22 to ice bank for evap. (before flow meter)	x	x
Vapor R-22 out of aux. evaporator	x	x
At copper wall prior to entering ice bank	x	
At copper wall after exiting ice bank	x	
Discharge from compressor		x
R-22 entering aux. evaporator	x	
R-22 entering aux. condenser	x	
R-22 exiting aux. condenser	x	
R-22 exiting water bath	x	
Brine entering aux. condenser	x	
Brine exiting aux. condenser	x	
Brine entering aux. evaporator	x	
Water entering water bath	x	

Table 5.3. Location of Additional Thermocouples and Pressure Transducers

Three Fluke Hydra Data Loggers, model #2625A, are used to acquire the data from the temperature probes, thermocouples, and pressure transducers. The data acquisition units are programmed to scan at thirty-second intervals throughout the experiment. At the end of the test, the data is uploaded from all three loggers to a Micron personal computer, in data file format. This format allows the data to be easily imported into Excel spreadsheets for analysis.

At the start of the test, it is desired to establish steady-state conditions in the main refrigerant loop prior to permitting flow to enter the ice bank. This is accomplished by adjusting brine flow, water flow, and refrigerant flow until the high and low pressures of the main refrigerant cycle are established at approximately 210 psia and 40 psia, respectively. At this point, the valve that allows liquid refrigerant to flow to the ice bank can be opened. This valve is a throttling valve and it drops the saturation pressure, and with it the saturation temperature, of the refrigerant entering the ice bank. The liquid refrigerant flows through an in-line flow meter ahead of the throttling valve without phase change then through the throttling valve which imposes a large pressure drop. This drop in pressure results in refrigerant quality between 0% and 17% entering the ice bank. The temperature and pressure recorded just prior to the flow meter are used to establish the point on a P-h diagram for R-22. The throttling process can be followed on the diagram to the pressure of the refrigerant upon entry to the ice bank. This establishes the quality of the refrigerant entering the ice bank. The panel which houses the flow-meters and valves is shown in Figure 5.5.

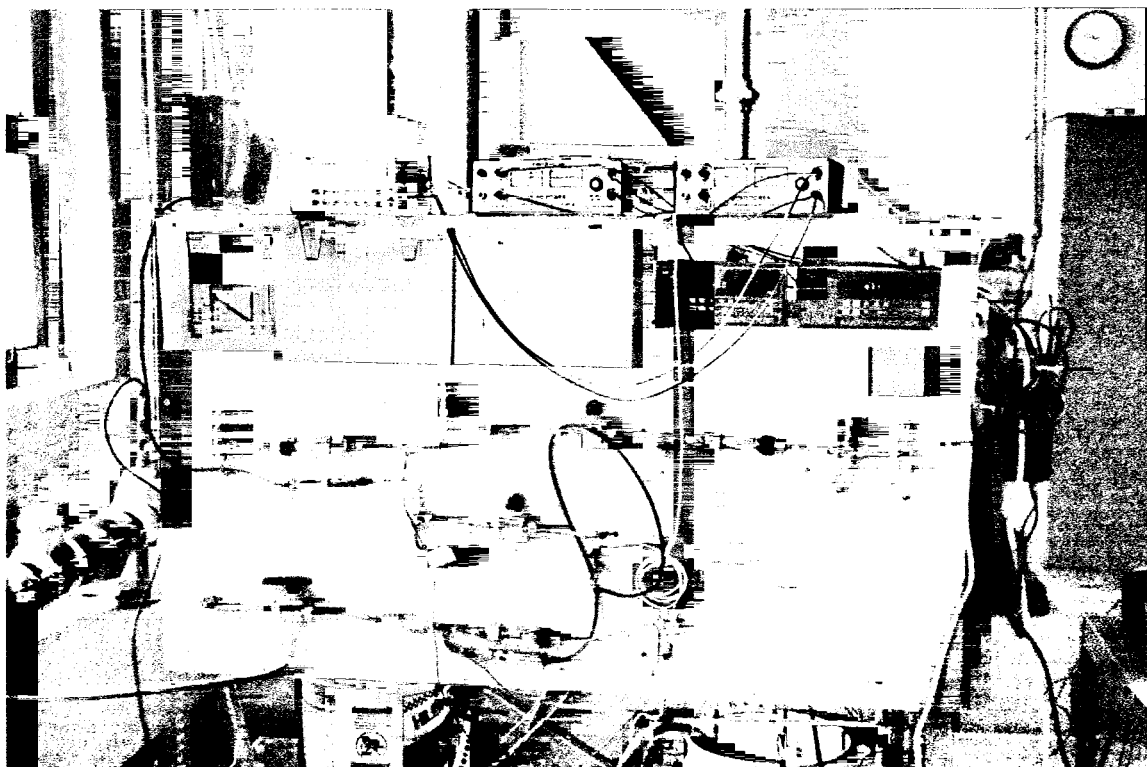


Figure 5.5. Flow Controls, Data Loggers and Power Supplies

Initially, the refrigerant exits the ice bank as superheated vapor at approximately room temperature. As the water in the annulus freezes, the refrigerant exits at a lower temperature but still as superheated vapor. Upon exiting the ice bank, the refrigerant is mixed with the main loop flow and continues to cycle.

When enough of the water has been frozen to permit condensing to take place (i.e., approximately four hours), refrigerant flow to the ice bank, for evaporation, is discontinued. It is desired to establish the high and low pressures of the main refrigerant flow loop to be approximately 160 psia and 34 psia, respectively, prior to allowing flow to the ice bank for condensing. The water flow and brine flow are readjusted to achieve this. The high pressure vapor out of the compressor is throttled down to a lower pressure and is cooled through the brine loop to release some of the super heat.

At the beginning of the condensing cycle, the liquid refrigerant that exits the ice bank is sub-cooled liquid. The refrigerant is passed again through the brine pail in order to absorb some energy so that the liquid flow meter will not develop frost on the outside, preventing it from being read. After passing through the flow meter, the condensed liquid refrigerant is mixed with the main loop flow and continues to cycle.

## Chapter 6

### MODEL VALIDATION

#### 6.1. Comparison of Numerical Model to 1-D Exact Solution of Paterson

In the freezing of pure substances such as water, solidification occurs at a discrete temperature and the solid and liquid phases are separated by a moving interface. The fundamental difficulty with obtaining an exact solution to this type of problem is that the solution of the parabolic heat conduction equation must be solved in a region where the boundary is unknown (Ozisik, 1993). The exact solutions to phase change problems are limited to a number of idealized situations in semi-infinite, or infinite, regions that are subject to simple boundary and initial conditions. One such solution is that of solidification of a line heat sink in an infinite medium (phase changing material) with cylindrical symmetry, by Paterson (1952), as outlined in Ozisik's text on heat conduction (1993). Paterson has shown that the solution to this one-dimensional heat conduction problem is possible if the solution is chosen as an exponential integral function in the form of  $Ei(-r^2/4\alpha t)$ . [Note:  $\alpha$  is defined as thermal diffusivity in this section *only*.]

A comparison was made between Paterson's exact solution and the numerical model described herein. For the purpose of comparison, the line heat sink was modeled as a 0.03-inch diameter refrigerant tube with a tube wall of negligible thickness. A finite length of 3 feet was selected as was a finite outer radius of the PCM of 0.6 inches. The problem begins with water initially at 32°F, and refrigerant running through the tube at 20°F, with a flow rate of 2 lbm/hr. At a Fourier number,  $Fo_s$ , of 7.78 and 35 (based on ice properties), Paterson's solution was plotted along with the solution of the numerical

model which is the subject of this dissertation. For the purpose of this comparison, the axial conduction in the model was set to zero. The results are shown in Figure 6.1.

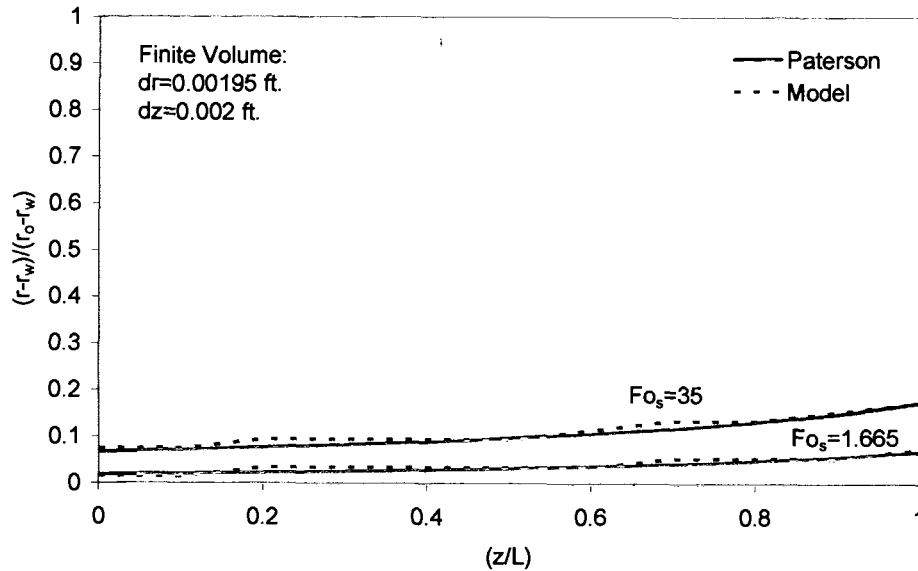


Figure 6.1. Comparison of Numerical Model to 1-D Exact Solution of Paterson – (Fo Computed with Ice Properties)

The solutions compare very well, for small  $Fo$ , indicating that similar volumes of water have been frozen in each solution. The excellent comparison between the numerical model and the exact 1-D solution of Paterson confirms the validity of the numerical model. The author will now apply the numerical model with both radial and axial conduction in the PCM for all other results.

## 6.2. Comparison of Numerical Model to Test Results

The experiment was performed as outlined in the chapter on Experimental Apparatus and Procedure. The parameters applied to the numerical model, to simulate the test conditions, are listed in Table 6.1.

Refrigerant Tube Inner Diameter	0.315 in.
Copper Tube Outer-Wall Diameter	0.375 in.
Outer Radius of PCM	1.2225 in.
Length of Ice Bank	43 ft.
Mass Flow for Evaporating Mode	28 lbm/hr
Initial Temperature of Water	70 F
Saturation Pressure	67.21 psia
Refrigerant Temperature	28.3 F
Quality of R-22 entering Ice Bank	3 %

Table 6.1. Parameters Applied During Evaporating Mode

The results of the comparison of the numerical model to the experiment, when functioning in evaporating mode, are contained in Figures 6.2., 6.3., and 6.4.

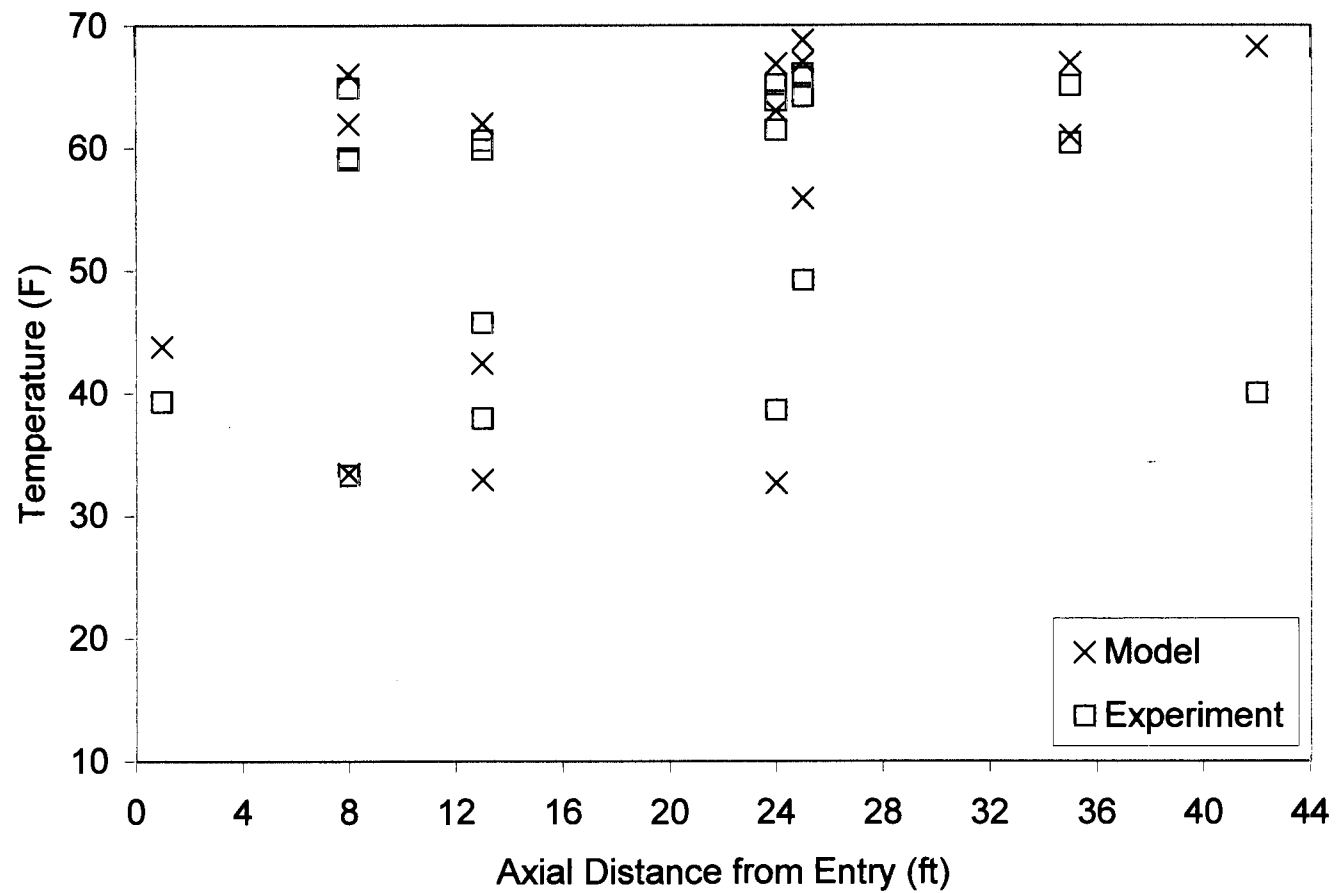


Figure 6.2. Comparison of Numerical Model to Experimental Results for Evaporation Mode,  $Fo=0.629$



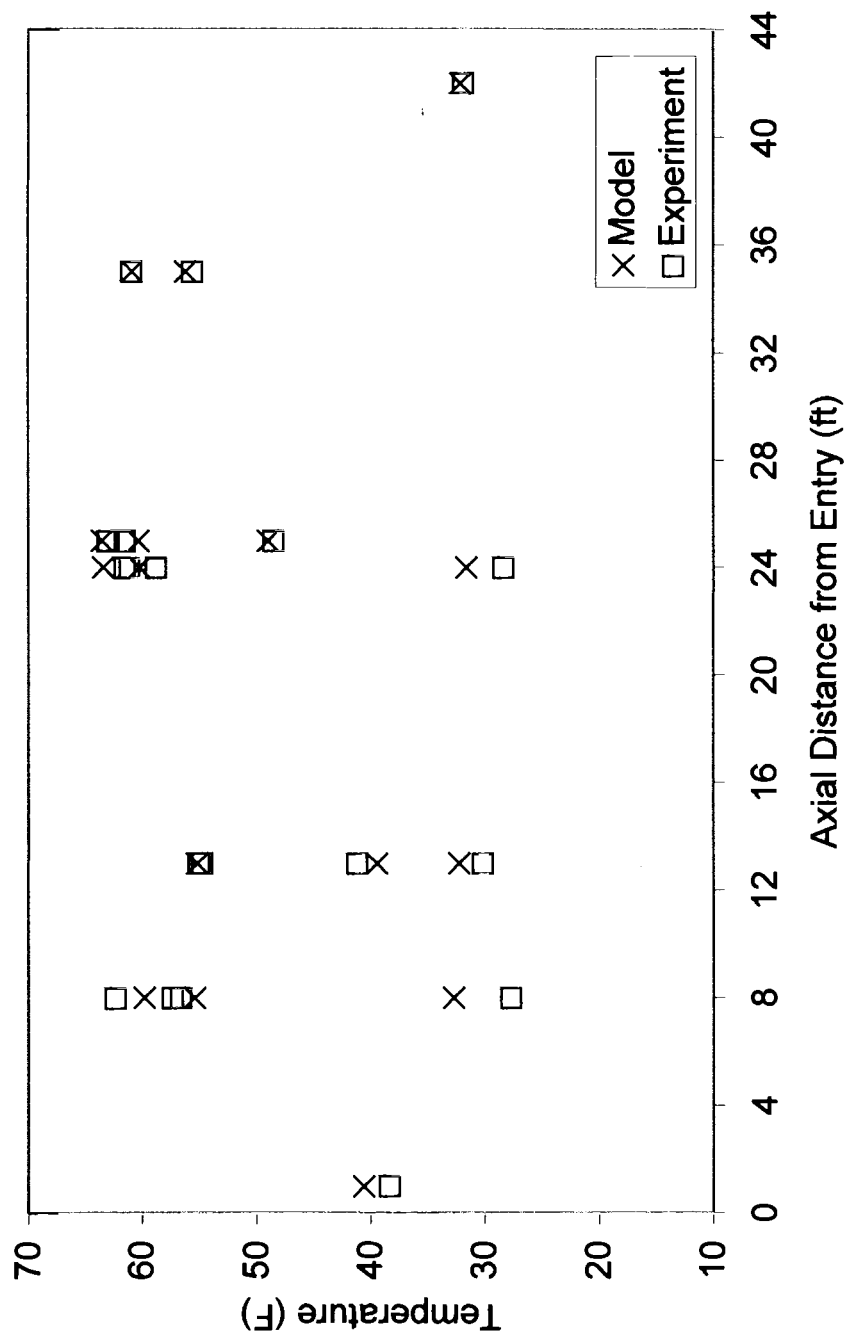


Figure 6.3. Comparison of Numerical Model to Experimental Results for Evaporation Mode,  $Fo=1.887$

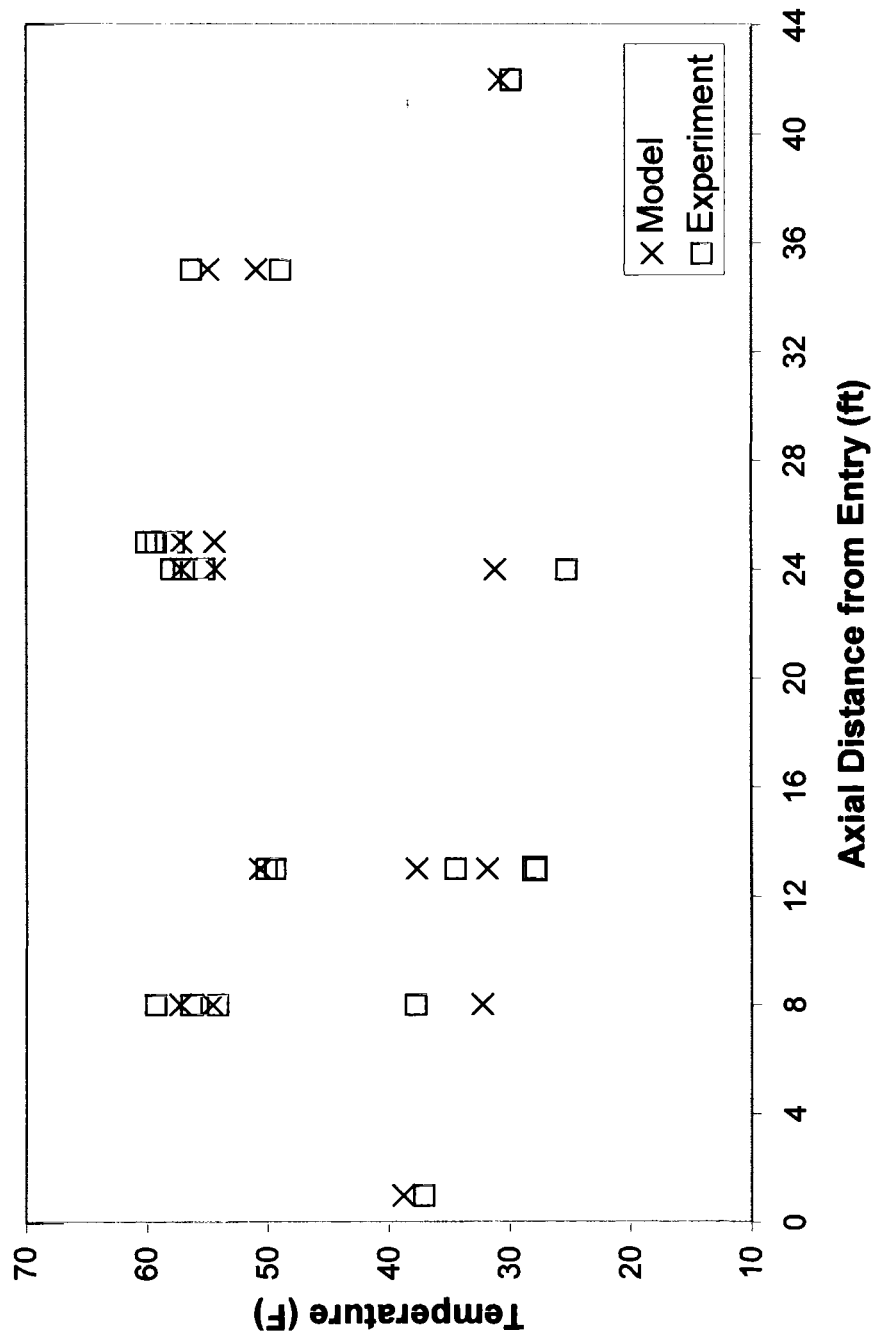


Figure 6.4. Comparison of Numerical Model to Experimental Results for Evaporation Mode,  $Fo=3.775$

The mean and average deviation for each set of data (i.e., data at each  $F_o$ ) are listed in Table 6.2. The deviations were computed as follows:

$$\text{Mean Deviation} = \frac{1}{n} \sum_1^n \left| \frac{(T_{\text{cal}} - T_{\text{exp}})100}{T_{\text{exp}}} \right| \quad (47)$$

$$\text{Average Deviation} = \frac{1}{n} \sum_1^n \frac{(T_{\text{cal}} - T_{\text{exp}})100}{T_{\text{exp}}} \quad (48)$$

<b><math>F_{ow}</math></b>	<b>Mean Deviation (%)</b>	<b>Average Deviation (%)</b>
0.629	8.79	5.22
1.887	3.67	1.17
3.775	5.44	1.42

Table 6.2. Mean and Average Deviation of Numerical vs. Experimental Data for Evaporation Mode

As stated earlier, pressure drop through the length of tube was expected to be greater in the experiment due to the U-bend added to the tubing at approximately the midpoint. The pressure drop was plotted for the section of pipe from the entry to the midpoint and from the midpoint to the end of the ice-bank, for evaporation times of 5 minutes and 15 minutes, as represented in Figure 6.5. Based on calculations of pressure drop, assuming all vapor flow, through one 90°-elbow and along the remainder of

approximately 22 feet, the pressure drop should be approximately 0.4 psi between the 2<sup>nd</sup> and 3<sup>rd</sup> pressure transducers which is approximately what was predicted by the numerical model. The third pressure transducer, as well as that particular channel of the data acquisition system will require some further investigation.

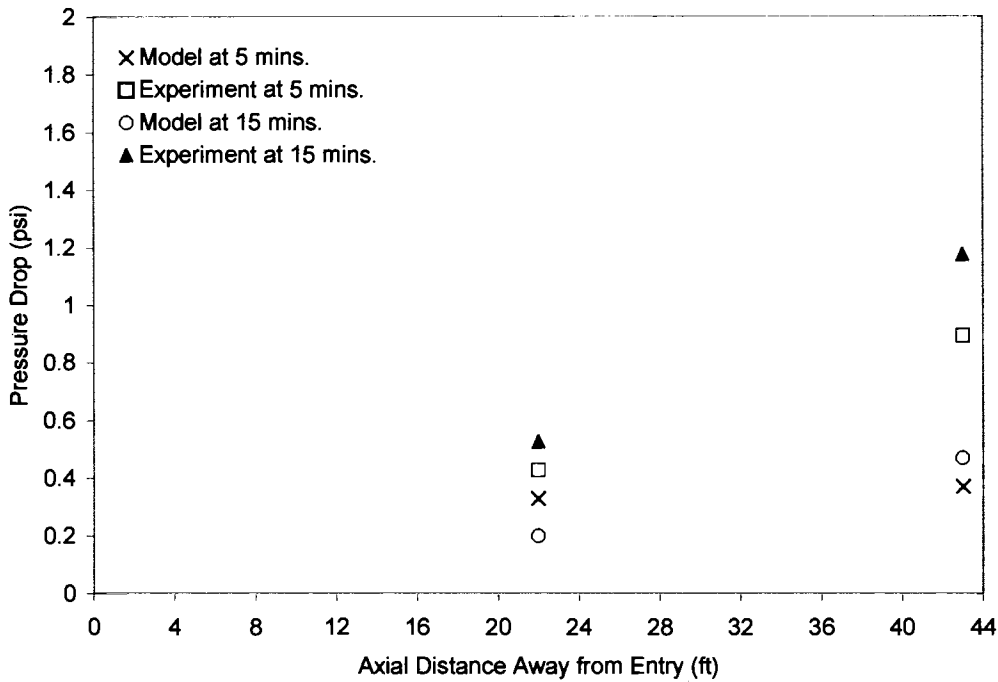


Figure 6.5. Comparison of Pressure Drop Along Tube

As a result of having the ice bank built in a room that is not refrigerated, condensing mode can never be tested with a homogeneous PCM. The ice in the annulus never reaches a constant temperature throughout the 43-foot length. Therefore, condensing mode can only be tested as a continuation from evaporation mode. After obtaining the data for evaporating mode, the test apparatus was converted to condensing mode with the parameters as listed in Table 6.3. The evaporating conditions defined in Table 6.1., were run for a period of 72 minutes, at which time the ice bank was converted

to condensing mode with the parameters defined in Table 6.3. Condensing mode was run for 6 minutes. Figure 6.6. compares numerical results to the experimental data

Mass Flow for Condensing Mode	29 lbm/hr
Saturation Pressure	160 psia
Refrigerant Temperature	80.78 F
Quality of R-22 entering Ice Bank	100 %

Table 6.3. Parameters applied during Condensing Mode.

obtained with the ice bank test. Deviations were computed for condensing mode results but they were a little greater than those for evaporating mode. This was expected due to the transient involved when shifting the testing apparatus from functioning in one mode to another. The deviations for condensing mode at  $Fo_s=7.055$  ( $Fo_s$  is not a continuation of the previous Evaporating  $Fo_w$ , but, rather, starting from Condensing Mode) are listed in Table 6.4.

$Fo_s$	Mean Deviation (%)	Average Deviation (%)
7.055	10.98	7.97

Table 6.4. Mean and Average Deviation of Numerical vs. Experimental Data for Condensing Mode

It was found that the numerical model in this study gives reasonable agreement with experimental data for both evaporating mode heat transfer as well as condensing mode.

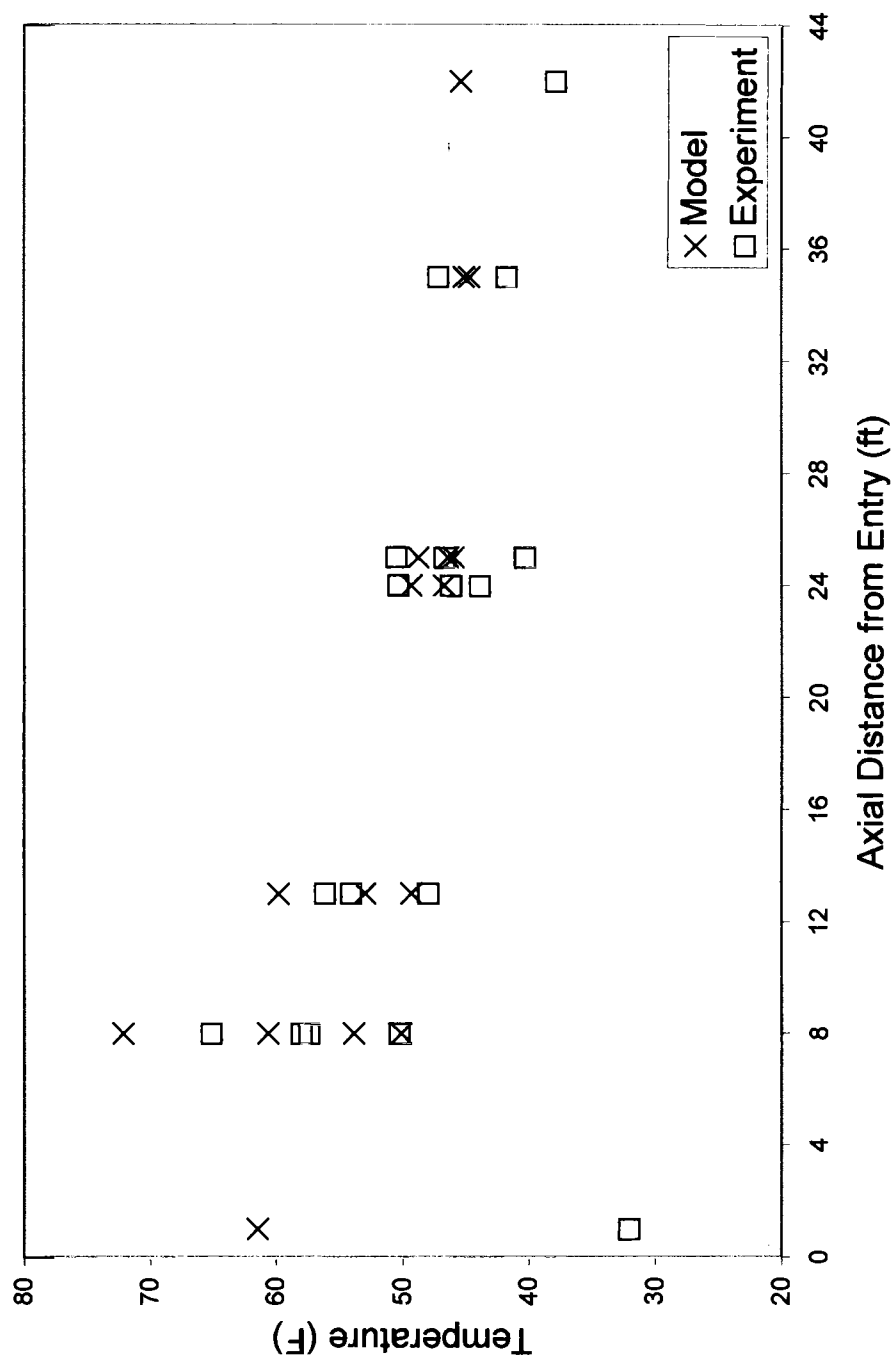


Figure 6.6. Comparison of Numerical Model to Experimental Results for Condensing Mode,  $Fo_s=7.055$

### **6.3. Uncertainty Analysis**

The results of temperature in the ice/water annulus were not absolute values, but had some uncertainties associated with them. Prior to beginning any testing, the temperature read by the probes, of the water in the annulus, was normalized to a single value indicated by a reliable temperature reading device situated in the room. The values of the probes deviated by as little as  $0.02^{\circ}\text{F}$  to as much as  $5.5^{\circ}\text{F}$ . The temperature probes were situated at radial distances away from the copper tubing, within the water/ice annulus, to within  $\pm 1/16''$ , or 5.1% of the overall thickness of the annulus. The deviation in temperatures taken by probes which were situated at the same radial and axial location was within 3.9%.

The pressure transducers which tracked the pressure drop of the refrigerant along the length of the copper tube were calibrated to within 1% error then were normalized to the same starting value. The adjusted values for normalizing the probes were all less than 0.3 psia.

### **6.4. Convergence of Model**

The grid size of the finite volume mesh was converged upon in both the  $i$  ( $\Delta z$ ) and the  $j$  ( $\Delta r$ ) directions. As shown in Table 6.5 and Table 6.6, the results of having run the computer model in Evaporation Mode for 0.4 hr., at a mass flow of 28 lbm/hr, with an initial wall temperature of  $70^{\circ}\text{F}$ , and an initial saturation pressure for R-22 of 57.6 psia, for dimensions of PCM as defined in the test apparatus of the previous section, both  $\Delta r$  and  $\Delta z$  were reduced in size to within an accuracy of less than 0.2%. These tables also indicate that there is global energy conservation between the PCM and the two-phase

heat transfer fluid to within 0.1%. Figure 6.7. and Figure 6.8. illustrate convergence of temperature in the PCM.

Converging on $\Delta r$					Deviation bet. $Q_{\text{water}}$ & $Q_{\text{R-22}}$ (%)	Deviation bet. Runs (%)
$\Delta r$ (ft)	$\Delta z$ (ft)	Dimensions of Grid	$Q_{\text{water}}$ (Btu)	$Q_{\text{R-22}}$ (Btu)		
0.0215625	0.005	4 x 8600	994.98	996.663	0.169187003	
0.014375	0.005	6 x 8600	995.7025	996.735	0.10369061	0.072621745
0.01078125	0.005	8 x 8600	997.0489	997.764	0.071698802	0.135217769

Table 6.5. Converging Finite Volume Mesh in i ( $\Delta r$ ) direction

Converging on $\Delta z$					Deviation bet. $Q_{\text{water}}$ & $Q_{\text{R-22}}$ (%)	Deviation bet. Runs (%)
$\Delta r$ (ft)	$\Delta z$ (ft)	Dimensions of Grid	$Q_{\text{water}}$ (Btu)	$Q_{\text{R-22}}$ (Btu)		
0.01078125	0.02	8 x 2150	998.9558	997.975	0.098166447	
0.01078125	0.01	8 x 4300	998.4658	998.123	0.034331037	0.049045189
0.01078125	0.005	8 x 8600	997.0489	997.764	0.071698802	0.141910568

Table 6.6. Converging Finite Volume Mesh in i ( $\Delta z$ ) direction.



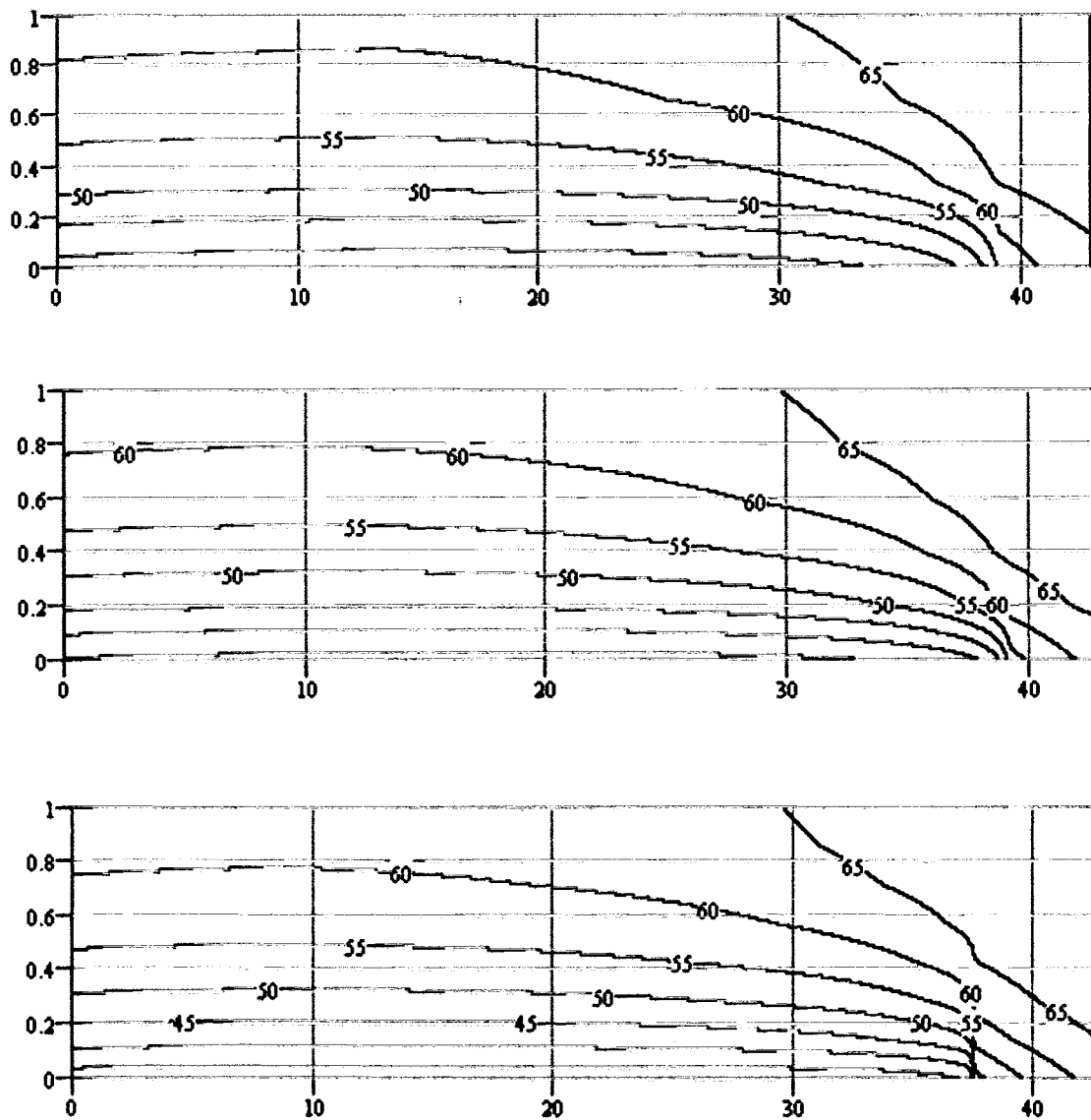


Figure 6.7. Convergence on  $\Delta r$  [Top to Bottom:  $\Delta r = 0.0215625$  ft.,  $0.01078125$  ft.,  $0.014375$  ft.] (Length of PCM is 43 ft., Thickness is 1 in.,  $\Delta z = 0.005$  ft.)

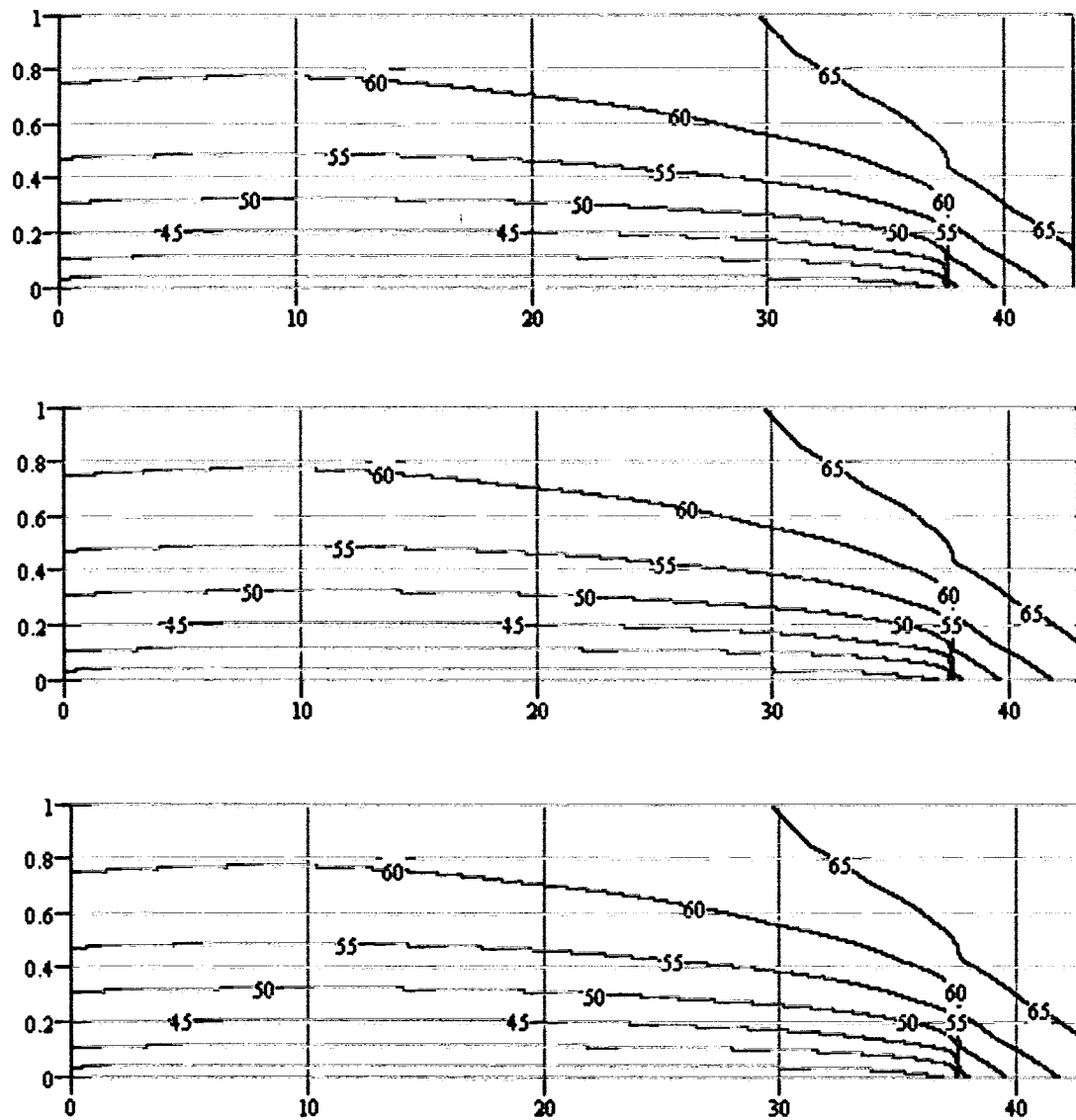


Figure 6.8. Convergence on  $\Delta z$  [Top to Bottom:  $\Delta z=0.02$  ft.,  $0.01$  ft.,  $0.005$  ft.]  
 (Length of PCM is 43 ft., Thickness is 1 in.,  $\Delta r=0.01078125$  ft.)

## Chapter 7

### RESULTS AND DISCUSSION

#### 7.1. Axial Conduction in PCM

Many researchers have opted to model freezing on the outside of a tube as a purely one-dimensional heat conduction problem (Shamsundar, 1982; Charach, Keizman & Sokolov, 1991; Zhang, Chen & Faghri, 1997; Yingqiu, Yinping, Yi, & Yanbing, 1999). Some have stated that axial conduction may be neglected due to the insignificance of the temperature variation of the fluid wall, in the axial direction (Zhang & Faghri, 1995). However, Zhang and Faghri's model incorporated a laminar, constant quality fluid flowing through a TES system in which sensible heat was neglected. The model described in the present work incorporates two-dimensional heat conduction as a result of having investigated the need to incorporate axial conduction.

##### 7.1.1. Freezing Front Position at Different Fourier Number

In an attempt to determine the influence of axial conduction on the cylindrical problem of solidification around a coolant-carrying tube, the freezing front position of the PCM was plotted at different durations of freezing. The only parameter that changed was the diameter ( $D$ ) of the refrigerant-carrying tube. The remainder of the parameters were non-dimensionalized and held constant as shown in Table 7.1. Figures 7.1. and 7.2 indicate that axial conduction is negligible at small Fourier number,  $Fo=10$ ; however, at larger  $Fo$ , the effects of axial conduction are visible at the far end of the PCM. When conduction takes place in a PCM, which is at an initial temperature other than the fusion

temperature of the material, and the heat-transfer-fluid is two-phase flow, the effects of axial conduction cannot be neglected other than at very small  $Fo$ .

Constant Parameters	Value
$C_p(T_{sat}-T_m)/LH = Ste$	0.084
$(T_o-T_m)/(T_{sat}-T_m)$	-2.75
$r_o/D$	5
$L/D$	2400
$Re_v$	60000

Table 7.1. Parameters Used in Thickness vs. Length Study

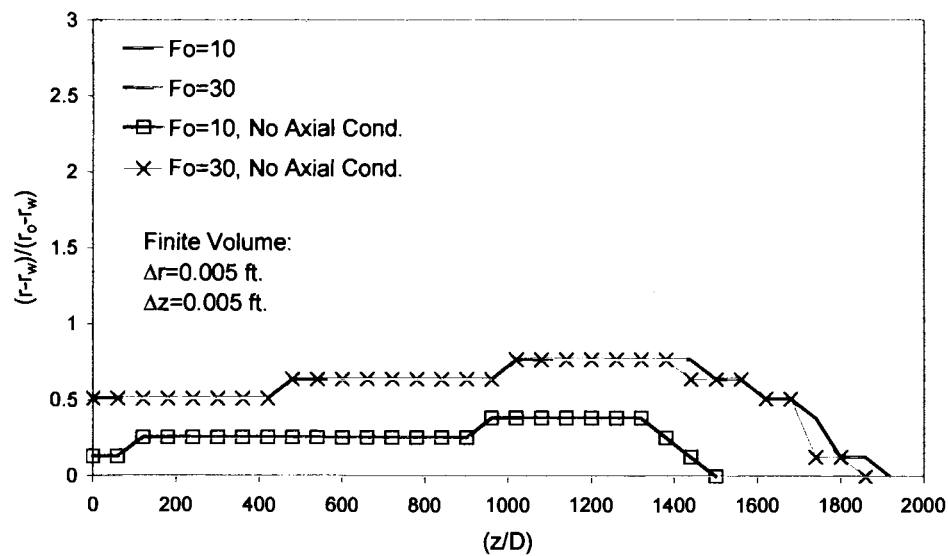


Figure 7.1. Freezing Front Position at Different Times for  $D=0.1$ " –  
( $Fo$  is Computed with Water Properties and Refrigerant Diameter)

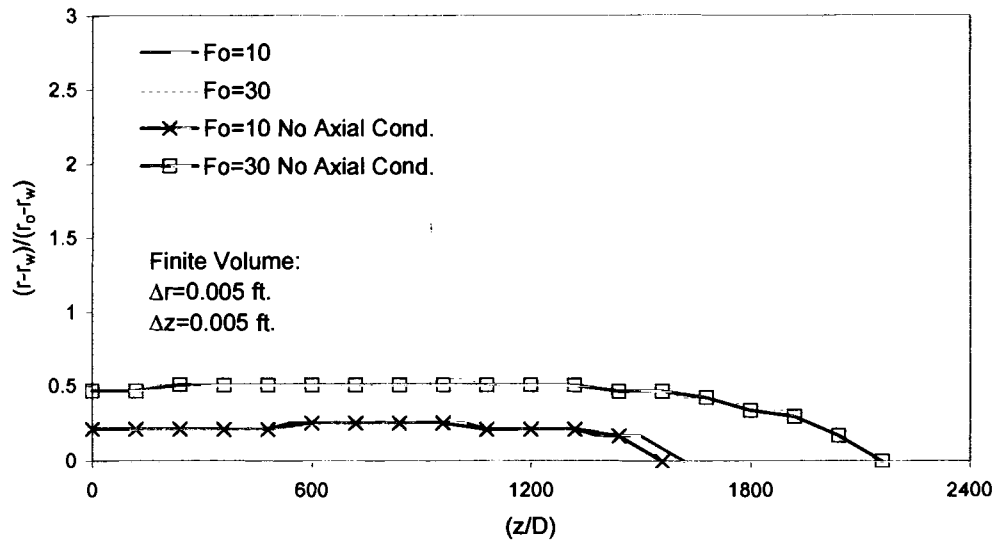


Figure 7.2. Freezing Front Position at Different Times for  $D=0.3$ " –  
( $Fo$  is Computed with Water Properties and Refrigerant Diameter)

### 7.1.2. Axial Variation of Freezing vs. Reynolds Number

In Figure 7.3, solidification front is plotted as a function of saturated liquid Reynolds number. It is shown that the rate of propagation of the freezing front, through the PCM, increases more greatly in the axial direction than in the radial direction, with increasing liquid Reynolds number.

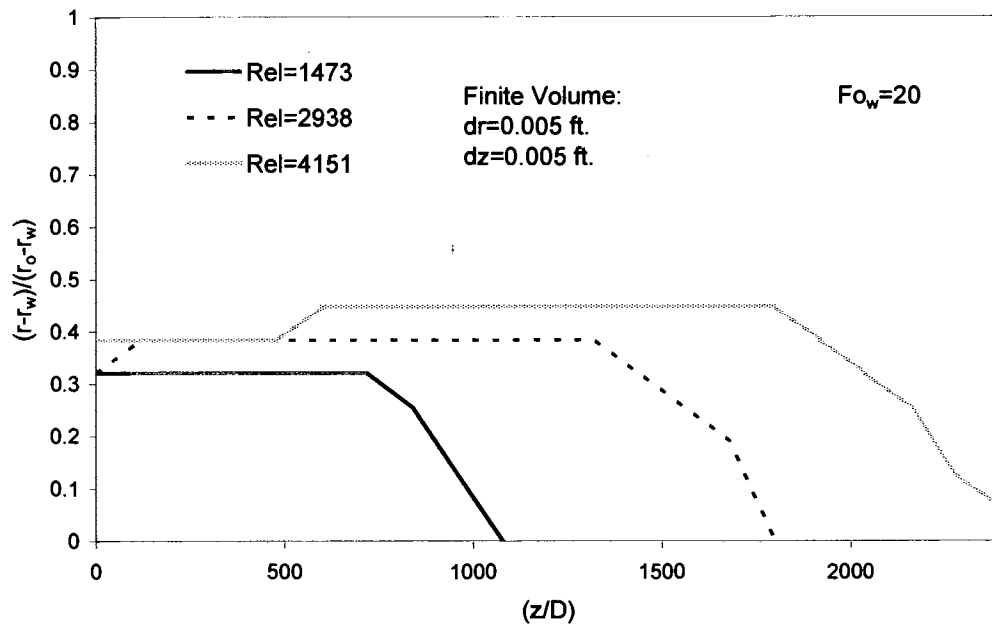


Figure 7.3. Axial Variation of Freezing vs. Saturated Liquid Reynolds Number -  $Fo$  Computed with Inner Refrigerant Diameter

## 7.2. Effects of Increasing Volume of PCM on Net Energy/Lost

The main goal of using ice banks is not only to shift power usage to off-peak times but also to save energy. This study investigated how increasing the volume of PCM affects the net amount of energy lost by the PCM, thereby producing more ice for cooling. Would it be more efficient to lengthen the annulus of the PCM or increase its outer diameter? For a given initial value of energy extracted from the water,  $Q_0$ , and a constant Reynolds number, the volume of the water annulus was increased. For each increase in volume,  $V/V_0$ , whether by increasing the length or increasing the outer radius, the net extractable energy,  $Q$ , was compared. The time required to extract that energy from the water was also plotted as the non-dimensional Fourier number. As is evident

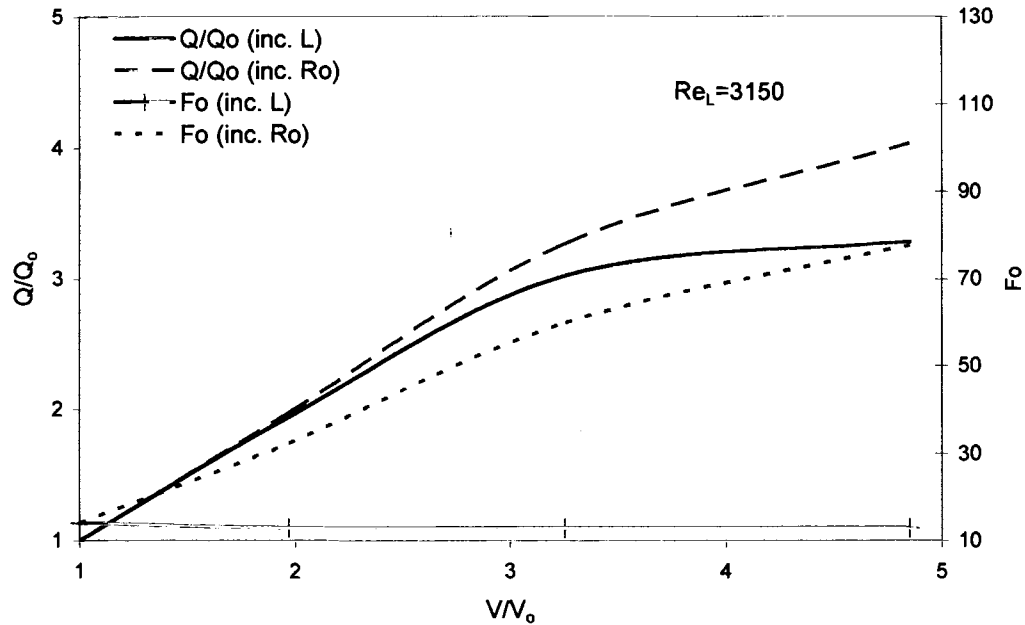


Figure 7.4. Effects of Increasing Volume of Water Annulus by Increasing Length vs. Increasing Outer Radius

in Figure 7.4, it is wiser to increase the length of the PCM rather than increasing its outer radius. From this figure, we see that up to approximately  $V/V_o=3$ , increasing length versus increasing outer radius produces virtually the same results. However, in order to obtain the same results (i.e., extract the same energy), more electricity would be required to *charge-up* the ice bank, if the radius of the annulus were increased, because the compressor would need to run much longer to manufacture the same amount of ice than it would if the length of the annulus were increased.

### 7.3. Effects of Stefan Number on Refrigerant Wall Temperature

The effects of sensible heat were examined by plotting the non-dimensional wall temperature (of the refrigerant tube) as a function of axial distance, as shown in Figure 7.5. For Stefan number equal to 0 (i.e., no sensible heat), the wall temperature behaves as

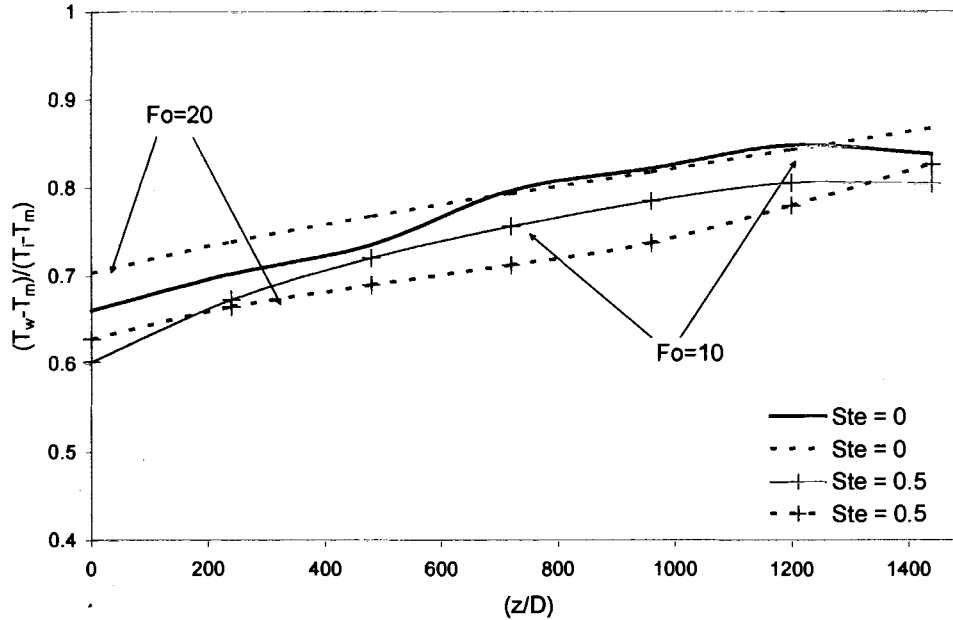


Figure 7.5. Effects of Stefan Number on Wall Temperature

expected. After more time goes by, larger  $Fo$ , the wall temperature of the refrigerant tube gets closer to the inlet temperature of the refrigerant, indicating that more solidification has taken place and that the PCM is dropping in temperature. Also, for  $Ste=0.5$ , the wall temperature behaves as expected at small  $Fo$ . The non-dimensional temperature differential, at  $Fo=10$ , is smaller at  $Ste=0.5$  than it is at  $Ste=0$ , demonstrating that the wall temperature is closer to the fusion temperature,  $T_m$ , of the PCM because of the higher sensible heat to latent heat ratio. However, something unexpected happens at  $Fo=20$ . For  $Ste=0.5$ , the non-dimensional temperature differential falls lower than it was at



$Fo=10$  for most of the length examined. This is a result of the thermal conductivity of the first row of cells, immediately along the wall of the refrigerant tube. At  $Fo=10$ , the first row of cells is still in the form of water which has a high thermal resistance, nearly 4 times greater than that of ice. Therefore, by  $Fo=20$ , when the first row of cells has turned to ice, the energy from the remainder of the *hot* water is pulled through the row of ice, thus warming the wall of the refrigerant tube. This is made clear in the graph of Biot number versus Stefan number, as shown in Figure 7.6.

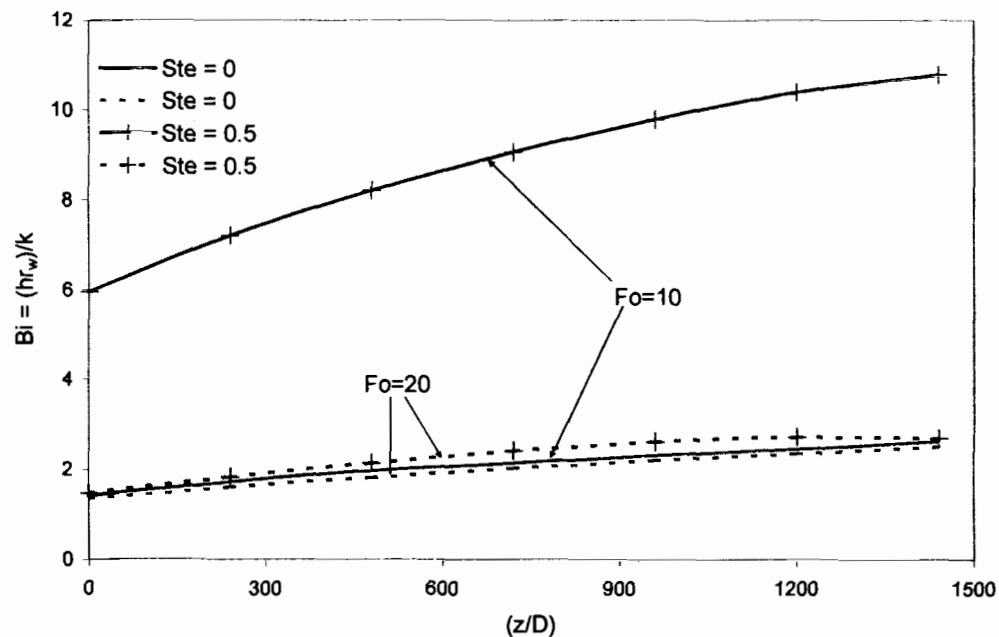


Figure 7.6. Effects of Stefan Number on Biot Number in the PCM (h of 2-phase fluid, k of PCM)

#### 7.4. Effects of Reynolds Number and Temperature on Evaporation Heat Transfer

During evaporation, increasing Reynolds number increases the rate of heat transferred from the PCM. Nusselt number not only increases with the magnitude of

Reynolds number but its *peak* shifts from being in lower vapor quality mixture at low Re to higher vapor quality mixture at high Re, as shown in Figure 7.7.

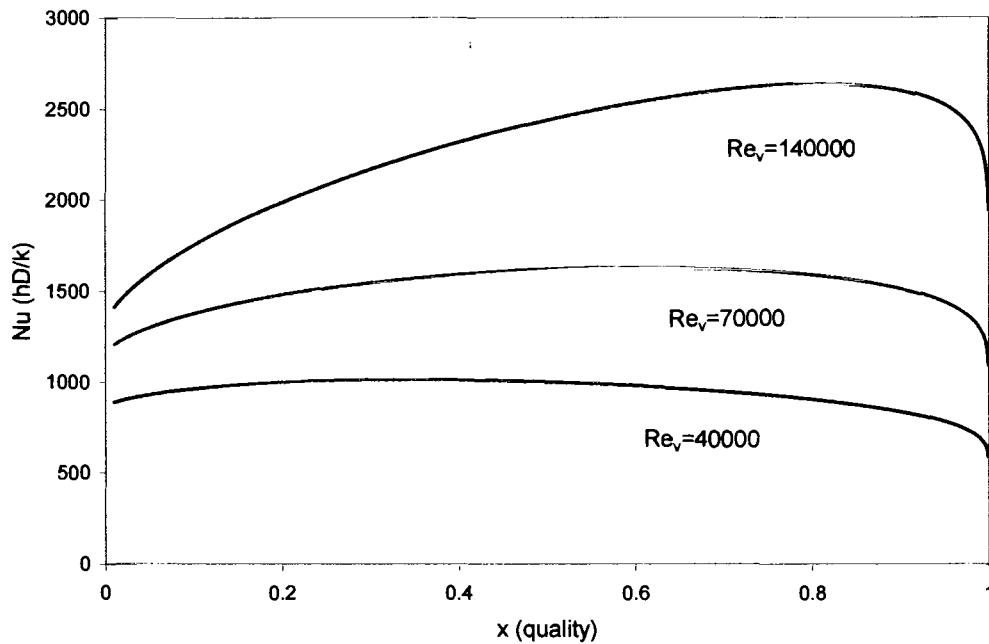


Figure 7.7. Effects of Re Number on Evaporation Heat Transfer in a Tube

The differential between the saturation temperature of the refrigerant entering the TES unit and the wall temperature influences the local Nusselt number only in the low-to-mid quality vapor regime, as shown in Figure 7.8.

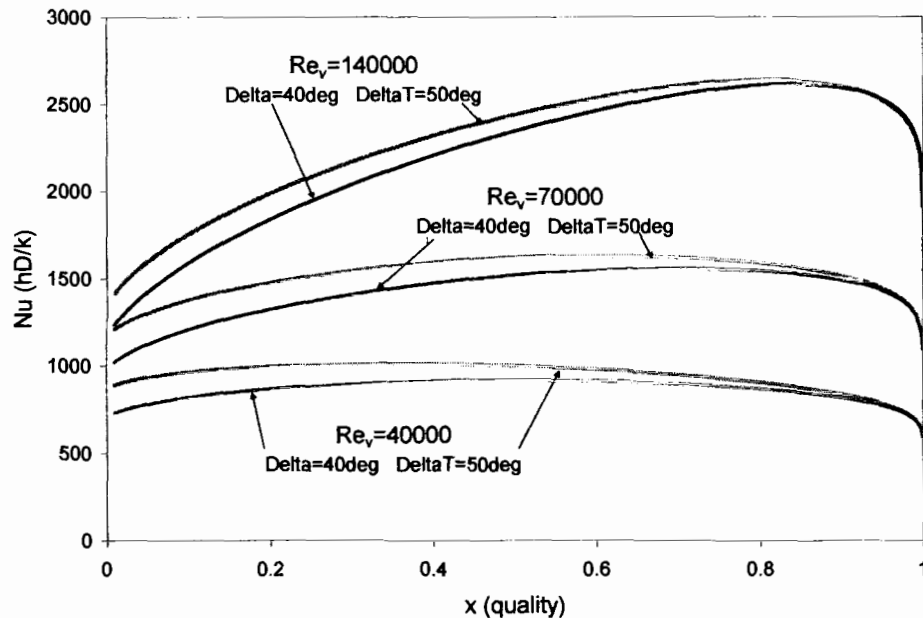


Figure 7.8. Effects of Temperature Differential on Evaporation Heat Transfer in a Tube

### 7.5. Effects of Reynolds Number and Temperature on Condensation Heat Transfer

Condensation heat transfer does not exhibit the same behavior as that of evaporation. Peak heat transfer occurs around 95% vapor for all annular flow condensation and at 100% vapor for stratified flow, as illustrated in Figure 7.9. Condensation heat transfer coefficient has a much smaller magnitude for a given  $Re$  than does evaporation. That is due to the resistance of the liquid film that is formed at the refrigerant inner wall as well as to the pool of liquid that accumulates at the bottom of the tube. The latter occurs primarily during stratified flow.

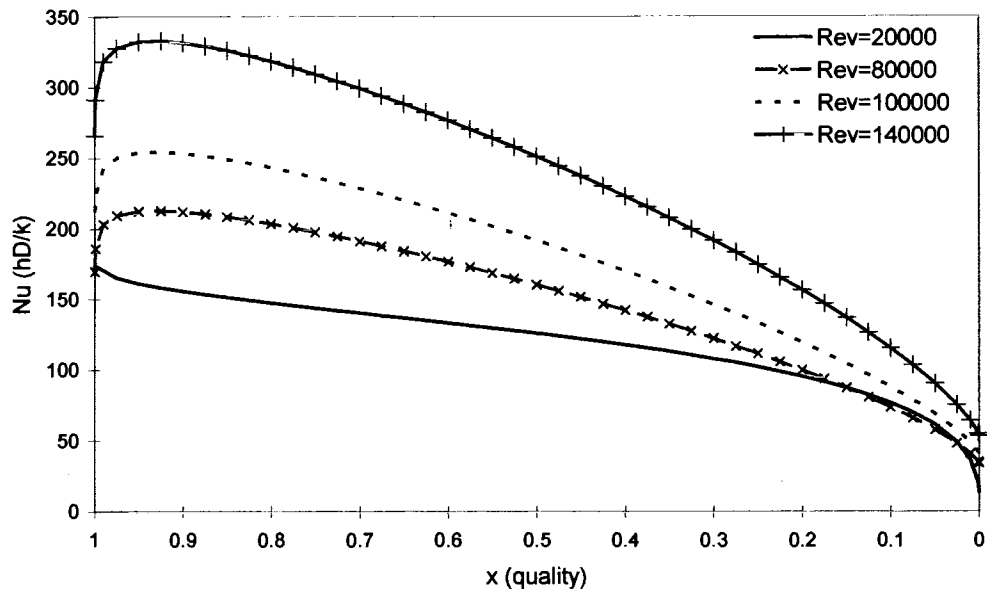


Figure 7.9. Effects of Reynolds Number on Condensation Heat Transfer in a Tube

As shown in Figure 7.10., condensing heat transfer has no dependence on wall temperature. Dobson and Chato have written that a large amount of experimental and analytical research suggests wall temperature has little to no impact on heat transfer in the annular flow regime (1998). The effect of temperature differential on stratified flow may appear peculiar at first glance. As shown, the larger temperature difference produces smaller local Nusselt number. In the stratified flow regime, a larger temperature difference produces a thicker pool of liquid at the bottom of the tube, as well as a thicker film around the inner circumference of the tube. This film lowers the heat transfer coefficient (Dobson & Chato, 1998).

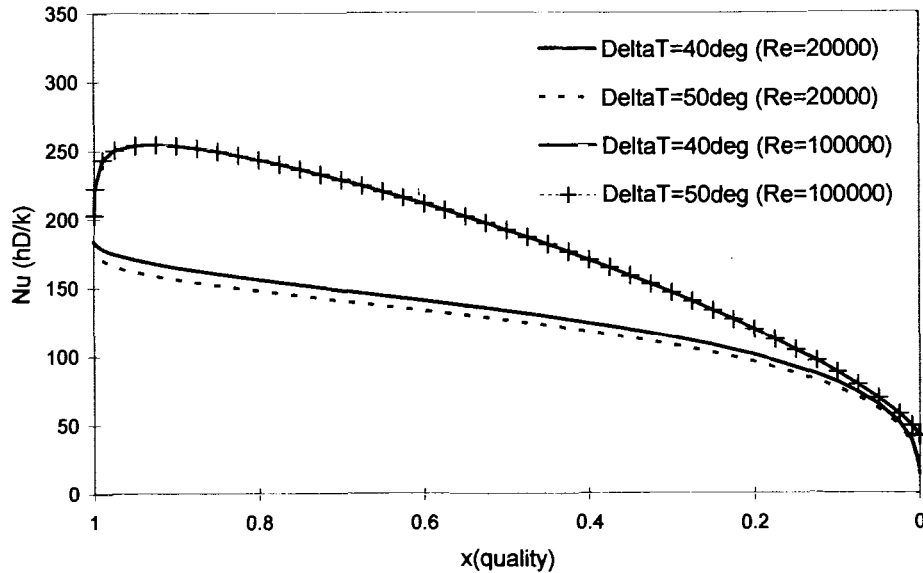


Figure 7.10. Effects of Temperature on Condensation Heat Transfer in a Tube

#### 7.6. Effect of Reynolds Number on Length of Tube Needed to Evaporate/Condense

The non-dimensional length of tube needed to fully evaporate and fully condense Refrigerant-22 was plotted as a function of Reynolds number for inner diameter equal to 0.3 inches and 0.6 inches, as shown in Figures 7.11. and 7.12., respectively. At constant diameter, the increased tube length required for increased Reynolds number is an expected trend for both evaporation and condensation heat transfer. However, the results of doubling diameter of the refrigerant tube show a slower rate of increase in length for increasing Reynolds number (i.e., a smaller slope) for both evaporation and condensation.

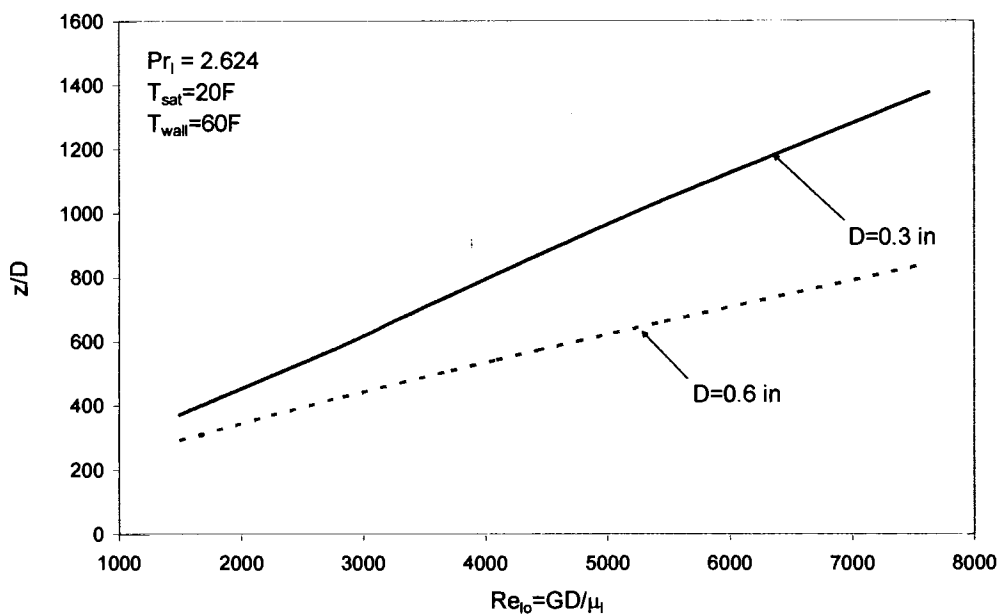


Figure 7.11. Effects of Liquid Reynolds Number on Minimum Length Required to Completely Evaporate Refrigerant

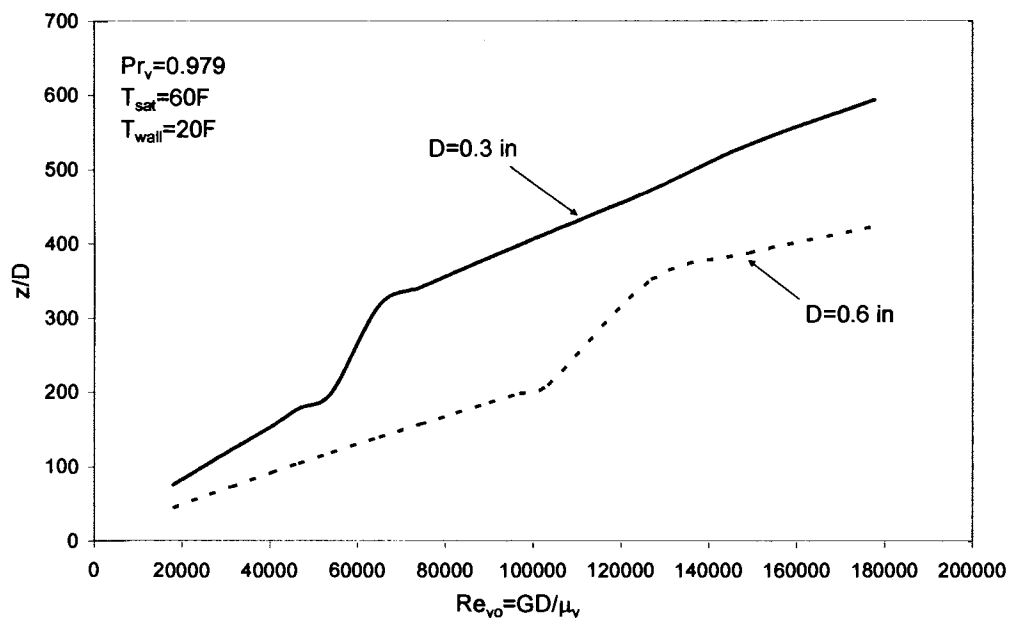


Figure 7.12. Effects of Vapor Reynolds Number on Minimum Length Required to Completely Condense Refrigerant

The non-linearity of the condensing profiles is illustrative of the transition from stratified flow to annular flow. Even with the non-linearity, the trend is still that of a faster increase in length required to fully condense with a smaller diameter of tubing.

### **7.7. Effect of Reynolds Number on Pressure Drop**

In this study, gravitational pressure drop is negligible due to the horizontal refrigerant tube. Therefore, total pressure drop consists of friction and momentum pressure drop. During evaporation of a two-phase fluid, total pressure drop increases with larger liquid Reynolds number, as illustrated in Figure 7.13. Since all of the coolant properties, including temperature, are a function of the saturation pressure of the coolant, a larger pressure drops result in a larger temperature differences between the coolant and the PCM, meaning larger heat transfer coefficients.

During condensation, the results are not immediately intuitive. With evaporation, the pressure drop due to momentum continues to increase while the refrigerant becomes a higher quality vapor, thus accelerating the flow through the pipe. With condensing, the opposite is true. Initially, when the refrigerant enters as vapor, both the friction and momentum pressure drop increase. However, as the vapor quality of the refrigerant decreases, becoming more liquid, the momentum pressure drop starts to decrease, slowing the flow of the liquid through the tube. Figure 7.14. shows that for small  $Re$  (i.e., stratified flow), the pressure drop constantly increases. However, at the larger  $Re$  (i.e., annular flow), the momentum pressure drop begins to decrease between 40% and 60% vapor; a partial pressure recovery takes place.

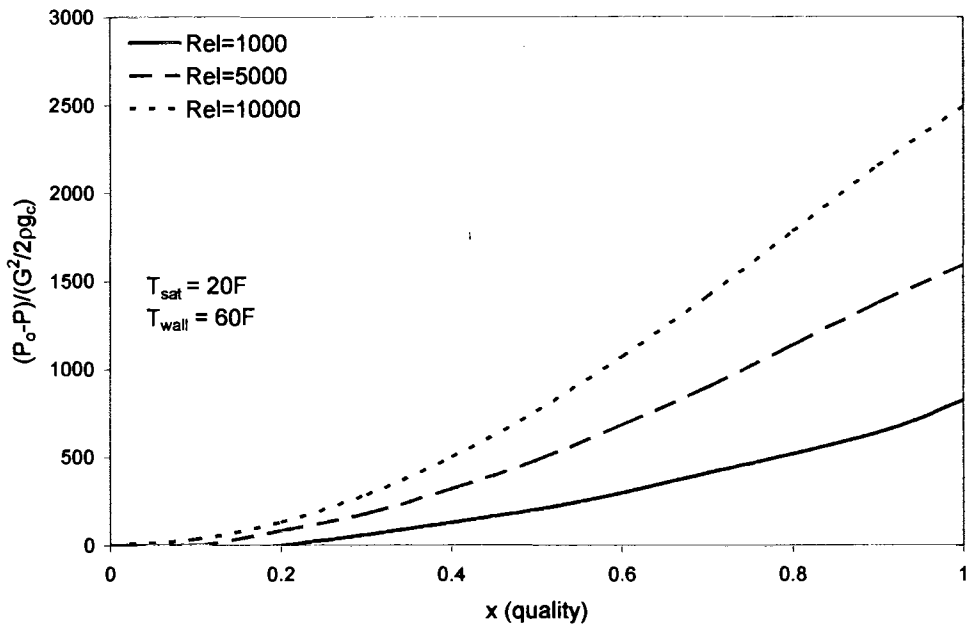


Figure 7.13. Effects of Saturated Liquid Re on Total Pressure Drop When Completely Evaporating Refrigerant

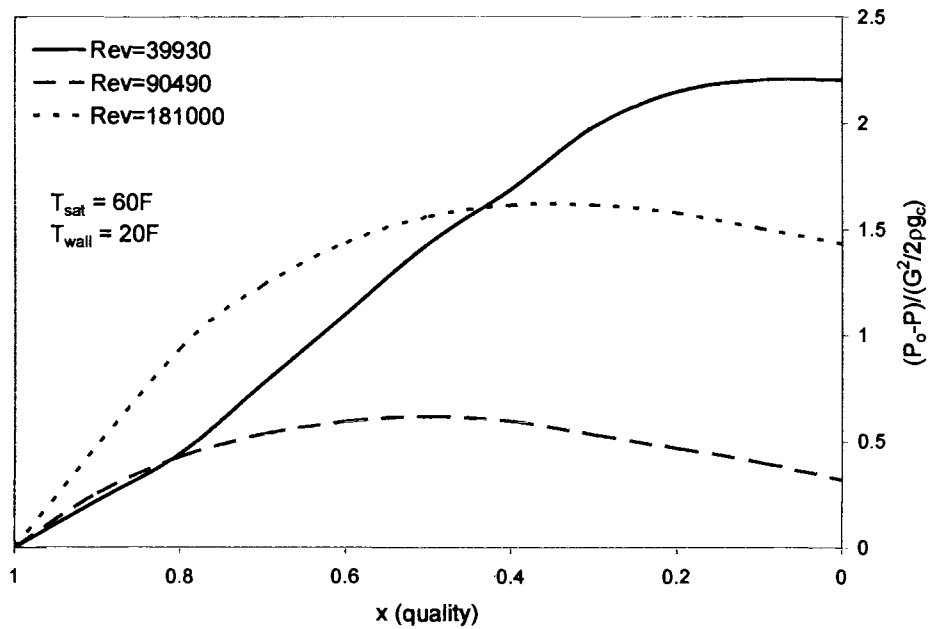


Figure 7.14. Effects of Saturated Vapor Re on Total Pressure Drop When Completely Condensing Refrigerant



## Chapter 8

### CONCLUSIONS

Thermal energy storage (TES) units are proving to be a useful and efficient method of space cooling. A numerical model has been presented to simulate the transient effects of two-dimensional, cylindrical solidification/melting of phase changing material (PCM) interacting with a two-phase fluid.

The phase changing process was modeled using the enthalpy method along with the finite volume approach. A good feature of the finite-volume approach is global energy conservation. The convective heat transfer of the fluid was modeled by existing, empirical correlations. The numerical model was validated both analytically and experimentally. The experimental TES unit consisted of water as the PCM and Refrigerant-22 as the phase-changing fluid. The mean and average deviation of the results, when compared to experimental data, were within 9% and 6%, respectively.

Results indicated that for a problem of heat conduction in a PCM, with conjugate forced convection of two-phase flow at its inner boundary, the effects of axial conduction are visible, at large  $Fo$ , when the initial temperature of the PCM is other than its fusion temperature.

It was shown that it is more cost efficient to add length to the PCM, as opposed to thickness, when attempting to increase the volume of extractable energy for cooling.

The effects of Stefan number on wall temperature and on Biot number were presented. It was shown that at Stefan numbers higher than 0 (i.e., sensible heat in

addition to latent heat in the PCM), the thermal conductivity of water creates thermal resistance in the PCM.

The effects of Reynolds number, and temperature, on two-phase heat transfer were illustrated. The length of tube needed to fully evaporate/condense R-22 was shown to be dependent upon Reynolds number.

Finally, the peculiarity of pressure recovery, during condensation, was presented graphically. The result is that of partial pressure recovery, at high Reynolds number, due to the momentum pressure drop term.

The numerical results present some useful criteria for the proper design of a TES system.

## REFERENCES

- Agrawal, S.S., Gregory, G.A., & Govier, G.W. (1973). An analysis of horizontal stratified two phase flow in pipes. *The Canadian Journal of Chemical Engineering*, 51, 280-286.
- Almogbel, M.A. (1997). *Modeling a thin ice-bank used as a refrigerant condenser*. Masters Thesis, Dept. of Mechanical Engineering, University of Maine, Orono, Maine.
- Begg, E., Khrustalev, D., & Faghri, A. (1999). Complete condensation of forced convection two-phase flow in a miniature tube. *ASME Journal of Heat Transfer*, 121, 904-915.
- Bellecci, C., & Conti, M. (1993). Phase change thermal storage: transient behaviour analysis of a solar receiver/storage module using the enthalpy method. *International Journal of Heat and Mass Transfer*, 36, (8), 2157-2163.
- Bergles, A.E., Collier, J.G., Delhay, J.M., Hewitt, G.F., & Mayinger, F. (1981). *Two-phase flow and heat transfer in the power and process industries*. New York: Hemisphere Publishing Corporation.
- Breber, G., Palen, J.W., & Taborek, J. (1980). Prediction of horizontal tubeside condensation of pure components using flow regime criteria. *ASME Journal of Heat Transfer*, 102, 471-476.
- Cao, Y., & Faghri, A. (1990). A numerical analysis of phase-change problems including natural convection. *ASME Journal of Heat Transfer*, 112, 812-816.
- Cao, Y., & Faghri, A. (1991). Performance characteristics of a thermal energy storage module: a transient PCM/forced convection conjugate analysis. *International Journal of Heat and Mass Transfer*, 34, (1), 93-101.
- Cao, Y., & Faghri, A. (1992). A study of thermal energy storage systems with conjugate turbulent forced convection. *ASME Journal of Heat Transfer*, 114, 1019-1027.
- Carey, V.P. (1992). *Liquid-vapor phase change phenomena: an introduction to the thermophysics of vaporization and condensation processes in heat transfer equipment*. New York: Hemisphere Publishing Corporation.
- Charach, C., Keizman, Y., & Sokolov, M. (1991). Small Stanton number axisymmetric freezing around a coolant-carrying tube. *International Communications in Heat and Mass Transfer*, 18, 639-657.

- Chato, J.C. (1962). Laminar condensation. *ASHRAE Journal*, 4, 52-60.
- Chisholm, D. (1973). Pressure gradients due to friction during the flow of evaporating two-phase mixtures in smooth tubes and channels. *International Journal of Heat and Mass Transfer*, 16, 347-348.
- Chitti, M.S., & Anand, N.K. (1996). A heat transfer correlation for condensation inside horizontal smooth tubes using the population balance approach. *International Journal of Heat and Mass Transfer*, 39, (14), 2947-2956.
- Dobson, M.K., & Chato, J.C. (1998). Condensation in smooth horizontal tubes. *ASME Journal of Heat Transfer*, 120, 193-213.
- Egolf, P.W., & Manz, H. (1994). Theory and modeling of phase change materials with and without mushy regions. *International Journal of Heat and Mass Transfer*, 37, (18), 2917-2924.
- Esen, M., & Ayhan, T. (1996). Development of a model compatible with solar assisted cylindrical energy storage tank and variation of stored energy with time for different phase change materials. *Energy Conversion and Management*, 37, (12), 1775-1785.
- Gnielinski, V. (1976). *International Journal of Chemical Engineering*, 16, 359-368.
- Gosney, W.B. (1982). *Principles of refrigeration*. Cambridge: Cambridge University Press.
- Gungor, K.E., & Winterton, R.H.S. (1986). A general correlation for flow boiling in tubes and annuli. *International Journal of Heat and Mass Transfer*, 29, (3), 351-358.
- Gungor, K.E., & Winterton, R.H.S. (1987). Simplified general correlation for saturated flow boiling and comparisons of correlations with data. *Chemical Engineering Research and Design*, 65, 148-156.
- Hamdan, M.A., & Elwerr, F.A. (1996). Thermal energy storage using a phase change material. *Solar Energy*, 56, (2), 183-189.
- Hansen, T. (1996). Cool storage may help solve peaking capacity dilemmas. *Power Engineering*, September, 32-39.
- Hasan, A. (1994). Thermal energy storage system with stearic acid as phase change material. *Energy Conversion and Management*, 35, (10), 843-856.

- Hsu, C.F., & Sparrow, E.M. (1981). A closed-form analytical solution for freezing adjacent to a plane wall cooled by forced convection. *ASME Journal of Heat Transfer*, 103, (3), 596-598.
- Hsu, C.F., Sparrow, E.M., & Patankar, S.V. (1981). Numerical solution of moving boundary problems by boundary immobilization and a control-volume-based finite-difference scheme. *International Journal of Heat and Mass Transfer*, 24, (8), 1335-1343.
- Jaster, H., & Kosky, P.G. (1976). Condensation heat transfer in a mixed flow regime. *International Journal of Heat and Mass Transfer*, 19, 95-99.
- Kandlikar, S.G. (1990). A general correlation for saturated two-phase flow boiling heat transfer inside horizontal and vertical tubes. *ASME Journal of Heat Transfer*, 112, 219-228.
- Kandlikar, S.G. (1991). Development of a flow boiling map for subcooled and saturated flow boiling of different fluids inside circular tubes. *ASME Journal of Heat Transfer*, 113, 190-200.
- Kandlikar, S.G. (Ed.). (1999). *Handbook of Phase Change*. Philadelphia. Taylor & Francis.
- Kays, W.M., & Crawford, M.E. (1993). *Convective Heat and Mass Transfer*. New York. McGraw Hill.
- Knebel, D.E. (1995). Predicting and evaluating the performance of ice harvesting thermal energy storage systems. *ASHRAE Journal*, 37, 22-30.
- Lee, A.H., & Jones, J.W. (1996). Laboratory performance of an ice-on-coil, thermal-energy storage system for residential and light commercial applications. *Energy*, 21, (2), 115-130.
- Lee, A.H., & Jones, J.W. (1996). Modeling of an ice-on-coil thermal energy storage system. *Energy Conversion and Management*, 37, (10), 1493-1507.
- Liu, X. (1997). Condensing and Evaporating Heat Transfer and Pressure Drop Characteristics of HFC-134a and HCFC-22. *ASME Journal of Heat and Mass Transfer*, 119, 158-163.
- Liu, Z., & Winterton, R.H.S. (1991). A general correlation for saturated and subcooled flow boiling in tubes and annuli, based on a nucleate pool boiling equation. *International Journal of Heat and Mass Transfer*, 34, (11), 2759-2766.

- Lockhart, R.W., & Martinelli, R.C. (1949). Proposed correlation of data for isothermal two-phase, two-component flow in pipes. *Chemical Engineering Progress*, 45, (1), 39-48.
- Masella, J.M., Tran, Q.H., Ferre, D., & Pauchon, C. (1998). Transient simulation of two-phase flows in pipes. *International Journal of Multiphase Flow*, 24, 739-755.
- McQuiston, F.C., & Parker, J.D. (1994). *Heating, ventilating, and air conditioning: analysis and design* (Fourth Edition). New York: John Wiley & Sons, Inc.
- Murray, W.D., & Landis, F. (1959). Numerical and machine solutions of transient heat-conduction problems involving melting or freezing. *ASME Journal of Heat Transfer*, 81, 106-112.
- National Renewable Energy Laboratory, a DOE national laboratory. (1995, July). Keep it cool with thermal energy storage. *Tomorrow's Energy Today*. Retrieved May 1, 2002, from [http://www.eren.doe.gov/cities\\_counties/thermal.html](http://www.eren.doe.gov/cities_counties/thermal.html).
- Off-Peak/Elite Energy Group, LLC. (2001, April 20). *Ice Thermal Storage*. Retrieved May 1, 2002, from <http://www.off-peak.com/>.
- Ozisik, M.N. (1993). *Heat conduction* (Second Edition). New York: John Wiley & Sons, Inc.
- Ozisik, M.N. (1994). *Finite difference methods in heat transfer*. Boca Raton: CRC Press, Inc.
- Petukhov, B.S. (1970). *Advances in heat transfer*. New York: Academic Press.
- Poland, J.H. (1991). A new household refrigerator/freezer design with three major advantages over present units. *Proceedings 42<sup>nd</sup> International Appliance Technical Conference*. Madison, Wisconsin: May 21 & 22, 1991.
- Ransom, V.H., & Ramshaw, V.H. (1992). *Discrete modeling considerations in multiphase fluid dynamics*. Boca Raton: CRC Press, Inc.
- Rufer, C.E., & Kezios, S.P. (1966). Analysis of two-phase, one-component stratified flow with condensation. *ASME Journal of Heat Transfer*, 88, 265-275.
- Schlager, L.M., Pate, M.B., & Bergles, A.E. (1990). Evaporation and condensation heat transfer and pressure drop in horizontal, 12.7-mm microfin tubes with refrigerant-22. *ASME Journal of Heat Transfer*, 112, 1041-1047.

- Seo, K., & Kim, Y. (2000). Evaporation heat transfer and pressure drop of R-22 in 7 and 9.52 mm smooth/micro-fin tubes. *International Journal of Heat and Mass Transfer*, 43, 2869-2882.
- Shah, M.M. (1979). A general correlation for heat transfer during film condensation inside pipes. *International Journal of Heat and Mass Transfer*, 22, 547-556.
- Shah, M.M. (1982). Chart correlation for saturated boiling heat transfer: equations and further study. *ASHRAE Transactions*, 88, (1), 185-196.
- Shamsundar, N. (1982). Formulae for freezing outside a circular tube with axial variation of coolant temperature. *International Journal of Heat and Mass Transfer*, 25, (10), 1614-1616.
- Smith, G.D. (1985). *Numerical Solution of Partial Differential Equations: Finite Difference Methods*. New York. Oxford University Press.
- Soliman, M., Schuster, J.R., & Berenson, P.J. (1968). A general heat transfer correlation for annular flow condensation. *ASME Journal of Heat Transfer*, 90, 267-276.
- Sparrow, E.M., & Hsu, C.F. (1981). Analysis of two-dimensional freezing on the outside of a coolant-carrying tube. *International Journal of Heat and Mass Transfer*, 24, (8), 1345-1357.
- Springer, G.S. (1969). The effects of axial heat conduction on the freezing or melting of cylinders. *International Journal of Heat and Mass Transfer*, 12, 521-524.
- Takamatsu, H., Momoki, S., & Fujii, T. (1993). A correlation for forced convective boiling heat transfer of pure refrigerants in a horizontal smooth tube. *International Journal of Heat and Mass Transfer*, 36, (13), 3351-3360.
- Tayeb, A.M. (1993). A simulation model for a phase-change energy storage system: experimental and verification. *Energy Conversion and Management*, 34, (4), 43-250.
- Traviss, D.P., Rohsenow, W.M., & Baron, A.B. (1973). Forced convection condensation inside tubes: A heat transfer equation for condenser design. *ASHRAE Transactions*, 79, 1973.
- Vargas, J.V.C., & Bejan, A. (1995). Fundamentals of ice making by convection cooling followed by contact melting. *International Journal of Heat and Mass Transfer*, 38, (15), 2833-2841.

- Yanbing, K., Yinping, Z., Yi, J., & Zhu, Y. (1999). A general model for analyzing the thermal characteristics of a class of latent heat thermal energy storage systems. *ASME Journal of Solar Energy Engineering*, 121, 185-193.
- Yingqiu, Z., Yinping, Z., Yi, J., & Yanbing, K. (1999). Thermal storage and heat transfer in phase change material outside a circular tube with axial variation of the heat transfer fluid temperature. *ASME Journal of Solar Energy Engineering*, 121, 145-149.
- Yoon, J.I., Kwon, O.K., Moon, C.G., Son, Y.S., Kim, J.D., & Kato, T. (2000). Numerical study on cooling phenomenon of water with supercooled region in a horizontal circular cylinder. *Numerical Heat Transfer, Part A*, 38, 357-376.
- Zhang, Y., & Faghri, A. (1996). Heat transfer enhancement in latent heat thermal energy storage system by using the internally finned tube. *International Journal of Heat and Mass Transfer*, 39, (15), 3165-3173.
- Zhang, Y., & Faghri, A. (1996). Semi-analytical solution of thermal energy storage system with conjugate laminar forced convection. *International Journal of Heat and Mass Transfer*, 39, (4), 717-724.
- Zhang, Y., Chen, Z., & Faghri, A. (1997). Heat transfer during solidification around a horizontal tube with internal convective cooling. *ASME Journal of Heat Transfer*, 119, 44-47.
- Zivi, S.M. (1964). Estimation of steady-state steam void-fraction by means of the principle of minimum entropy production. *ASME Journal of Heat Transfer*, 86, 247-252.
- Zuber, N. (1960). On the variable-density single-fluid model for two-phase flow. *ASME Journal of Heat Transfer*, 82, 255-258.
- Zuber, N., & Findlay, J.A. (1965). Average volumetric concentration in two-phase flow systems. *ASME Journal of Heat Transfer*, 87, 453-468.



## APPENDIX A

### The Algorithm

```
PROGRAM Ice Bank Model
C
C
C*****
C
C    You must first set the refrigerant properties for
C    the refrigerant you are using in Subroutine 'REFRIGPROPS'
C    and adjust the Variable Properties in Subroutine
C    'VARIABLEPROPS'
C
C*****
C
C    INCLUDE 'PARSOL.FOR'
C    INCLUDE 'PRESOL.FOR'
C    INCLUDE 'COMSOL.FOR'
C
C*****
C
C    Define File for Results
C
C    OPEN(UNIT=8,FILE='RefOut')
C    OPEN(UNIT=9,FILE='IceOut')
C
C*****
C
C    Select System of Units in which Program will compute
C    If U.S. Units (1), SI Units (2):
C
C    UNITS = 1
C
C*****
C
C    Indicate whether you want to run this program in Condensing
C    Mode (1), Evaporating Mode (2), or Start-Up Mode (3) [Start-Up
C    Mode always begins with Evaporating Mode in order to build
C    Ice Bank and is used with N=1 below.]
C
C    MODE = 2
C
C    IF(MODE.EQ.1)THEN
C        WRITE(8,*)'Condensing Mode'
C    ELSE
C        WRITE(8,*)'Evaporating Mode'
C    ENDIF
C
C*****
C
C    If you are running only one mode, N=0;
C    if alternating modes, N=1
C
C    N=0
C
```

```

C*****
C
C      CALL VARIABLEPROPS
C
C      CALL REFRIGPROPS
C
C      WRITE(8,*) 'REFRIGERANT PROPERTIES:'
C      WRITE(8,*)
C      IF(UNITS.EQ.1) THEN
C
C          WRITE(8,4991) REFRIG, TSAT, PSAT, HFG, SPVOLL, SPVOLV, MUL, MUV, KL, KV,
C          &
C          CPL, CPV
C          ELSE
C
C          WRITE(8,4992) REFRIG, TSAT, PSAT, HFG, SPVOLL, SPVOLV, MUL, MUV, KL, KV,
C          &
C          CPL, CPV
C      ENDIF
4991 FORMAT(1X, 'REFRIGERANT'           = ',A5,/1X,
&'SATURATION TEMPERATURE             = ',F7.4,' DEG F'/1X,
&'SATURATION PRESSURE                 = ',F9.4,' PSIA'/1X,
&'LATENT HEAT OF VAPORIZATION          = ',F7.4,' BTU/LBM'/1X,
&'SPECIFIC VOLUME OF LIQUID            = ',F7.4,' FT^3/LBM'/1X,
&'SPECIFIC VOLUME OF VAPOR             = ',F7.4,' FT^3/LBM'/1X,
&'VISCOSITY OF LIQUID                  = ',F7.4,' LBM/H-FT'/1X,
&'VISCOSITY OF VAPOR                   = ',F7.4,' LBM/H-FT'/1X,
&'THERMAL CONDUCTIVITY OF LIQ.         = ',F7.4,' BTU/H-FT-F'/1X,
&'THERMAL CONDUCTIVITY OF VAP.         = ',F7.4,' BTU/H-FT-F'/1X,
&'SPECIFIC HEAT OF LIQUID              = ',F7.4,' BTU/LBM-F'/1X,
&'SPECIFIC HEAT OF VAPOR               = ',F7.4,' BTU/LBM-F'//)
C
4992 FORMAT(1X, 'REFRIGERANT'           = ',A5,/1X,
&'SATURATION TEMPERATURE             = ',F7.4,' DEG K'/1X,
&'SATURATION PRESSURE                 = ',F9.4,' kPa'/1X,
&'LATENT HEAT OF VAPORIZATION          = ',F7.4,' J/kg'/1X,
&'SPECIFIC VOLUME OF LIQUID            = ',F7.4,' m^3/kg'/1X,
&'SPECIFIC VOLUME OF VAPOR             = ',F7.4,' m^3/kg'/1X,
&'VISCOSITY OF LIQUID                  = ',F7.4,' N-s/m^2'/1X,
&'VISCOSITY OF VAPOR                   = ',F7.4,' N-s/m^2'/1X,
&'THERMAL CONDUCTIVITY OF LIQ.         = ',F7.4,' J/s-m-K'/1X,
&'THERMAL CONDUCTIVITY OF VAP.         = ',F7.4,' J/s-m-K'/1X,
&'SPECIFIC HEAT OF LIQUID              = ',F7.4,' J/kg-K'/1X,
&'SPECIFIC HEAT OF VAPOR               = ',F7.4,' J/kg-K'//)
C
C      CALL ICEBANKPROPS
C
C      CALL CLEAR
C
C      PARAMETERS WHICH ARE CONSTANT AND USED REPEATEDLY:
C
C      IF(UNITS.EQ.1) THEN
C          D=DIA/12.0D0                !(ft)Pipe Diameter
C      ELSE
C          D=DIA
C      ENDIF
C      PI = 3.1415927D0
C      ACS = PI*(D**2D0)/4D0          !(ft^2)Pipe X-Sect. Area
C      MASSVEL = MDOT/ACS

```

```

VISRATIO = MUL/MUV
VOLRATIO = SPVOLL/SPVOLV
PRL = MUL*CPL/KL
PRV = MUV*CPV/KV
G = 9.81 ! (m/s^2)
GC = 32.174D0*(3600.0D0**2D0) ! (lbm-ft/lbf-hr^2)
REL=MASSVEL*D/MUL
VL=MASSVEL*SPVOLL
VV=MASSVEL*SPVOLV
HL = CPL*(1/SPVOLL)*VL*EXP(-3.796-0.205D0*DLOG(REL) -
& 0.505D0*DLOG(PRL)-0.0225D0*DLOG(PRL)**2D0)
REV=MASSVEL*D/MUV
NU = 0.023D0*(PRV**0.4D0)*(REV**0.8D0)
HV = NU*KV/D !HeatTransf.Coeff.Vapor

C
C*****
C
C SET INITIAL CONDITIONS FOR
C REFRIGERANT TUBE
C
C*****
Q=0.D0
DO I=1,IMAX
    TR(I)=TSAT
    TW(I)=TWALL
    P(I)=PSAT
ENDDO
C*****
C
C SET INITIAL CONDITIONS FOR ICE BANK
C
C*****
QICE=0.D0
VTOTAL=0.D0
DO I=2,IM1
    DO J=2,JM1
        T(I,J)=TWALL
        IF(MODE.EQ.1) THEN
            QUALITY(I,J)='SOLID'
            HWS(I,J)=(T(I,J)-TM)*CPS-LH
            K(I,J)=KS
            RHO(I,J)=RHOS
        ELSE
            QUALITY(I,J)='LIQUID'
            HWS(I,J)=(T(I,J)-TM)*CPW
            K(I,J)=KW
            RHO(I,J)=RHOW
        ENDIF
        V=(PI*DZ/4.D0)*(((2.D0*(J-1D0)*DR+D)**2.D0)-
& ((2.D0*(J-2D0)*DR+D)**2.D0))
        VTOTAL=VTOTAL+V
    ENDDO
ENDDO
WRITE(9,*)'Total Volume of Ice Bank=',VTOTAL
C*****
C

```

```

C      INITIALIZES REFRIGERANT TUBE BY SELECTING MODE:
C
C*****
      IF (MODE.EQ.1) THEN
          CALL CONDENSING
      ELSE
          CALL EVAPORATING
      ENDIF
C*****
C
C      BEGIN TRANSIENT PROBLEM :
C
C*****
C*****Compute Time Increment
C
      DT=(RHOS*CPS*(DR**2.)*(DZ**2.))/(2.*KS*(2*(DZ**2.)+ DR**2.))
C      WRITE(9,*) 'DT=', DT
C      WRITE(9,*) 'DT=', DT*3600., 'SECONDS'
C      WRITE(9,*) 'END TIME  =', TEND*3600, 'SECONDS'
C
C*****Initialize Time
C
      TC = 0.D0                !Overall Time Counter
      TC2= 0.D0                !Time Counter for each mode
C
C*****MAIN LOOP
C
      DO WHILE (TC.LE.TEND)
          TC=TC+DT
          TC2=TC2+DT
          WRITE(6,*) 'TIME=', TC, 'hours'
          WRITE(9,*) 'TIME=', TC, 'hours'
C
C      *****Set Boundary Condition Temperatures
C
C      *****AT Z = 0 (Insulated Boundary):
          DO J=2, JM1
              T(1, J)=T(2, J)
          ENDDO
C
C      *****AT Z = LENGTH (Insulated Boundary):
          DO J=2, JM1
              T(IMAX, J)=T(IM1, J)
          ENDDO
C
C      *****AT R = RO of Ice Bank (Insulated Boundary):
          DO I=1, IMAX
              T(I, JMAX)=T(I, JM1)
          ENDDO
C
C      *****Update cell properties:
C
          DO J=2, JM1
              DO I=2, IM1
                  IF (QUALITY(I, J).EQ.'SOLID') THEN
                      K(I, J)=KS

```

```

                                RHO(I,J)=RHOS
ELSEIF(QUALITY(I,J).EQ.'LIQUID') THEN
                                K(I,J)=KW
                                RHO(I,J)=RHOW
ELSE
                                K(I,J)=KW-HWS(I,J)*(KS-KW)/LH
                                RHO(I,J)=RHOW-HWS(I,J)*(RHOS-RHOW)/LH
ENDIF
ENDDO
ENDDO
C
C *****Compute New Temperatures of Real Cells:
C
C *****AT FIRST REAL ROW (J=2):
C      DO I=2,IM1
C          LEFT2=(K(I-1,2)+K(I,2))*((DW+2.D0*DR)**2.D0)-
&          (DW**2.D0)*(T(I-1,2)-T(I,2))/(8.D0*DZ)
C
C          BOTTOM2=H(I)*D*DZ*(TR(I)-TW(I))
C
C          RIGHT2=(K(I,2)+K(I+1,2))*((DW+2.D0*DR)**2.D0)-
&          (DW**2.D0)*(T(I,2)-T(I+1,2))/(8.D0*DZ)
C
C          TOP2=((DW+DR)*K(I,2)+(DW+3.D0*DR)*K(I,3))*(DW+2.D0*DR)*DZ*
&          (T(I,2)-T(I,3))/((2.D0*DW+4.D0*DR)*DR)
C
C          HWSN(I,2)=HWS(I,2)+4.D0*DT*(LEFT2+BOTTOM2-RIGHT2-
&          TOP2)/(RHO(I,2)*DZ*((DW+2.D0*DR)**2.D0)-(DW**2.D0))
C      ENDDO
C
C *****Remainder of Real Cells:
C
C      DO J=3,JM1
C          DO I=2,IM1
C
C              VJBOT=((J-2)*2.D0*DR+DW)**2.D0-((J-
&              3)*2.D0*DR+DW)**2.D0)
C
C              VJ=((J-1)*2.D0*DR+DW)**2.D0-((J-
&              2)*2.D0*DR+DW)**2.D0)
C
C              VJTOP=((J*2.D0*DR+DW)**2.D0-((J-
&              1)*2.D0*DR+DW)**2.D0)
C
C              LEFT=(K(I-1,J)+K(I,J))*VJ*(T(I-1,J)-
&              T(I,J))/(8.D0*DZ)
C
C              BOTTOM=(VJBOT*K(I,J-1)+VJ*K(I,J))*((J-
&              2)*2.D0*DR+DW)*DZ*(T(I,J-1)-
&              T(I,J))/((VJBOT+VJ)*DR)
C
C              RIGHT=(K(I,J)+K(I+1,J))*VJ*(T(I,J)-T(I+1,J))
&              /(8.D0*DZ)
C
C              TOP=(VJ*K(I,J)+VJTOP*K(I,J+1))*((J-
&              1)*2.D0*DR+DW)*DZ*(T(I,J)-

```

```

C      &          T(I,J+1))/((VJ+VJTOP)*DR)
C
C      &          HWSN(I,J)=HWS(I,J)+4.D0*DT*(LEFT+BOTTOM-RIGHT-
C      &          TOP)/(RHO(I,J)*DZ*VJ)
C
C          ENDDO
C      ENDDO
C
C      *****Compute Heat Transferred
C
C          DO J=2,JM1
C              DO I=2,IM1
C
C                  V=(PI*DZ/4.D0)*((2.D0*(J-1)*DR+DW)**2.D0)-
C      &          ((2.D0*(J-2)*DR+DW)**2.D0)
C                  QICE=QICE+RHO(I,J)*V*(HWSN(I,J)-HWS(I,J))
C
C      *****Designate Quality of Each Cell
C
C                  IF(HWSN(I,J).LE.-LH) THEN
C                      QUALITY(I,J)='SOLID'
C                      TN(I,J)=TM+(HWSN(I,J)+LH)/CPS
C                  ELSEIF(HWSN(I,J).GE.0.) THEN
C                      QUALITY(I,J)='LIQUID'
C                      TN(I,J)=TM+HWSN(I,J)/CPW
C                  ELSE
C                      QUALITY(I,J)='MIXED'
C                      TN(I,J)=TM
C                  ENDIF
C              ENDDO
C          ENDDO
C
C      *****Assign New Enthalpy and Temp. Values to Old Arrays:
C
C          DO J=2,JM1
C              DO I=2,IM1
C                  HWS(I,J)=HWSN(I,J)
C                  T(I,J)=TN(I,J)
C              ENDDO
C          ENDDO
C
C      *****Write Output to Icebank Output File:
C      IF(TC.GT.TEND-DT) THEN
C      IF(TC2.GT.Tstartup-DT) THEN
C          WRITE(9,*)'QEND=',QICE
C          WRITE(9,*)
C          WRITE(9,*)'CELL'          TEMP.
C      &      ENTHALPY      QUALITY'
C          IF(UNITS.EQ.1) THEN
C              WRITE(9,*)'ROW'      COLUMN      (F)
C      &      (Btu/lbm)'
C
C          DO J=2,JM1
C              DO I=2,IM1
C
C              WRITE(9,7000)J,I,T(I,J),HWS(I,J),QUALITY(I,J)
7000      FORMAT(I3,2X,I7,F7.2,F10.3,5X,A6)

```



```

C
      ENDDO                                     !End Of Main Loop

      end

C*****
C
C      SET VARIABLE PROPERTIES:
C
C*****
      SUBROUTINE VARIABLEPROPS
C
      INCLUDE 'PARSOL.FOR'
      INCLUDE 'PRESOL.FOR'
      INCLUDE 'COMSOL.FOR'
C
      IF(UNITS.EQ.1) THEN
          QDOT=4200.D0      !(Btu/hr-ft^2) Heat Flux, Init.
          PSAT=115.8d0      !(psia)Entering Sat.Pressure
          PSATC=115.8D0     !For 1st cell of Cond. Tube 115.8 for 60F
          PSATE=67.21D0     !For 1st cell of Evap. Tube 57.6 for 20F
          MDOT=18.41D0      !(lbm/hr)Mass Flow Rate through Cond.
          MDOTE=28.D0       !(lbm/hr)Mass Flow Rate through Evap.
          MDOTST=11.8D0     !(lbm/hr)Mass Flow through Evap.@Start-up

          DIA=0.315D0       !(inches)Inside Diameter of Ref.Tube
          DW=0.375/12D0     !(ft)Outside Diameter of Ref. Tube
          RI=DIA/(2.D0*12.D0)  !(feet)Inside Radius (Ref.Tube)
          RO=1.2225D0/12.D0  !(feet)Outside Radius (Ice Bank) (1.2225)
          DR=0.01078125D0    !Increment in r-dir. 0.01078125
          TWALL=70.D0        !(F)Initial Wall Temperature
          THETA=0.0          !(degrees)Angle of Inclination
          LENGTH=43.D0       !(feet)Length of Pipe
          DZ=0.005D0         !(feet)Cell Width in i-direction
          TCOND=0.002D0      !(hour)Time in Condensing Mode
          TEVAP=0.083333D0   !(hour)Time in Evaporating Mode
          TSTARTUP=1.2D0     !(hour)Time in Start-up
          TEND=0.083333D0    !(hour)End Time of TransientProblem
      ELSE
          QDOT=50.D0         !(W/m^2)Heat Flux, Initial Guess
          PSAT=798.413d0     !(kPa)Entering Sat.Pressure
          PSATC=798.413D0    !For 1st cell of Cond. Tube
          PSATE=397.D0       !For 1st cell of Evap. Tube
          MDOT=0.00504D0     !(kg/s)Mass Flow Rate through Cond.
          MDOTE=0.0063D0     !(kg/s)Mass Flow Rate through Evap.
          MDOTST=0.0063D0    !(kg/s)Mass Flow at Start-up

          DIA=0.008D0        !(m)Inside Diameter of Ref. Tube
          DW=0.008D0         !(m)Outside Diameter of Ref. Tube
          RI=DIA/2.D0        !(m)Inside Radius (Ref.Tube)
          RO=0.064D0         !(m)Outside Radius (Ice Bank)
          DR=0.001463D0      !Increment in r-dir.
          TWALL=288.D0       !(K)Initial Wall Temperature
          THETA=0.0          !(degrees)Angle of Inclination
          LENGTH=9.144D0     !(m)Length of Pipe
          DZ=0.001829D0      !(m)Cell Width in i-direction
          TCOND=600.D0       !(s)Time in Condensing Mode
      ENDIF
    END
  END

```



```

                TEVAP=360.D0                !(s)Time in Evaporating Mode
                TSTARTUP=720.D0            !(s)Time in Evap. Mode with Ice
C                                                initially at room temp
                TEND=600.0D0                !(s)End Time of Transient Problem
C
                ENDIF
C
                IBAR=INT(LENGTH/DZ)        !Number of real cells in i-dir.
                IMAX=IBAR+2                !Number of real cells + 2 fict.
C                                                cells
                IM1=IMAX-1                ;
                JBAR=INT((RO-RI)/DR)        !Number of real cells in j-dir
                JMAX=JBAR+2                !Number of real cells + 2 fict. cells
                JM1=JMAX-1
C
                WRITE(8,*) 'VARIABLE PROPERTIES:'
                WRITE(8,*)
                IF(UNITS.EQ.1) THEN
                    WRITE(8,4990)MDOT,DIA,RO*2*12,TWALL,THETA,DZ
                ELSE
                    WRITE(8,4993)MDOT,DIA,RO*2,TWALL,THETA,DZ
                ENDIF
4990 FORMAT(1X,'MASS FLOW RATE                = ',F7.4,' LBM/HR'/1X,
&'REF.TUBE INNER DIAMETER                = ',F7.4,' IN'/1X,
&'ICE BANK TUBE DIAMETER                = ',F7.4,' IN'/1X,
&'WALL TEMPERATURE                = ',F7.4,' DEG F'/1X,
&'ANGLE OF INCLINE                = ',F7.4,' DEGREES'/1X,
&'CELL INCREMENT ALONG TUBE                = ',F7.4,' FEET'/)
C
4993 FORMAT(1X,'MASS FLOW RATE                = ',F7.4,' kg/s'/1X,
&'REF.TUBE INNER DIAMETER                = ',F7.4,' m'/1X,
&'ICE BANK TUBE DIAMETER                = ',F7.4,' m'/1X,
&'WALL TEMPERATURE                = ',F7.4,' DEG K'/1X,
&'ANGLE OF INCLINE                = ',F7.4,' DEGREES'/1X,
&'CELL INCREMENT ALONG TUBE                = ',F7.4,' m'/)
                RETURN
                END
C
C*****
C
C    SET REFRIGERANT PROPERTIES
C
C*****
                SUBROUTINE REFRIGPROPS
C
                INCLUDE 'PARSOL.FOR'
                INCLUDE 'PRESOL.FOR'

                INCLUDE 'COMSOL.FOR'
C
                REFRIG ='R-22'
C
                IF(UNITS.EQ.1) THEN
C
C    The following expression for TSAT applies for only values
C    of 2<PSAT<210 psia
C

```

```

C      TSAT=93.81D0*(PSAT**(1D0/4.43D0))-214.2D0  !(F) Saturation Temp.
C
C      TBOIL =-41.35D0          !(F) Boiling Pt. Temp.
C      TCRT  =204.8D0          !(F) Critical Temp.
C      PC    =4986.0D0         !(kPa) Critical Pressure
C      PCRT  =723.74D0         !(psia)Critical Pressure
C
C      PWALL=3E-05*(TWALL**3D0)+6.5E-03*(TWALL**2D0)
C      & +0.8118D0*TWALL+38.735D0
C      MUL  = 2.1491D0*(PSAT**(-0.3386D0))
C      MUV  = 3E-03*DLOG(PSAT)+0.0159D0
C      SPVOLL = 1.1E-03*DLOG(PSAT)+0.0079D0
C      SPVOLV = 46.151D0*(PSAT**(-0.963D0))
C      VFG = SPVOLV - SPVOLL
C      KL = 0.0954D0*(PSAT**(-0.1279D0))
C      KV = 2.35E-03*(PSAT**0.1977D0)
C      CPL = -2E-07*(PSAT**2D0)+3E-04*PSAT+0.257D0
C      CPV = -1E-06*(PSAT**2D0)+6E-04*PSAT+0.1379D0
C      HFG = 4E-04*(PSAT**2D0)-0.2131D0*PSAT+101.9D0
C
C      ELSE
C
C      The following expressions apply for only values
C      of 105<PSAT<1725 kPa
C
C      TSAT=137.6D0*(PSAT**0.1113)  !(K) Saturation Temp.
C
C      TBOIL =232.41D0          !(K) Boiling Pt. Temp.
C      TCRT  =369.3D0          !(K) Critical Temp.
C      PC    =4986.0D0         !(kPa) Critical Pressure
C
C      PWALL=1.45E-16*(TWALL**7.63)-64.D0          !kPa
C      MUL  = 9E-04*(PSAT**(-0.219))+5E-06          !N-s/m^2
C      MUV  = -6E-13*(PSAT**2)+4E-04*PSAT+1E-05
C      SPVOLL = 3E-14*(PSAT**3)-1E-10*(PSAT**2)+2E-07*PSAT+7E-04  !m^3/kg
C      SPVOLV = 19.638*(PSAT**(-0.9742))
C      VFG = SPVOLV - SPVOLL
C      KL = -0.01*(PSAT**0.28)+0.155                !W/m-K
C      KV = 1.9E-04*(PSAT**0.5)+0.0053
C      CPL = -2E-11*(PSAT**4)+1E-07*(PSAT**3)-2E-04*(PSAT**2)
C      & +0.2917*PSAT+1074.1
C      CPV =-6E-07*(PSAT**2)+0.2481*PSAT+587.18      !J/kg-K
C      HFG = 1.34E-08*(PSAT**2)-7E-05*PSAT+0.2384    !J/kg
C
C      ENDIF
C
C      RETURN
C      END
C
C      *****
C
C      SET ICEBANK PROPERTIES
C
C      *****
C      SUBROUTINE ICEBANKPROPS
C
C      INCLUDE 'PARSOL.FOR'

```

```

      INCLUDE 'PRESOL.FOR'
      INCLUDE 'COMSOL.FOR'
C
      IF(UNITS.EQ.1) THEN
C
      LH = 143.34d0                !(Btu/lbm)Latent Heat of Fusion of
C                                  Water
C
      RHOW = 62.4141805d0          !(lb/ft^3)Density of Water
      RHOS = 57.2409845d0          !(lb/ft^3)Density of Ice
C
      KW = 0.326D0                !(Btu/hr-f-F)Thermal Conductivity
C                                  of Water
      KS = 1.28D0                 !(Btu/hr-f-F)Thermal Conductivity
C                                  of Ice
C
      CPW = 1.0041d0              !(Btu/lb-F)Specific Heat of Water
      CPS = 0.46D0                !(Btu/lb-F)Specific Heat of Ice
C
      TM = 32.0d0                 !(F)Melting Temperature of Ice
C
      KCOPPER=224.0d0              !(BTU/hr-ft-F)
C
      Write Icebank Properties to Output File
C
      WRITE(9,*)'ICEBANK PROPERTIES:'
      WRITE(9,*)
      WRITE(9,6999) LH, RHOW, RHOS, KW, KS, CPW, CPS, TM
6999 FORMAT(1X,'LATENT HEAT OF FUSION      = ',F7.2,' BTU/LBM'/1X,
&'DENSITY OF WATER          = ',F7.4,' LB/FT^3'/1X,
&'DENSITY OF ICE            = ',F7.4,' LB/FT^3'/1X,
&'THERMAL CONDUCT. OF WATER = ',F7.3,' BTU/H-FT-F'/1X,
&'THERMAL CONDUCT. OF ICE  = ',F7.3,' BTU/H-FT-F'/1X,
&'SPECIFIC HEAT OF WATER   = ',F7.4,' BTU/LBM-F'/1X,
&'SPECIFIC HEAT OF ICE     = ',F7.4,' BTU/LBM-F'/1X,
&'MELTING TEMP. OF ICE    = ',F7.2,' F'//)
C
      ELSE
C
      LH = 0.3334d0                !(J/kg)Latent Heat of Fusion of Water
C
      RHOW = 1000.d0               !(kg/m^3)Density of Water
      RHOS = 913.d0               !(kg/m^3)Density of Ice
C
      KW = 0.585D0                !(W/m-K)Thermal Conductivity of
Water
      KS = 2.22D0                 !(W/m-K)Thermal Conductivity of Ice
C
      CPW = 4.202d0               !(J/kg-K)Specific Heat of Water
      CPS = 1.93D0                !(J/kg-K)Specific Heat of Ice
C
      TM = 273.15d0               !(K)Melting Temperature of Ice
C
      KCOPPER=387.7               !(W/m-K)
C
      Write Icebank Properties to Output File
C

```

```

        WRITE(9,*) 'ICEBANK PROPERTIES:'
        WRITE(9,*)
        WRITE(9,6998) LH*1000, RHOW, RHOS, KW, KS, CPW, CPS, TM
6998 FORMAT(1X, 'LATENT HEAT OF FUSION      = ', F7.2, ' kJ/kg'/1X,
&'DENSITY OF WATER                      = ', F7.4, ' kg/m^3'/1X,
&'DENSITY OF ICE                        = ', F7.4, ' kg/m^3'/1X,
&'THERMAL CONDUCT. OF WATER             = ', F7.3, ' W/m-K'/1X,
&'THERMAL CONDUCT. OF ICE               = ', F7.3, ' W/m-K'/1X,
&'SPECIFIC HEAT OF WATER                = ', F7.4, ' J/kg-K'/1X,
&'SPECIFIC HEAT OF ICE                  = ', F7.4, ' J/kg-K'/1X,
&'MELTING TEMP. OF ICE                  = ', F7.2, ' K'//)
C
        ENDIF
        RETURN
        END
C
C*****
C
C      CLEAR ARRAYS
C
C*****
C      SUBROUTINE CLEAR
C
C      INCLUDE 'PARSOL.FOR'
C      INCLUDE 'PRESOL.FOR'
C      INCLUDE 'COMSOL.FOR'
C
C      DO I=1, IMAX
C
C          XI(I)=0.
C          H(I)=0.
C          TR(I)=0.
C          TW(I)=0.
C          DO J=1, JMAX
C              T(I,J)=0.
C              QS(I,J)=0.
C          ENDDO
C      ENDDO
C
C      Q=0. D0
C      RETURN
C      END
C
C*****
C
C      CONDENSING SUBROUTINE
C
C*****
C      SUBROUTINE CONDENSING
C
C      INCLUDE 'PARSOL.FOR'
C      INCLUDE 'PRESOL.FOR'
C      INCLUDE 'COMSOL.FOR'
C
C      PSAT=PSATC
C      CALL REFRIGPROPS
C      TR(2)=TSAT

```

```

C      MASSVEL=MDOT/ACS  !Mass Flux for Condensing mode
      IC = 0
      X = 0.9999D0
      Z = 0.0
      P(2) = PSATC
      IF(TC.GE.TEND-DT) THEN
C      IF(TC2.GE.TCOND-DT) THEN
      WRITE(8,*) 'Cell#      X      Rel      Vliq      Rev      Vvap      h
&      Q      z      P      TR      TW'
      IF(UNITS.EQ.1) THEN
      WRITE(8,*) '
B/hf2F      f/m      f/m
&      Btu/h      ft      psia      F      F'
      ELSE
      WRITE(8,*) '
      m/s      W/m^2-K      m/s
&      W      m      kPa      K      K'
      ENDIF
      ENDIF
5000 FORMAT(I7,1x,F6.4,F7.0,F7.2,F9.0,F7.0,F9.2,F10.1,F8.3,F9.3,
&          2X,F7.2,2X,F7.2)
C
C*****
C
C      Determine Value of DX for
C      given constant DZ:
C
C*****
C
      I = 2
      DO WHILE((X.GT.0.).AND.(Z.LT.LENGTH).AND.(TC.LT.TEND))
        IC = IC+1
C
        REL = (1.0 - X)*MASSVEL*D/MUL
        REV = X*MASSVEL*D/MUV
        ALPHA=1.0/(1.0 + ((1.0-X)/X)*(VOLRATIO**(2/3)))
        IF(UNITS.EQ.1) THEN
          VLIQ = (1.0 - X)*MASSVEL*SPVOLL/60.
          VVAP = X*MASSVEL*SPVOLV/60.
        ELSE
          VLIQ = (1.0 - X)*MASSVEL*SPVOLL
          VVAP = X*MASSVEL*SPVOLV
        ENDIF
C
C*****Need to choose between using Shah correlation (massflux
C      greater than 100 kg/m^2*s or 73730 lb/ft^2*hr) or
C      Dobson-Chato correlation (4/8/02)
C
      IF(UNITS.EQ.1) THEN
        IF(MASSVEL.GE.73730.D0) THEN
          GOTO 5003
        ELSE
          GOTO 5001
        ENDIF
      ELSEIF(UNITS.EQ.2) THEN
        IF(MASSVEL.GE.100.D0) THEN

```

```

                                GOTO 5003
                        ELSE
                                GOTO 5001
                        ENDIF
    ENDIF
C*****Using Method of Dobson & Chato (1998) Stratified Flow portion
c*****only.
    5001    GA=GC*((1/SPVOLL)-(1/SPVOLV))*(D**3.)/(SPVOLL*(MUL**2.))
            CHI=(VISRATIO**0.1)*(((1.0-X)/X)**0.9)*(VOLRATIO**0.5)
            THETAL=PI*(1-(ACOS(2*ALPHA-1))/PI)
            IF(UNITS.EQ.1) THEN
                    FRL=((MASSVEL**2.)*(SPVOLL**2.))/(GC*D)
            ELSE
                    FRL=((MASSVEL**2.)*(SPVOLL**2.))/(G*D)
            ENDIF
            IF(FRL.LE.0.7) THEN
                    C1=4.172D0+5.48D0*FRL-1.564D0*(FRL**2)
                    C2=1.773D0-0.169D0*FRL
            ELSE
                    C1=7.242D0
                    C2=1.655D0
            ENDIF
            PHIL=(1.376D0+(C1/(CHI**C2)))**0.5
            REVO=MASSVEL*D/MUV
    5002    JAL=CPL*(TR(I)-TW(I))/HFG
            NUF=0.0195D0*(REL**0.8)*(PRL**0.4)*PHIL
            NU=0.23*(REVO**0.12)*((GA*PRL/JAL)**0.25)
            &          /(1+1.11*(CHI**0.58))+(1-THETAL/PI)*NUF
            H(I)=KL*NU/D
            NUC(I)=NU
    C          ENDIF
C*****Update wall temperature and recalculate h if necessary:
            IF((TR(I)-TW(I)).LE.0.D0) THEN
                    WRITE(6,*)'You need a larger temperature difference
                    &          to maintain Condensation.'
                    write(9,*)'T=',t
                    write(9,*)'z=',z
                    STOP
            ENDIF
    C
            QPRIME=(TR(I)-T(I,2))/(((H(I)*PI*D)**(-1))+
            &          ((2*PI*KCOPPER)**(-1))*DLOG(DW/D)+
            &          ((2*PI*K(I,2))**(-1))*DLOG((DW+DR)/DW))
            TWALL=TR(I)-QPRIME/(H(I)*PI*D)
    C
            IF(ABS(TW(I)-TWALL).GT.0.1) THEN
                    TW(I)=TWALL
                    GOTO 5002
            ENDIF
            GOTO 5004
    C
C*****Using Method of Shah (1989)
C*****Recommended for  $11 < \text{massvel} < 211 \text{ kg/m}^2\text{-s}$ ,  $0 < x < 1$ ,  $1 < \text{Prl} < 13$ 
    5003    RELO=MASSVEL*D/MUL
            HLO=0.023*KL*(RELO**0.8D0)*(PRL**0.4D0)/D
            IF(UNITS.EQ.1) THEN
                    H(I)=HLO*((1-X)**0.8D0)+(3.8D0*(X**0.76D0))*((1-

```

```

&          X)**0.04D0)) / ((P(I)/PCRT)**0.38D0))
      NUC(I)=H(I)*D/KL
    ELSE
      H(I)=HLO*((1-X)**0.8D0)+(3.8D0*(X**0.76D0)*((1-
&          X)**0.04D0)) / ((P(I)/PC)**0.38D0))
      NUC(I)=H(I)*D/KL
    ENDIF
C*****Update wall temperature:
    IF((TR(I)-TW(I)).LE.0.D0) THEN
      WRITE(6,*)'You need a larger temperature difference
&          to maintain Condensation.'
      write(9,*)'T=',t
      write(9,*)'z=',z
      STOP
    ENDIF
    QPRIME=(TR(I)-T(I,2))/(((H(I)*PI*D)**(-1))+
&          ((2*PI*KCOPPER)**(-1))*DLOG(DW/D)+
&          ((2*PI*K(I,2))**(-1))*DLOG((DW+DR)/DW))
    TWALL=TR(I)-QPRIME/(H(I)*PI*D)
    TW(I)=TWALL
C
  5004      DX=DZ*4.D0*(H(I))*(TR(I)-TW(I))/(MASSVEL*HFG*D)
C
C*****Write results to output file
C
      IF(TC.GE.TEND-DT) THEN
c          if(tc2.ge.tcond-dt) then

      WRITE(8,5000) I,X,REL,VLIQ,REV,VVAP,NUC(I),Q,Z,P(I),TR(I),TW(I)
      endif
C
      IF(IC.EQ.1) THEN

      WRITE(6,5000) I,X,REL,VLIQ,REV,VVAP,H(I),Q,Z,P(I),TR(I),
&          TW(I)
      ENDIF
C
      Q = Q + H(I)*PI*D*DZ*(TW(I)-TR(I))
C
C*****
C
C      Now procede to calculate the corresponding pressure gradient
C      and drop in the tube.
C*****
C
      DXDZ=-DX/DZ
      IF(UNITS.EQ.1) THEN
C
      DPDZFA=(MUV**0.2D0)*((MASSVEL*X)**1.8D0)*SPVOLV/
&          (GC*(D**1.2D0))
      DPDZF=-0.09D0*((1.D0+2.85D0*(CHI**0.523D0))**2)*DPDZFA
      DPDZMB=(MASSVEL**2.D0)*DXDZ*SPVOLV/GC
      DPDZM=-DPDZMB*(2.D0*X+(1.D0-2.D0*X)*(VOLRATIO**(1.D0/3.D0)
&          +VOLRATIO**(2.D0/3.D0))-(2.D0-2.D0*X)*VOLRATIO)
      DPDZG=SIN(THETA)*GC/GC*(ALPHA/SPVOLV+(1.0-ALPHA)/SPVOLL)
      DPDZ=DPDZF+DPDZM+DPDZG
      P(I+1)= P(I)+DPDZ*DZ/144.0D0

```

```

C          PSAT=P(I+1)
C
C          ELSE
C
C          DPDZFA=(MUV**0.2)*((MASSVEL*X)**1.8)*SPVOLV/(D**1.2)
C          DPDZF=-0.09D0*((1.D0+2.85D0*(CHI**0.523))**2)*DPDZFA
C          DPDZMB=(MASSVEL**2)*DXDZ*SPVOLV
C          DPDZM=-DPDZMB*(2.0D0*X+(1.0D0-2.0D0*X)*(VOLRATIO**(1D0/3D0)
&          + VOLRATIO**(2D0/3D0))-(2.0D0-2.0D0*X)*VOLRATIO)
C          DPDZG=SIN(THETA)*G*(ALPHA/SPVOLV+(1.0-ALPHA)/SPVOLL)
C          DPDZ=DPDZF+DPDZM+DPDZG
C          P(I+1)= P(I)+DPDZ*DZ*1E+03          ! kPa
C          PSAT=P(I+1)
C
C          ENDIF
C
C          NLCONDC=I          !# of Last Condensing Cell
C
C          Z=Z+DZ
C
C          I=I+1
C
C          Update Saturation Temp. and Refrigerant Props.
C
C          CALL REFRIGPROPS
C          TR(I)=TSAT
C
C          X=X-DX
C
C          IF(X.LE.0)GOTO 8000
C
C          ENDDO
C
C          8000 WRITE(6,5000) I,X,REL,VLIQ,REV,VVAP,NUC(I),Q,Z,P(I),TR(I),TW(I)
C
C          *****
C
C          ALL-LIQUID ZONE
C
C          *****
C
C          IF(TC.GE.TEND-DT) THEN
C          IF(TC2.GE.TCOND-DT) THEN
C          WRITE(8,*)
C          WRITE(8,*) 'Cell#      X      Rel      VLIQ      h      Q      z
&      P      TR      TW'
C          IF(UNITS.EQ.1) THEN
C          WRITE(8,*) '
&psia      F'
C          ELSE
C          WRITE(8,*) '
&kPa      K'
C          ENDIF
C          ENDIF
C
C          DO I=NLCONDC+1,IM1

```



```

      X=0.
C
C*****Compute mean temperature
C
      8002          TSAT=(TR(I)+TW(I))/2.D0
C
C*****Update vapor properties as a function of temperature
      IF(UNITS.EQ.1) THEN
          SPVOLL=0.012D0*EXP(0.0014D0*TSAT)          ! (ft^3/lbm)
          MUL=0.6158D0*EXP(-0.0006D0*TSAT)          ! (lbm/ft-h)
          KL=0.06D0*EXP(-0.0024D0*TSAT)             ! (Btu/h-ft-F)
          CPL=2E-06*(TSAT**2D0)+0.0003D0*TSAT+0.2696D0 ! (Btu/lbm-F)
C
          VLIQ=MASSVEL*SPVOLL/60.D0
      ELSE
          SPVOLL=-4E-05+9E-06*(TSAT**0.8052D0)      ! (m^3/kg)
          MUL=8314D0*(TSAT**(-1.8679D0))            ! (N-s/m^2)
          KL=-0.1371*DLOG(TSAT)+0.8687
          ! (W/m-K)
          CPL=580.43D0*EXP(0.0026D0*TSAT)           ! (J/kg-K)
C
          VLIQ=MASSVEL*SPVOLL
      ENDIF
C
      PRL=MUL*CPL/KL
      REL=MASSVEL*D/MUL
C
C*****According to Gnielinski (1976), applicable over the range
c      of 0.5<Pr<2000 and 2300<Re<5e6
c
      IF(REL.LT.10000) THEN
          CF=16.D0/REL ! D'Arcy Friction Factor for Laminar Flow
      ELSE
          CF=2.D0*((2.236*DLOG(REL)-4.639D0)**(-2.D0))
          !Above eq. is #12-14 in Kayes & Crawford, pg.249
          !correlation for friction coeff. given by Petukhov
          !applicable in the range of 1e04<Re<5e06
      ENDIF
      TOP2=(REL-1000.D0)*PRL*CF/2.D0
      BOTTOM2=1.D0+12.7D0*((CF/2.D0)**0.5D0)*((PRL**(2.D0/3.D0))
&          -1.D0)
      NUL=TOP2/BOTTOM2

      H(I)=KL*NUL/D
C
C*****Update wall temperature:
      QPRIME=(TR(I)-T(I,2))/(((H(I)*PI*D)**(-1))+
&          ((2*PI*KCOPPER)**(-1))*DLOG(DW/D)+
&          ((2*PI*K(I,2))**(-1))*DLOG((DW+DR)/DW))
      TWALL=TR(I)-QPRIME/(H(I)*PI*D)
C
      IF(ABS(TW(I)-TWALL).GT.0.1) THEN
          TW(I)=TWALL
          GOTO 8002
      ENDIF
C
      TW(I)=TWALL

```

```

C          IF(TC.GE.TEND-DT) THEN
c          if(tc2.ge.tcond-dt) then
8003      WRITE(8,8003) I,X,REL,vliq,H(I),Q,Z,P(I),TR(I),TW(I)
      &      FORMAT(I7,1x,F6.4,F7.0,F9.2,F9.0,F10.1,F8.3,F9.2,4x,
      &      F7.2,2X,F7.2)
      endif
C
C
      Q=Q+H(I)*PI*D*DZ*(TW(I)-TR(I))
C
c*****Compute Pressure Drop for All-Liquid Flow:
      IF(REL.LE.10000) THEN
          fv=64.d0/rel !Laminar Flow (d'Arcy) Friction Factor
      ELSE
          fv=0.3164d0*(rel**(-0.25d0)) !Turbulent Flow
C          (Blasius) F.F.
      ENDIF
c      Pressure drop in a pipe due to an apparent shear stress
c      in fully developed flow, laminar or turbulent, (Pg. 78
c      of Kays & Crawford)
      IF(UNITS.EQ.1) THEN
          dpdz=(-fv*(massvel**2.D0)*spvoll)/(2d0*gc*d)
          P(I+1)=P(I)+DPDZ*DZ/144.D0
          PSAT=P(I+1)
      ELSE
          dpdz=(-fv*(massvel**2.D0)*spvoll)/(2d0*d)
          P(I+1)=P(I)+DPDZ*DZ*1E+03 ! kPa
          PSAT=P(I+1)
      ENDIF
C
      IF(UNITS.EQ.1) THEN
          TR(I+1)=TR(I)+(4.D0*DZ*H(I)*SPVOLL*(TW(I)-TR(I)))/
      &      (VLIQ*60.D0*D*CPL)
      ELSE
          TR(I+1)=TR(I)+(4.D0*DZ*H(I)*SPVOLL*(TW(I)-TR(I)))/
      &      (VLIQ*D*CPL)
      &
      ENDIF
C
C
      Z=Z+DZ
C
      ENDDO
C
      IF(TC.GE.TEND-DT) THEN
          WRITE(8,*) 'Q=',Q*DT
      ENDIF
C
8004 RETURN
      END
C*****
C
C      EVAPORATING SUBROUTINE
C
C*****
      SUBROUTINE EVAPORATING
C

```

```

      INCLUDE 'PARSOL.FOR'
      INCLUDE 'PRESOL.FOR'
      INCLUDE 'COMSOL.FOR'

C
      PSAT=PSATE
      CALL REFRIGPROPS
      TR(2)=TSAT

C
      IF(MODE.EQ.2) THEN
            MASSVEL = MDOTE/ACS           !Evaporating Mode
      ELSE
            MASSVEL = MDOTST/ACS         !Start-up Mode
      ENDIF
      X=0.03D0
      Z = 0.0D0
      IC = 0
      P(2)=PSATE
C
      IF(TC.GE.TEND-DT) THEN
      IF(TC2.GE.TEVAP-DT) THEN
      WRITE(8,*) 'Cell#      X      Rel      Vliq      Rev      Vvap      h
& Q      z      P      TR      TW'
      WRITE(8,*) '
& Btu/h      ft      psia'
      ENDIF
6000 FORMAT(I7,1X,F6.4,F7.0,F7.2,F9.0,1X,F8.2,F9.2,2X,F12.3,F7.3,
&          F7.2,2X,F7.2,2X,F7.2)

C
      I=2

      DO WHILE((X.LT.1.0).AND.(Z.LT.LENGTH).AND.(TC.LT.TEND))
            IC=IC+1

C
            REL=(1.0-X)*MASSVEL*D/MUL
            REV=X*MASSVEL*D/MUV
            VLIQ=(1.0-X)*MASSVEL*SPVOLL/60.D0
            VVAP=X*MASSVEL*SPVOLV/60.D0

C
C      *****Martinelli Parameter*****
            CHI=(VISRATIO**(0.1D0))*(((1.0-X)/X)**(0.9D0))
&            *(VOLRATIO**(0.5D0))
            IF((TW(I)-TR(I)).LE.0.D0) THEN
&            WRITE(6,*) 'You need a larger temperature difference
            to maintain Evaporation.'
            WRITE(9,*) 'END TIME=',TC,'HOURS'
            STOP
            ENDIF

C
C      *****
C
C      *****Using Gungor-Winterton (1987) correlation which compares
C      extremely well with experimental data of Seo et als.,
C      Int.J.Heat Mass Transfer 43 (2000) 2869-2882, Figure 6.
C
C      *****Dittus-Boelter Eq. for single-phase (liq.)****
            HL=0.023D0*KL*(REL**(0.8D0))*(PRL**(0.4D0))/D

C
            FRLO=(MASSVEL**2.D0)*(SPVOLL**2.D0)/(GC*D)           !Froude

```

```

C                               Number - all liq.

C
C   The following is true for horizontal tubes.
C
C       IF(FRLO.LT.0.05D0) THEN
C           E2=FRLO**(0.1D0-2.D0*FRLO)
C       ELSE
C           E2=1.D0
C       ENDIF

C   6002       BO=QDOT/(MASSVEL*HFG)                                !Boiling Number
C
C       TERM1=1.D0+3000.D0*(BO**0.86D0)
C       TERM2=1.12D0*( (X/(1.D0-
C   &           X) ) **0.75D0) * ( (SPVOLV/SPVOLL) **0.41D0)
C
C       H(I)=HL*E2*(TERM1+TERM2)
C       NUE(I)=H(I)*D/KV

C
C   *****
C*****Update wall temperature:
C       QPRIME=(T(I,2)-TR(I))/((H(I)*PI*D)**(-1))+
C   &           ((2*PI*KCOPPER)**(-1))*DLOG(DW/D)+
C   &           ((2*PI*K(I,2))**(-1))*DLOG((DW+DR)/DW)
C       TW(I)=TR(I)+QPRIME/(H(I)*PI*D)

C
C*****Check for convergence of wall heat flux:
C       QDOT2=H(I)*(TW(I)-TR(I))
C       IF(ABS(QDOT2-QDOT).GT.0.01) THEN
C           QDOT=QDOT2
C           GOTO 6002
C       ENDIF

C
C*****Compute change in quality
C       DX=DZ*4.D0*(H(I))*(TW(I)-TR(I))/(MASSVEL*HFG*D)

C
C       ALPHA=1.D0/(1.D0+((1.D0-X)/X)*(VOLRATIO**(2.D0/3.D0)))

C
C*****Write results to output file
C
C       IF(TC.GE.TEND-DT) THEN
C   c       if(tc2.ge.tevap-dt) then

WRITE(8,6000) I,X,REL,VLIQ,REV,VVAP,NUE(I),Q,Z,P(I),TR(I),TW(I)
C       endif

C
C       IF(IC.EQ.1) THEN

WRITE(6,6000) I,X,REL,VLIQ,REV,VVAP,H(I),Q,Z,P(I),TR(I),TW(I)
C       ENDIF

C
C       Q = Q + H(I)*PI*D*DZ*(TW(I)-TR(I))    !(Btu/hr)Total
C   c       Q = H(I)*PI*D*(TW(I)-TR(I))        !(Btu/hr*ft)
C
C
C*****
C

```

```

C      Now procede to calculate the corresponding pressure gradient
C      and drop in the tube.
C
C*****
C      DXDZ = DX/DZ
C      IF (UNITS.EQ.1) THEN
C          DPZFA=(MUV**0.2D0)*( (MASSVEL*X)**1.8D0)*SPVOLV/
C          &      (GC*(D**1.2D0))
C          DPZF=-0.09D0*( (1.D0+2.85D0*(CHI**0.523D0))**2.D0)*DPZFA
C          DPZMB=(MASSVEL**2.D0)*DXDZ*SPVOLV/GC
C          DPZM=-DPZMB*(2.D0*X+(1.D0-2.D0*X)*(VOLRATIO**(1.D0/3.D0)+
C          &      VOLRATIO**(2.D0/3.D0))-(2.D0-2.D0*X)*VOLRATIO)
C          DPZG=SIN(THETA)*G/GC*(ALPHA/SPVOLV+(1.0-ALPHA)/SPVOLL)
C          DPZ=DPZF+DPZM+DPZG
C          P(I+1)=P(I)+DPZ*DZ/144.D0
C          PSAT=P(I+1)
C
C      ELSE
C
C          DPZFA=(MUV**0.2)*( (MASSVEL*X)**1.8)*SPVOLV/(D**1.2)
C          DPZF=-0.09D0*( (1.D0+2.85D0*(CHI**0.523))**2)*DPZFA
C          DPZMB=(MASSVEL**2)*DXDZ*SPVOLV
C          DPZM=-DPZMB*(2.0D0*X+(1.0D0-2.0D0*X)*(VOLRATIO**(1D0/3D0)
C          &      + VOLRATIO**(2D0/3D0))-(2.0D0-2.0D0*X)*VOLRATIO)
C          DPZG=SIN(THETA)*G*(ALPHA/SPVOLV+(1.0-ALPHA)/SPVOLL)
C          DPZ=DPZF+DPZM+DPZG
C          P(I+1)= P(I)+DPZ*DZ*1E+03      ! kPa
C          PSAT=P(I+1)
C      ENDIF
C
C      NLEVAPC=I
C
C      Z=Z+DZ
C
C      I=I+1
C
C*****Update Saturation Temp. and Refrigerant Props.
C
C      CALL REFRIGPROPS
C      TR(I)=TSAT
C
C      X=X+DX
C
C      IF(x.gt.0.9999)GOTO 7000
C
C      ENDDO
C
C      7000 WRITE(6,6000)I,X,REL,VLIQ,REV,VVAP,H(I),Q,Z,P(I),TR(I),TW(I)
C
C*****
C
C      ALL-VAPOR ZONE
C
C*****
C
C      IF(TC.GE.TEND-DT) THEN
C      IF(TC2.GE.TEVAP-DT) THEN

```

```

7001 WRITE(8,*)
      WRITE(8,*) 'Cell#      X      Rev      VVap      h      Q      z
&      P      TR      TW'
      WRITE(8,*) '
& psia      F'
      ENDIF
C
      DO I=NLEVAPC+1,IM1
C
C*****Compute mean temperature
C
7002      TSAT=(TR(I)+TW(I))/2.D0
C
C*****Update vapor properties as a function of temperature
      IF(UNITS.EQ.1)THEN
          SPVOLV=1.3992D0*EXP(-0.0185D0*TSAT)
          MUV=5E-05*TSAT+0.0268D0
          KV=2E-05*TSAT+4.9E-03
          CPV=0.1617D0*EXP(0.0031D0*TSAT)
C
          VVAP=MASSVEL*SPVOLV/60.D0
      ELSE
          SPVOLV=2E+19*(TSAT**(-8.4644D0))          ! (m^3/kg)
          MUV=0.003433D0+1E-05*(TSAT**1.2036D0)    ! (N-s/m^2)
          KV=0.0017*EXP(0.0063D0*TSAT)             ! (W/m-K)
          CPV=129.43*EXP(0.0063D0*TSAT)             ! (J/kg-K)
C
          VVAP=MASSVEL*SPVOLV
      ENDIF
C
      PRV=MUV*CPV/KV
      REV=MASSVEL*D/MUV
C
      X=1.
C
C*****According to Gnielinski (1976), applicable over the range
c      of 0.5<Pr<2000 and 2300<Re<5e6
C
      IF(REV.LT.10000)THEN
          CF=16.D0/REV !D'Arcy Friction Factor for Laminar Flow
      ELSE
          CF=2.D0*((2.236*DLOG(REV)-4.639D0)**(-2.D0))
          !Above eq. is #12-14 in Kayes & Crawford, pg.249
          !correlation for friction coeff. given by Petukhov
          !applicable in the range of 1e04<Re<5e06
      ENDIF
      TOP2=(REV-1000.D0)*PRV*CF/2.D0
      &
      BOTTOM2=1.D0+12.7D0*((CF/2.D0)**0.5D0)*((PRV**(2.D0/3.D0))
          -1.D0)
      NUV=TOP2/BOTTOM2
      H(I)=KV*NUV/D
C
C*****Update wall temperature:

```

```

      QPRIME=(T(I,2)-TR(I))/(((H(I)*PI*D)**(-1))+
&      ((2*PI*KCOPPER)**(-1))*DLOG(DW/D)+
&      ((2*PI*K(I,2))**(-1))*DLOG((DW+DR)/DW))
      TWALL=TR(I)+QPRIME/(H(I)*PI*D)
C
      IF(ABS(TW(I)-TWALL).GT.0.1) THEN
          TW(I)=TWALL
          GOTO 7002
      ENDIF
C
      TW(I)=TWALL
C
      IF(TC.GE.TEND-DT) THEN
c
      if(tc2.ge.tevap-dt) then
7003      WRITE(8,7003) I,X,REV,vvap,H(I),Q,Z,P(I),TR(I),TW(I)
&      FORMAT(I7,3x,F6.4,F7.0,F9.2,F9.0,F10.1,F8.3,F9.2,4x,
&      F7.2,2X,F7.2)
      endif
C
      Q=Q+H(I)*PI*D*DZ*(TW(I)-TR(I))
C
c*****Compute Pressure Drop for All Vapor Flow:
      IF(REV.LE.10000) THEN
          fv=64.d0/rev !Laminar Flow (d'Arcy) Friction Factor
      ELSE
          fv=0.3164d0*(rev**(-0.25d0)) !Turbulent Flow
C          (Blasius) F.F.
      ENDIF
      IF(UNITS.EQ.1) THEN
          dpdz=(-fv*(massvel**2.D0)*spvolv)/(2d0*gc*d)
          P(I+1)=P(I)+DPDZ*DZ/144.D0
          PSAT=P(I+1)
      ELSE
          dpdz=(-fv*(massvel**2.D0)*spvolv)/(2d0*d)
          P(I+1)=P(I)+DPDZ*DZ*1E+03 !kPa
          PSAT=P(I+1)
      ENDIF
C
      IF(UNITS.EQ.1) THEN
          TR(I+1)=TR(I)+(4.D0*DZ*H(I)*SPVOLV*(TW(I)-TR(I)) /
&          (VVAP*60.D0*D*CPV))
      ELSE
          TR(I+1)=TR(I)+(4.D0*DZ*H(I)*SPVOLV*(TW(I)-TR(I)) /
&          (VVAP*D*CPV))
      ENDIF
C
      Z=Z+DZ
C
      ENDDO
C
C
      IF(TC.GE.TEND-DT) THEN
          WRITE(8,*) 'Q=',Q*DT
      ENDIF
7004 RETURN
      END

```

```

C   BEGINNING OF FILE (COMSOL.FOR)
COMMON/RCOM/
1       MDOT,                      DIA,                      TWALL,
2       THETA,                    X,                      TSAT,
3       TBOIL,                    TC,                      PSAT,
4       HFG,                      SPVOLL,                 SPVOLV,
5       MUL,                      MUV,                   KL,
6       KV,                      CPL,                      CPV,
7       PI,                      D,                      ACS,
8       MASSVEL,                 VISRATIO,              VOLRATIO,
9       PRL,                      PRV,                   G,
1      GC,                      PC,                     LENGTH,
2      DZ,                      RO,                     RI,
3      DR,                      XI (MXNCZ),             VLIQ,
4      VVAP,                    H (MXNCZ),             Q,
5      TR (MXNCZ),              TW (MXNCZ),            P (MXNCZ),
6      T (MXNCZ,MXNCR),         QS (MXNCZ,MXNCR),     MHFG,
7      REL,                      REV,                   HL,
8      VL,                      HV,                    NU,
9      IDZ,                     VFG,                   FC,
1     XSC,                      SC,                     EN,
2     ED,                      HMIC,                  HMAC,
3     DX,                      VV,                    NSPVOL (MXNCZ),
4     NVV (MXNCZ),              NCP (MXNCZ),           NKV,
5     NMUV,                    NVL (MXNCZ),           NKL,
6     NMUL,                    LH,                    RHOW,
7     RHOS,                    KW,                    KS,
8     CPW,                     CPS,                   TM,
9     TEND,                    DT,                    HWS (MXNCZ,MXNCR),
1     HWSN (MXNCZ,MXNCR),       TN (MXNCZ,MXNCR),     TCRT,
2     TCRTK,                    K (MXNCZ,MXNCR),     RHO (MXNCZ,MXNCR),
3     DENOM,                    DELT,                  F,
4     B,                        FG,                    NUV,
5     TWn (MXNCZ),              ospolv,                RC,
6     SIG,                      MUW,                   GA,
7     FRSO,                     THETAL,                FRL,
8     C1,                       C2,                    PHIL,
9     JAL,                      REVO,                  NUF,
1     QICE,                    HWSN1 (MXNCZ,MXNCR),   HWSN2 (MXNCZ,MXNCR),
2     HWSN3 (MXNCZ,MXNCR),      HWSN4 (MXNCZ,MXNCR),   HWSN5 (MXNCZ,MXNCR),
3     LEFT,                     BOTTOM,                 RIGHT,
4     TOP,                      TC2,                   TCOND,
5     TEVAP,                    PSATC,                 PSATE,
6     XO,                      PCRT,                  RELO,
7     HLO,                     TSTARTUP,              MDOTE,
8     MDOTST,                  DW,                    FRLO,
9     E2,                      S2,                    QDOT,
1     QDOT2,                    BO,                    TERM1,
2     TERM2,                    K1,                    K2,
3     TOP2,                     BOTTOM2,                NUE (MXNCZ),
4     R,                        Z,                     KCOPPER,
5     CF,                      NUC (MXNCZ),           qp (mxncz),
6     qpold (mxncz)
REAL*8
1     MDOT,                      MUL,                    MUV,
2     KL,                      KV,                    MASSVEL,
3     LENGTH,                  MHFG,                  NU,

```



	4	IDZ,	NSPVOL,	NVV,
	5	NCP,	NKV,	NMUV,
	6	NVL,	NKL,	NMUL,
	7	LH,	KW,	KS,
	8	K,	DENOM,	DELT,
	9	NUV,	ospolv,	MUW,
	1	JAL,	NUF,	LEFT,
	2	MDOTE,	MDOTST,	K1,
	3	K2,	NUE,	KCOPPER,
	4	NUC		
	COMMON/ICOM/			
	1	MODE,	IBAR,	IMAX,
	2	IM1,	JBAR,	JMAX,
	3	JM1,	NLCONDC,	I,
	4	IC,	JC,	KC,
	5	NLEVAPC,	A,	N,
	6	NEVAPC,	M,	UNITS,
	7	Y		
	INTEGER			
	1	A,	UNITS,	Y
	COMMON/CCOM/			
	1	REFRIG		
	CHARACTER			
	1	REFRIG*5,	QUALITY*6	
C	LOGICAL CHARACTER			
	COMMON/LCOM/			
	1	QUALITY (MXNCZ, MXNCR),	SOLID,	
	2	LIQUID,	MIXED	
C	END OF FILE (COMSOL.FOR)			
□				

```
C BEGINNING OF FILE (PARSOL.FOR)
  PARAMETER (MXNCZ=20000, MXNCR=30)
C
C END OF FILE (PARSOL.FOR)
□
```

```
C  BEGINNING OF FILE (PRESOL.FOR)
C
C  FOR DOUBLE PRECISION ACCURACY:
C    1) ACTIVATE THE FOLLOWING STATEMENT
      IMPLICIT REAL*8 (A-H,O-Z)
C    2) REPLACE INTRINSIC FUNCTIONS IN FILE (FUNSOL COPY A)
C
C  END OF FILE (PRESOL.FOR)
```

## APPENDIX B

### Sample Of Fluid-Side Output

Evaporating Mode  
VARIABLE PROPERTIES:

MASS FLOW RATE = 34.0000 LBM/HR  
REF.TUBE INNER DIAMETER = .3150 IN  
ICE BANK TUBE DIAMETER = 2.4450 IN  
WALL TEMPERATURE = 70.0000 DEG F  
ANGLE OF INCLINE = .0000 DEGREES  
CELL INCREMENT ALONG TUBE = .0050 FEET

REFRIGERANT PROPERTIES:

REFRIGERANT = R-22  
SATURATION TEMPERATURE = 20.0263 DEG F  
SATURATION PRESSURE = 57.6000 PSIA  
LATENT HEAT OF VAPORIZATION = 90.9525 BTU/LBM  
SPECIFIC VOLUME OF LIQUID = .0124 FT^3/LBM  
SPECIFIC VOLUME OF VAPOR = .9309 FT^3/LBM  
VISCOSITY OF LIQUID = .5447 LBM/H-FT  
VISCOSITY OF VAPOR = .0281 LBM/H-FT  
THERMAL CONDUCTIVITY OF LIQ. = .0568 BTU/H-FT-F  
THERMAL CONDUCTIVITY OF VAP. = .0052 BTU/H-FT-F  
SPECIFIC HEAT OF LIQUID = .2736 BTU/LBM-F  
SPECIFIC HEAT OF VAPOR = .1691 BTU/LBM-F

Q= 58.576059849705250

Cell#	X	Rel	Vliq	Rev	Vvap	h	Q	z	P	TR	TW
			f/m		f/m	B/hf2F	Btu/h	ft	psia	F	F
2	.1100	2694.	11.52	6465.	107.22	995.94	127569.31	.000	57.60	20.03	27.64
3	.1102	2694.	11.51	6477.	107.41	996.20	127569.93	.005	57.60	20.03	27.64
4	.1104	2693.	11.51	6489.	107.61	996.47	127570.56	.010	57.60	20.03	27.64
5	.1106	2693.	11.51	6500.	107.81	996.73	127571.18	.015	57.60	20.03	27.63
6	.1108	2692.	11.51	6512.	108.00	997.00	127571.81	.020	57.60	20.03	27.63
7	.1110	2691.	11.50	6524.	108.20	997.27	127572.43	.025	57.60	20.03	27.63
8	.1112	2691.	11.50	6536.	108.40	997.53	127573.05	.030	57.60	20.03	27.63
9	.1114	2690.	11.50	6548.	108.59	997.80	127573.68	.035	57.60	20.03	27.63
10	.1116	2690.	11.50	6560.	108.79	998.06	127574.30	.040	57.60	20.03	27.63
11	.1118	2689.	11.49	6572.	108.99	998.33	127574.93	.045	57.60	20.03	27.62
12	.1120	2688.	11.49	6583.	109.18	998.60	127575.55	.050	57.60	20.03	27.62
13	.1122	2688.	11.49	6595.	109.38	998.86	127576.17	.055	57.60	20.03	27.62
14	.1124	2687.	11.49	6607.	109.58	999.13	127576.80	.060	57.60	20.03	27.62
15	.1126	2687.	11.48	6619.	109.77	999.39	127577.42	.065	57.60	20.03	27.62
16	.1128	2686.	11.48	6631.	109.97	999.65	127578.05	.070	57.60	20.03	27.61
17	.1130	2685.	11.48	6643.	110.17	999.92	127578.67	.075	57.60	20.03	27.61
18	.1132	2685.	11.48	6655.	110.37	1000.18	127579.29	.080	57.60	20.03	27.61
19	.1134	2684.	11.47	6666.	110.56	1000.45	127579.92	.085	57.60	20.03	27.61
20	.1136	2683.	11.47	6678.	110.76	1000.71	127580.54	.090	57.60	20.03	27.61
21	.1138	2683.	11.47	6690.	110.96	1000.97	127581.17	.095	57.60	20.03	27.61
22	.1140	2682.	11.46	6702.	111.15	1001.24	127581.79	.100	57.60	20.03	27.60
23	.1142	2682.	11.46	6714.	111.35	1001.50	127582.41	.105	57.60	20.03	27.60
24	.1144	2681.	11.46	6726.	111.55	1001.76	127583.04	.110	57.60	20.03	27.60
25	.1146	2680.	11.46	6738.	111.74	1002.03	127583.66	.115	57.60	20.03	27.60
26	.1148	2680.	11.45	6749.	111.94	1002.29	127584.29	.120	57.60	20.03	27.60
27	.1150	2679.	11.45	6761.	112.14	1002.55	127584.91	.125	57.60	20.03	27.60
28	.1152	2679.	11.45	6773.	112.33	1002.81	127585.54	.130	57.60	20.03	27.59

29	.1154	2678.	11.45	6785.	112.53	1003.08	127586.16	.135	57.60	20.03	27.59
30	.1157	2677.	11.44	6797.	112.73	1003.34	127586.78	.140	57.60	20.03	27.59
31	.1159	2677.	11.44	6809.	112.92	1003.60	127587.41	.145	57.60	20.03	27.59
32	.1161	2676.	11.44	6821.	113.12	1003.86	127588.03	.150	57.60	20.03	27.59
33	.1163	2676.	11.44	6833.	113.32	1004.12	127588.66	.155	57.60	20.03	27.58
34	.1165	2675.	11.43	6844.	113.51	1004.38	127589.28	.160	57.60	20.03	27.58
35	.1167	2674.	11.43	6856.	113.71	1004.64	127589.91	.165	57.60	20.03	27.58
36	.1169	2674.	11.43	6868.	113.91	1004.91	127590.53	.170	57.60	20.03	27.58
37	.1171	2673.	11.43	6880.	114.11	1005.17	127591.16	.175	57.60	20.03	27.58
38	.1173	2672.	11.42	6892.	114.30	1005.43	127591.78	.180	57.60	20.03	27.58
39	.1175	2672.	11.42	6904.	114.50	1005.69	127592.40	.185	57.60	20.02	27.57
40	.1177	2671.	11.42	6916.	114.70	1005.95	127593.03	.190	57.60	20.02	27.57
41	.1179	2671.	11.42	6927.	114.89	1006.21	127593.65	.195	57.60	20.02	27.57
42	.1181	2670.	11.41	6939.	115.09	1006.47	127594.28	.200	57.60	20.02	27.57
43	.1183	2669.	11.41	6951.	115.29	1006.73	127594.90	.205	57.60	20.02	27.57
44	.1185	2669.	11.41	6963.	115.48	1006.98	127595.53	.210	57.60	20.02	27.57
45	.1187	2668.	11.40	6975.	115.68	1007.24	127596.15	.215	57.60	20.02	27.56
46	.1189	2668.	11.40	6987.	115.88	1007.50	127596.78	.220	57.60	20.02	27.56
47	.1191	2667.	11.40	6999.	116.08	1007.76	127597.40	.225	57.60	20.02	27.56
48	.1193	2666.	11.40	7011.	116.27	1008.02	127598.03	.230	57.60	20.02	27.56
49	.1195	2666.	11.39	7022.	116.47	1008.28	127598.65	.235	57.60	20.02	27.56
50	.1197	2665.	11.39	7034.	116.67	1008.54	127599.28	.240	57.60	20.02	27.56
51	.1199	2664.	11.39	7046.	116.86	1008.79	127599.90	.245	57.60	20.02	27.55
52	.1201	2664.	11.39	7058.	117.06	1009.05	127600.53	.250	57.60	20.02	27.55
53	.1203	2663.	11.38	7070.	117.26	1009.31	127601.15	.255	57.60	20.02	27.55
54	.1205	2663.	11.38	7082.	117.45	1009.57	127601.78	.260	57.60	20.02	27.55
55	.1207	2662.	11.38	7094.	117.65	1009.82	127602.40	.265	57.60	20.02	27.55
56	.1209	2661.	11.38	7106.	117.85	1010.08	127603.03	.270	57.60	20.02	27.54
57	.1211	2661.	11.37	7117.	118.05	1010.34	127603.65	.275	57.60	20.02	27.54
58	.1213	2660.	11.37	7129.	118.24	1010.60	127604.28	.280	57.60	20.02	27.54
59	.1215	2660.	11.37	7141.	118.44	1010.85	127604.90	.285	57.60	20.02	27.54
60	.1217	2659.	11.37	7153.	118.64	1011.11	127605.53	.290	57.60	20.02	27.54
61	.1219	2658.	11.36	7165.	118.83	1011.36	127606.15	.295	57.60	20.02	27.54
62	.1221	2658.	11.36	7177.	119.03	1011.62	127606.78	.300	57.60	20.02	27.53
63	.1223	2657.	11.36	7189.	119.23	1011.88	127607.40	.305	57.60	20.02	27.53
64	.1225	2657.	11.36	7201.	119.43	1012.13	127608.03	.310	57.60	20.02	27.53
65	.1227	2656.	11.35	7212.	119.62	1012.39	127608.65	.315	57.60	20.02	27.53
66	.1229	2655.	11.35	7224.	119.82	1012.64	127609.28	.320	57.60	20.02	27.53
67	.1231	2655.	11.35	7236.	120.02	1012.90	127609.90	.325	57.60	20.02	27.53
68	.1233	2654.	11.34	7248.	120.21	1013.15	127610.53	.330	57.60	20.02	27.52
69	.1235	2653.	11.34	7260.	120.41	1013.41	127611.15	.335	57.60	20.02	27.52
70	.1237	2653.	11.34	7272.	120.61	1013.66	127611.78	.340	57.60	20.02	27.52
71	.1239	2652.	11.34	7284.	120.81	1013.92	127612.40	.345	57.60	20.02	27.52
72	.1241	2652.	11.33	7296.	121.00	1014.17	127613.03	.350	57.60	20.02	27.52
73	.1243	2651.	11.33	7308.	121.20	1014.43	127613.65	.355	57.60	20.02	27.52
74	.1245	2650.	11.33	7319.	121.40	1014.68	127614.28	.360	57.60	20.02	27.51
75	.1247	2650.	11.33	7331.	121.59	1014.93	127614.90	.365	57.60	20.02	27.51
76	.1249	2649.	11.32	7343.	121.79	1015.19	127615.53	.370	57.60	20.02	27.51
77	.1251	2649.	11.32	7355.	121.99	1015.44	127616.15	.375	57.60	20.02	27.51
78	.1253	2648.	11.32	7367.	122.19	1015.69	127616.78	.380	57.60	20.02	27.51
79	.1256	2647.	11.32	7379.	122.38	1015.95	127617.40	.385	57.60	20.02	27.51
80	.1258	2647.	11.31	7391.	122.58	1016.20	127618.03	.390	57.60	20.02	27.50
81	.1260	2646.	11.31	7403.	122.78	1016.45	127618.65	.395	57.60	20.02	27.50
82	.1262	2645.	11.31	7415.	122.97	1016.70	127619.28	.400	57.60	20.02	27.50
83	.1264	2645.	11.31	7426.	123.17	1016.96	127619.91	.405	57.60	20.02	27.50
84	.1266	2644.	11.30	7438.	123.37	1017.21	127620.53	.410	57.60	20.02	27.50
85	.1268	2644.	11.30	7450.	123.57	1017.46	127621.16	.415	57.60	20.02	27.50
86	.1270	2643.	11.30	7462.	123.76	1017.71	127621.78	.420	57.60	20.02	27.49
87	.1272	2642.	11.29	7474.	123.96	1017.96	127622.41	.425	57.60	20.02	27.49
88	.1274	2642.	11.29	7486.	124.16	1018.22	127623.03	.430	57.60	20.02	27.49
89	.1276	2641.	11.29	7498.	124.36	1018.47	127623.66	.435	57.60	20.02	27.49
90	.1278	2641.	11.29	7510.	124.55	1018.72	127624.28	.440	57.60	20.02	27.49
91	.1280	2640.	11.28	7522.	124.75	1018.97	127624.91	.445	57.60	20.02	27.49
92	.1282	2639.	11.28	7533.	124.95	1019.22	127625.54	.450	57.60	20.02	27.49
93	.1284	2639.	11.28	7545.	125.14	1019.47	127626.16	.455	57.60	20.02	27.48
94	.1286	2638.	11.28	7557.	125.34	1019.72	127626.79	.460	57.60	20.02	27.48
95	.1288	2638.	11.27	7569.	125.54	1019.97	127627.41	.465	57.60	20.02	27.48
96	.1290	2637.	11.27	7581.	125.74	1020.22	127628.04	.470	57.60	20.02	27.48
97	.1292	2636.	11.27	7593.	125.93	1020.47	127628.66	.475	57.60	20.02	27.48
98	.1294	2636.	11.27	7605.	126.13	1020.72	127629.29	.480	57.60	20.02	27.48
99	.1296	2635.	11.26	7617.	126.33	1020.97	127629.92	.485	57.60	20.02	27.47

## APPENDIX C

### Sample Of PCM-Side Output

#### ICEBANK PROPERTIES:

LATENT HEAT OF FUSION	= 143.34 BTU/LBM
DENSITY OF WATER	= 62.4142 LB/FT^3
DENSITY OF ICE	= 57.2410 LB/FT^3
THERMAL CONDUCT. OF WATER	= .326 BTU/H-FT-F
THERMAL CONDUCT. OF ICE	= 1.280 BTU/H-FT-F
SPECIFIC HEAT OF WATER	= 1.0041 BTU/LBM-F
SPECIFIC HEAT OF ICE	= .4600 BTU/LBM-F
MELTING TEMP. OF ICE	= 32.00 F

Total Volume of Ice Bank= 6.096653333437171E-001  
 QEND= -59.843602427201510

CELL ROW	COLUMN	TEMP. (F)	ENTHALPY (Btu/lbm)	QUALITY
2	2	45.51	13.570	LIQUID
2	3	45.51	13.569	LIQUID
2	4	45.51	13.568	LIQUID
2	5	45.51	13.567	LIQUID
2	6	45.51	13.565	LIQUID
2	7	45.51	13.564	LIQUID
2	8	45.51	13.563	LIQUID
2	9	45.51	13.562	LIQUID
2	10	45.51	13.561	LIQUID
2	11	45.50	13.560	LIQUID
2	12	45.50	13.558	LIQUID
2	13	45.50	13.557	LIQUID
2	14	45.50	13.556	LIQUID
2	15	45.50	13.555	LIQUID
2	16	45.50	13.554	LIQUID
2	17	45.50	13.553	LIQUID
2	18	45.50	13.551	LIQUID
2	19	45.49	13.550	LIQUID
2	20	45.49	13.549	LIQUID
2	21	45.49	13.548	LIQUID
2	22	45.49	13.547	LIQUID
2	23	45.49	13.546	LIQUID
2	24	45.49	13.544	LIQUID
2	25	45.49	13.543	LIQUID
2	26	45.49	13.542	LIQUID
2	27	45.49	13.541	LIQUID
2	28	45.48	13.540	LIQUID
2	29	45.48	13.539	LIQUID
2	30	45.48	13.538	LIQUID
2	31	45.48	13.537	LIQUID
2	32	45.48	13.535	LIQUID
2	33	45.48	13.534	LIQUID
2	34	45.48	13.533	LIQUID
2	35	45.48	13.532	LIQUID
2	36	45.48	13.531	LIQUID

2	37	45.47	13.530	LIQUID
2	38	45.47	13.529	LIQUID
2	39	45.47	13.527	LIQUID
2	40	45.47	13.526	LIQUID
2	41	45.47	13.525	LIQUID
2	42	45.47	13.524	LIQUID
2	43	45.47	13.523	LIQUID
2	44	45.47	13.522	LIQUID
2	45	45.47	13.521	LIQUID
2	46	45.46	13.520	LIQUID
2	47	45.46	13.519	LIQUID
2	48	45.46	13.517	LIQUID
2	49	45.46	13.516	LIQUID
2	50	45.46	13.515	LIQUID
2	51	45.46	13.514	LIQUID
2	52	45.46	13.513	LIQUID
2	53	45.46	13.512	LIQUID
2	54	45.46	13.511	LIQUID
2	55	45.45	13.510	LIQUID
2	56	45.45	13.509	LIQUID
2	57	45.45	13.508	LIQUID
2	58	45.45	13.506	LIQUID
2	59	45.45	13.505	LIQUID
2	60	45.45	13.504	LIQUID
2	61	45.45	13.503	LIQUID
2	62	45.45	13.502	LIQUID
2	63	45.45	13.501	LIQUID
2	64	45.44	13.500	LIQUID
2	65	45.44	13.499	LIQUID
2	66	45.44	13.498	LIQUID
2	67	45.44	13.497	LIQUID
2	68	45.44	13.496	LIQUID
2	69	45.44	13.495	LIQUID
2	70	45.44	13.494	LIQUID
2	71	45.44	13.492	LIQUID
2	72	45.44	13.491	LIQUID
2	73	45.44	13.490	LIQUID
2	74	45.43	13.489	LIQUID
2	75	45.43	13.488	LIQUID
2	76	45.43	13.487	LIQUID
2	77	45.43	13.486	LIQUID
2	78	45.43	13.485	LIQUID
2	79	45.43	13.484	LIQUID
2	80	45.43	13.483	LIQUID
2	81	45.43	13.482	LIQUID
2	82	45.43	13.481	LIQUID
2	83	45.42	13.480	LIQUID
2	84	45.42	13.479	LIQUID
2	85	45.42	13.478	LIQUID
2	86	45.42	13.477	LIQUID
2	87	45.42	13.475	LIQUID
2	88	45.42	13.474	LIQUID

etc.....

END TIME= 2.020350046681588E-002HOURS

## **BIOGRAPHY OF THE AUTHOR**

Anne-Marie Bechard Thibodeau was born in Waterville, Maine on July 28, 1963. In 1981, she graduated from Waterville High School. She attended Long Island University and Anna Maria College where she graduated in 1985 with a Bachelor's degree in Music. In 1990, she entered the Mechanical Engineering program at The University of Maine. She graduated with a Bachelor's degree in 1993 and a Master's degree in 1996.

Anne-Marie worked as a research engineer at Applied Thermal Sciences, in Sanford, Maine, for three years. She is currently employed by Pratt & Whitney, as a senior aero-thermal engineer. Anne-Marie is a candidate for the Doctor of Philosophy degree Individualized in Mechanical Engineering from The University of Maine in December, 2002.